Electronic correlation and magnetism in multi-band Kondo lattice model

Application for disorder materials

D I S S E R T A T I O N

zur Erlangung des akademischen Grades

Dr. Rer. Nat.
im Fach Physik

eingereicht an der
Mathematisch-Naturwissenschaftlichen Fakultät I
Humboldt-Universität zu Berlin

von
Dipl.-Phys. Vadym Bryksa Ph.D.
geboren am 01.01.1979 in Oleksandrija (Ukraine)

Präsident der Humboldt-Universität zu Berlin:
Prof. Dr. Christoph Markschies

Dekan der Mathematisch-Naturwissenschaftlichen Fakultät I:
Prof. Dr. Lutz-Helmut Schön

Gutachter:
1. Prof. Dr. W. Nolting
2. Prof. Dr. W. Borgiel
3. Prof. Dr. G. Tarasov

eingereicht am: 31.03.2009
Tag der mündlichen Prüfung: 23.10.2009

Abstract

We propose a self-consistent approximate solution of the disordered Kondo-lattice model (KLM) to get the interconnected electronic and magnetic properties of 'local-moment' systems like diluted ferromagnetic semiconductors. Aiming at $(A_{1-x}M_x)$ compounds, where magnetic (M) and non-magnetic (A) atoms are distributed randomly over a crystal lattice, we present a theory which treats the subsystems of itinerant charge carriers and localized magnetic moments in a homologous manner. The coupling between the localized moments due to the itinerant electrons (holes) is treated by a modified RKKY-theory which maps the KLM onto an effective Heisenberg model. The disordered electronic and magnetic moment systems are both treated by coherent potential approximation (CPA) methods.

An extension of CPA to perform a self-consistent model calculation of the electronic and magnetic properties of diluted local-moment systems $A_{1-x}M_x$ described by ferromagnetic Kondo-lattice model ($s-f$ model), where we included disorder in the first environment shell by use of crystal field parameters between two non-magnetic, one magnetic and non-magnetic, and two magnetic atoms, respectively $\lambda^{AA}, \lambda^{AM}, \lambda^{MM}$, and to get the interconnected electronic and magnetic properties of systems like diluted ferromagnetic semiconductors (DMS) is proposed.

We discuss in detail the dependencies of the key-terms such as the long range and oscillating effectice exchange integrals and the Curie temperature as well as the electronic and magnonic quasiparticle densities of states on the concentration x of magnetic ions, the carrier concentration n, the exchange coupling J and the crystal field parameters.

Zusammenfassung

Es wird eine selbstkonsistente, approximative Lösung für das verdünnte, ungeordnete Kondo-Gitter-Modell (KLM) vorgeschlagen, um die miteinander verknüpften elektronischen und magnetischen Eigenschaften von sogenannten 'local moment'-Systemen wie den verdünnten magnetischen Halbleitern zu diskutieren. Untersucht werden Verbindungen der Form $A_{1-x}M_x$, in denen magnetische (M) und nichtmagnetische Atome (A) statistisch über das Kristallgitter verteilt sind. Die Kopplung zwischen den lokalisierten Momente und den quasi-freien Elektronen (Löcher) wird im Rahmen einer modifizierten RKKY-Theorie behandelt, die das KLM auf ein effektives Heisenberg-Modell abbildet. Die Unordnungen in dem elektronischen Teilsystem und in dem magnetischen Momentensystem werden nach Methoden behandelt, die der 'coherent potential approximation' (CPA) angepaßt sind.

Es wird eine Erweiterung der CPA zur Berechnung der sich wechselseitig bedingenden elektronischen und magnetischen Eigenschaften verdünnter 'local moment'-Systeme vom Typ $A_{1-x}M_x$ für die Situation vorgeschlagen, in der eine durch Kristallfeldparameter bedingte Unordnung in der Nächste-Nachbar-Schale des Aufatoms berücksichtigt werden muß. Dabei werden Kristallfeldparameter zwischen zwei nichtmagnetischen Atomen (λ^{AA}), zwischen einem magnetischen und einem nicht-magnetischen Atom (λ^{AM}) und zwischen zwei magnetischen Atomen (λ^{MM}) unterschieden.

Schlüsselgrößen wie die langreichweitigen und oszillierenden effektiven Austauschintegrale und die Curie-Temperatur und die elektronischen und magnonischen Quasiteilchen-Zustandsdichten werden im Detail in Abhängigkeit der Konzentration x der magnetischen Ionen, der Ladungsträger-Konzentration n, der Interband-Austauschkopplung J, der Temperatur und der Kristallfeldparameter untersucht.

Inhaltsverzeichnis

1. Introduction **1**
- 1.1. Transitional metals in semiconductors . . . 1
- 1.2. The disorder Kondo Lattice Model . . . 4
- 1.3. Outline . . . 6

2. Disordered Heisenberg model **9**
- 2.1. Introduction to the HM(x=1) . . . 9
- 2.2. Disordered HM . . . 11
- 2.3. Configurational average . . . 13
- 2.4. Thermodynamics of disorder Heisenberg model . . . 17

3. Electronic structure of disorder materials **21**
- 3.1. Theoretical techniques . . . 22
- 3.2. Theoretical Model . . . 24
  - 3.2.1. Electron Subsystem: Zero-bandwidth limit of the correlated KLM . . . 25
  - 3.2.2. Electron Subsystem: Interpolating self-energy approach . 29
- 3.3. Electron Subsystem: Cluster CPA treatment . . . 31

4. Self-Consistent Task **43**
- 4.1. Direct and Indirect mechanisms . . . 43
- 4.2. Exchange interaction in the disorder KLM . . . 44
- 4.3. Ferromagnetism in the disorder KLM . . . 53

5. Summary & Outlook **63**

A. Finite lattice calculation **67**

B. Cumulant technique **73**

C. Larking presentation **77**

1. Introduction

1.1. Transitional metals in semiconductors

It is known that transition metal atoms generate deep levels within the energy gap of II-VI, III-V semiconductors (Refs. Omelanovskii and Fistul [1983], Kikoin and Fleurov [1994]). The statements related to the problem of deep levels in wide-gap semiconductors doped with the transition metal atoms of low concentration ($x < 0.0001$) can be summarized as follow: i) The transition metal atom occurs the substitution defect in the cationic sub-lattice of semiconductor; ii) Unfilled atomic d-orbital of transition elements is occupied following the Hunds rules for free atom and is clamped to the vacuum level of semiconductor rather than to the top of valence band or to the bottom of conduction band. The deep levels in semiconductors are generated following the scheme of resonant crystal field or broken bonds (Ref. Kikoin and Fleurov [1994]); iii) Peculiarities of electron spectra in magnetically doped semiconductors can not be explained basing on the solution of two-band model in the tight-binding approximation (Ref. Kikoin and Fleurov [1994]). This latter problem being essentially many-body one requires taking into account besides the crystal field the coulomb coupling of electrons and the covalence of binding between the transition element atom and the matrix as well. Narrow-gap magnetically doped semiconductors generally do not follow the behavior of the wide-gap semiconductors containing magnetic atoms (Ref. Kikoin and Fleurov [1994]).

Traditionally it has been considered that the microscopic description of the Mn effect in wide-gap semiconductors can be performed using the Kondo-Vonsovskii Hamiltonian (Refs. Kondo [1964], Abrikosov et al. [1958], Vonsovskii [1946]) with two exchange constants and in the mean field approximation. Thus one has in the case of exchange interaction between the spin of conduction band electron and the localized magnetic moment of the Mn ion

$$H^e_{exch} = \alpha \sum_i (\vec{S}_i \sigma)_{\sigma\sigma'} a^+_{i\sigma} a_{i\sigma'} \rightarrow \alpha \langle S^z \rangle \overline{\sigma}^e, \tag{1.1}$$

whereas in case of the valence band hole this coupling takes the form of paper Bhattacharjee [1992]

$$H^h_{exch} = \beta \sum_i (\vec{S}_i \sigma)_{\sigma\sigma'} b^+_{i\sigma} b_{i\sigma'} \rightarrow \beta \langle S^z \rangle \overline{\sigma}^h, \tag{1.2}$$

where $a^+_{i\sigma}$ ($a_{i\sigma}$) and $b^+_{i\sigma}$ ($b_{i\sigma}$) are the creation (annihilation) operators for the Wannier electron and hole with the spin σ ($\sigma = \uparrow, \downarrow$) at the site $\vec{R}_i$, respectively, (S^x, S^y, S^z) is a local magnetic moment of the transition metal, $(\sigma^x, \sigma^y, \sigma^z)$

are the Pauli matrix, $\langle S^z \rangle$ is an average magnetization of localized moments of the magnetic atoms and $\overline{\sigma}^e$, $\overline{\sigma}^h$ are average values of the electron, hole spins, respectively.

Usually the α, β exchange coupling parameters being derived from magneto-optical or magneto-transport experiments reveal a strong scatter both by values and signs even for the most investigated wide-gap semiconductors (Refs. Bhattacharjee [1992], Ley et al. [1987], Persson and Zunger [2003], Furdyna [1988], Mizokawa and Fujimory [1997]). Moreover in case of narrow-gap semiconductors demonstrating the metallic properties it is problematically to determine these microscopic parameters from experiments (Furdyna [1988], Hoerstel et al. [1999]). In the limiting case of metal there exists only one band and only one parameter remains to describe the exchange interaction between the collectivized carriers and the localized spins. Thus the problem becomes the Kondo problem. The magnetic properties of the Mn doped semiconductors are predicted to be diamagnetic at high temperatures, whereas at low temperatures the Van Vleck paramagnetism caused by the transition metal ions is expected under such approach (Ref. Omelanovskii and Fistul [1983]). It should be noticed that the Kondo-Vonsovskii Hamiltonian, being widely used for the description of the magnetic semiconductors Nagaev [1979], the materials demonstrating the metal-insulator transition Loseva et al. [1983], and the magnets with the semi-metallic properties Moriya [1985], is valid in case of diluted magnetic semiconductors under the condition of randomly distributed transition ions over the cationic sub-lattice of the semiconductors.

Recently the $Ga_{1-x}Mn_xAs$ and $In_{1-x}Mn_xAs$ semiconductors with high molar percentage of Mn ($x > 0.01$) have been studied in Refs. Ohno [1999], Iye et al. [1999]. The growth conditions allow the Mn ions to be randomly distributed over the cationic sub-lattice and the $MnAs$ clusters do not arise interior the bulk $Ga_{1-x}Mn_xAs$ due to the condition of ($x < x_c$), where x_c is the percolation limit for the creation of the finite percolation clusters in the face-centered cubic cationic sub-lattice ($x_c \approx 0.195$). It has been shown that these semiconductors turn out in the magnetically ordered state like to the ferromagnetic phase (Refs. Ohno [1999], Iye et al. [1999], Dietl et al. [2000]). Such state can be easily manipulated allowing the spintronic application (Ref. Ohno et al. [2002]). Changing the wide-gap semiconductors $Ga_{1-x}Mn_xAs$ by the narrow-gap $In_{1-x}Mn_xAs$ compounds possessing larger lattice constant it is possible to get the homogeneous semiconductors of the higher Mn doping. The $In_{1-x}Mn_xSb$ semiconductor with $x = 0.02, 0.028$ has been successfully synthesized (Ref. Wojtowicz et al. [2003]).

The ferromagnetic ordering in the $A_{1-x}Mn_xB$ DMS can not be referred directly to a typical phenomenon of magnetic systems. It has been concluded in Refs. Hirakawa et al. [2002], Singley et al. [2002], Craco et al. [2003] that in the DMS the double exchange is the mechanism responsible for the ferromagnetic ordering rather than the RKKY mechanism in case of the metallic conductivity as it is stated in Refs. Ohno [1999], Iye et al. [1999]. In spite of low Mn concentrations in the diluted magnetic semiconductors these latter belong to the magnetic systems, the type of Heisenberg magnetic semiconductors (EuO, EuS, $EuSe$, $EuTe$, $Ca_{1-x}La_xMnO_3$) (Refs. Nagaev [1979], Nol-

ting et al. [1988] or the Heusler alloys possessing the structure $C1b$ ($PtMnSb$, $NiMnSb$, CrO_2, $MnSb$, $MnAs$) (Refs. Irkhin and Katsnelson [1994], Sandratskii and Bruno [2003], Sanyal et al. [2003]). It is known that the ferromagnetism and the antiferromagnetism coexist in the Heisenberg magnetic semiconductors (Ref. Nagaev [1979]) resulting in the inhomogeneous magnetic ordering, what can explain a non-monotonic temperature dependence of the resistance (Refs.Nagaev [1979], Ohno [1999], Iye et al. [1999]). Thus on the one hand the problem of meta-stable magnetic properties of the DMS arises. On the other hand it is known that even the diamagnetic properties of the narrow-gap DMS are inhomogeneous. The departure from the Fermi-behavior of free electrons is observed in the magnetic semiconductors of high conductivity also (Ref. Irkhin and Katsnelson [1994]). This property is proved for the model serving an example of the strongly correlated electron system. All experimental findings mentioned above are of great importance for understanding of the DMS properties. The DMS materials based on III-V and II-VI semiconductors exhibit also a very striking correlation between the transport and magnetic properties Jungwirth et al. [2006]. Ideally, each Mn dopant atom represents an acceptor that introduces a local spin and a hole carrier. The ferromagnetism is driven by a charge-carrier mediated mechanism as a consequence of an interband exchange interaction between the localized magnetic moments and the carrier(hole) spins. Experimentally, the Curie temperature T_c of the DMS is enhanced by postgrowth annealing of the samples, which changes positions of defects and the hole concentration Jungwirth et al. [2006].

There exist various theoretical schemes in the DMS study. One resembles the computer modeling for strongly frustrated spin glasses Refs. Kennet et al. [2002a,b]. Such approach is based on the random distribution of transition metal over the cationic sub-lattice of the semiconductor and predicts significant deviation from the 3/2 law for the temperature dependence of magnetization if the temperature tends zero. The approximation of mean field or the approximation of a virtual crystal is widely used in Refs. Yang et al. [2001], Sun and Lin [2003]. Here after the configuration averaging in the DMS the search of the electron Green's functions reduces to the similar problem of the magnetic semiconductor with the mean splitting performed following the Bogolyubov-Tyablikov procedure (Ref. Nolting et al. [1996b]). Both the disorder and the possibility of the inhomogeneous magnetism are ignored. The contribution of the disorder can be taken into account using the technique of the coherent potential (Refs. Takahashi and Mitsui [1996], Takahashi and Kubo [1999, 2002]). This technique proved to be a powerful tool in the study of magnetic systems of high conductivity; however it is of importance to account for correctly the electron correlations and the dynamic character of scattering. The dynamic mean field technique (Ref. Georges et al. [1996]) allows the investigation of the strongly correlated systems and the DMS as well. This technique broadens the resources of the coherent potential method (Ref. Craco et al. [2003]). The standard technique of the Fermi-systems is also used for the study of the correlated carriers in the DMS (Refs. Lebedeva and Kuivalainen [2002], Ivanov et al. [2003]). However it is difficult to solve a self-consistent problem for the magnetic sub-system together with the problem of the electron-hole spectrum

in the semiconductor.

The ab-initio calculations are considered to be of use to get the information about the electron spectrum in the $A_{1-x}Mn_xB$ DMS (Refs. Craco et al. [2003], Sanyal et al. [2003], Sandratskii and Bruno [2003]). Nevertheless the uniqueness of the results as well as their certainty has to be particularly analyzed in such calculations. Therefore the analytical schemes developed for the investigation of the $A_{1-x}Mn_xB$ DMS with a metallic type conductivity are of extreme importance. These materials are considered as an example of correlated electron systems combining the electrical and magnetic properties (Refs. Ohno [1999], Iye et al. [1999], Dietl et al. [2000], Ohno et al. [2002], Wojtowicz et al. [2003], Hirakawa et al. [2002], Singley et al. [2002], Craco et al. [2003]).

So the magnetism in the DMS is heavily depending on the impurity (Mn ion) disorder and dilution, carrier concentration and compensation, and the coupling mechanism between the localized Mn spins and the itinerant holes. Therefore, it is very hard to study these materials without some approximations. There are many theoretical approaches attempting to understand DMS physics Zhou et al. [2004], Singh et al. [2003], Kudrnovsky et al. [2004], Bouzerar and Bruno [2002], Hilbert and Nolting [2004], Bouzerar et al. [2003, 2006a], Takahashi [2004], Nolting et al. [2004], Subrat and Singh [2005], Priour and Sarma [2006]. However, the mutual influence of interband-coupling effects and disorder effects with respect to the ferromagnetic phase transition have not been completely understood so far. So we propose first of all to study the ferromagnetic properties of the ideal alloy $A_{1-x}M_x$ system Tang and Nolting [2007], Bryksa and Nolting [2008a,b].

1.2. The disorder Kondo Lattice Model

There are many analytical models such as the Hubbard and the Anderson models which are very useful for the description of real correlated electron systems. The Kondo-lattice Model (KLM) Hewson [1997] is another one. The KLM describes an interplay of itinerant electrons in a partially filled energy band with magnetic moments localized at certain lattice sites Nolting et al. [1996b], Nolting et al. [2001], Nolting and Oles [1980], Edwards et al. [1999], Hilbert and Nolting [2004]. The characteristic model properties result from an interband exchange interaction between two well-defined subsystems: itinerant electrons and localized spins.

Problems connected with the substitutional disorder have recently become more and more important in different fields of material science as there are, e.g., the diluted magnetic semiconductors Jungwirth et al. [2006], the transition metal dielectrics Gusev et al. [2001], the perovskite manganese oxides Motome and Furukawa [2005], and so on. The disorder is also very important in different technological routes. Here we are interested mainly how the disorder influences the characteristic properties of local-moment systems such as the DMS, where magnetic (M) and non-magnetic (A) atoms are distributed randomly over a crystal lattice ($A_{1-x}M_x$) with a given concentration of magnetic atoms x. In order to answer this question different approaches were proposed Harris

et al. [1974], Theumann and Tahir-Kheli [1975], Jones [1971], Dvey-Aharon and Fibich [1978], Kudrnovsky et al. [2004], Bouzerar and Bruno [2002]. More or less realistic electronic structure calculations based on density functional theory (DFT) Parr and Yang [989] or simulation methods as classical Quantum Monte Carlo investigations for standard models like the Heisenberg Hilbert and Nolting [2004] one were used. However, the disadvantage of the realistic DFT-calculations come from their strong material dependence Kudrnovsky et al. [2004]. Therefor, they do not explain the basic physics of disordered local-moment systems in a simple way. The better results in this respect are obtained from model study of the disordered Kondo lattice.

A special challenge when treating the random Kondo-lattice model arises with the fact that both the electron and the spin subsystem have to be considered simultaneously and on the same level. Most of the KLM investigations are focused on the electronic Takahashi [2004], Blackman et al. [1971] or magnetic Theumann and Tahir-Kheli [1975], Dvey-Aharon and Fibich [1978], Harris et al. [1974], Hilbert and Nolting [2004], Bouzerar and Bruno [2002], Bouzerar et al. [2006a] subsystem only. A special goal of our study is the homologous treatment of the electronic and magnetic properties of the random KLM, which mutually condition each other and, therefore, should be determined self-consistently.

As mentioned, a very important aspect of these alloys is the disorder, the magnetic and non-magnetic atoms are distributed randomly over the crystal lattice. The magnetic exchange interactions are to be taken into account for all distances between the different moments. This defines an effective Heisenberg model for the magnetic moments. The concentration x controls the average distance between two magnetic atoms. On the other hand, the effective Heisenberg interaction also depends on x. The same holds for interband-coupling effects Nolting et al. [1996b], Liechtenstein et al. [1987]. Both effects are important for understanding the ferromagnetic transition in such component Tang and Nolting [2007], Bryksa and Nolting [2008a].

Nevertheless, we are forced to apply different methods to study the influence of the disorder and dilution of the magnetic moments subsystem on the properties of these two aforementioned subsystems. For the itinerant electron system a proper alloy analogy with the respective coherent potential approximation (CPA) Elliott et al. [1974] may be used. For the random spin system, for which the situation is not so clear, an equivalent ansatz must be found. As it was done successfully for the periodic KLM Nolting et al. [1996b] (*'modified' RKKY (MRKKY)*) one can map the KLM-interband exchange on an effective and random Heisenberg model. The resulting effective exchange integrals between the localized spins will be long range and complicated functionals of the electronic self-energy. The conventional RKKY, resulting from second order perturbation theory may be insufficient even with a phenomenological damping factor Kudrnovsky et al. [2004], Bouzerar et al. [2006a]. Higher order conduction electron self-energy effects, being taken into account by *'modified' RKKY* but neglected by conventional $RKKY$, provide the self-consistency of the full KLM. They drastically influence the magnetic properties such as the Curie temperature.

The most developed approach for incorporation of the carrier disorder is the CPA (Refs. Elliott et al. [1974], Matsubara and Yonezawa [1966], Nolting et al. [2001], Tang and Nolting [2007], Bryksa and Nolting [2008a], Takahashi [2004], Nolting et al. [2004], Bouzerar and Bruno [2002]). However, there are many indications that this method is not sufficient for the explanation of certain properties of the disordered ferromagnetic semiconductors Elliott et al. [1974], Butler [1972]. For example, the CPA does not incorporate the electron scattering on the crystal field fluctuations, which are important and can change the Curie temperature very drastically Jungwirth et al. [2006]. One attempt of treating the crystal field fluctuation in the DMS systems using numerical simulation for finite systems has recently been used in ref. Bouzerar et al. [2006b]. However, the authors use only the effect of chemical substitution that accompanies the presence of the magnetic atom.

1.3. Outline

There are many real materials where disorder plays an important role for electronic as well as magnetic properties (binary substitutional alloys, diluted magnetic semiconductors, perovskite manganese oxides, spin glass materials, transition metal dielectrics and so on). Of course, these real systems are much more complicated than the simple Kondo-lattice model predicts (complicated crystal lattice, multi-band structure, hybridization effects, spin-orbit coupling). However, we believe that the main microscopic mechanisms are well described in terms of the characteristic KLM features. The final goal is to make a quantitative description of those materials combining the present analytic model investigations with realistic *'ab initio'* calculations of the band structure as it was done previously for concentrated local-moment systems Hilbert and Nolting [2004], Müller and Nolting [2002], Schiller [2000].

In this paper we discuss the influence of moment disorder on the electron and spin excitation spectra of the disorder ferromagnetic $A_{1-x}M_x$ KLM. Starting from an different alloy analogy technique of the KLM we applied a CPA procedure to find out the reaction of the electronic spectrum on the random mixture of magnetic and nonmagnetic atoms Tang and Nolting [2007], Bryksa and Nolting [2008a,b]. The analytical expression for the electronic selfenergy has been used then to get the effective exchange integrals of the modified RKKY theory Nolting et al. [1996b]. The latter results from a mapping of the interband exchange onto a random Heisenberg model which was subsequently treated in the spirit of the well-known Tyablikov approximation. The disorder in the localized spin system turned out the most involved part of our study. Its was incorporated using the equation of motion method and the technique of configurational averaging. In order to decouple the higher-order averaged Green functions we used an approximation of independent fluctuations Yukhnovskii [1987], Yukhnovskii and Gurskii [1991]. The expression for the averaged magnon Green function is generalized by using the structure factor of disordered distribution of magnetic atoms over a crystal lattice. Here we also used an approximation, identical to the low quadratic approach Dvey-Aharon and Fibich

[1978]. There is no direct interaction between the localized moments. Therefore the collective order is caused by the indirect interaction mediated by the itinerant band electrons. Consequently, the indirect momentum coupling strongly depends on electronic model parameters such as exchange coupling J and band occupation n. A further important parameter is of course the concentration of magnetic atoms x.

The organization of the thesis is as follows. In chapter 2, we first introduce the disordered Heisenberg model (inter-atomic exchange between two localized moments of the magnetic atoms). Within the Green function motion technique we try to evaluate the temperature dependent physical properties of the system like quasi-particle magnon density of states for a given quantum spin and an exchange coupling of the localized spins. We further extend our theory to an alloy with magnetic and nonmagnetic atoms and determine the similar physical properties for the disorder Heisenberg case with an additional parameter x being the concentration of the magnetic atoms. In chapter 3, we perform the calculations of the quasi-particle electron density of states for the $A_{1-x}M_x$ alloy using the CPA procedure in order to obtain the exchange coupling between magnetic atoms and to study the temperature dependent correlation effects in the bands. In chapter 4 we derive the self-consistent calculations of the magnetic and electronic quasi-particle density of states for the disorder $A_{1-x}M_x$ Kondo lattice model by used of the technique of mapping the disordered Heisenberg model on the disordered KLM. Using this theory we try to explain the role of a substitutional disorder in stabilizing the ferromagnetism in the DMS systems. Finally in chapter 5, we summarize our findings and conclude the thesis with an outlook. In order to keep the content of the thesis in a self-contained manner, we briefly describe the method of the finite lattice calculation, the cumulant technique and the Larking presentation as a part of appendixes.

2. Disordered Heisenberg model

2.1. Introduction to the HM(x=1)

Let me start directly with the Heisenberg model Heisenberg [1928] for pure magnetic systems:

$$H = -\frac{1}{2}\sum_{i,j} J_{ij}\vec{S}_i\vec{S}_j, \tag{2.1}$$

where $J_{ij} = J(\vec{R}_j - \vec{R}_i)$ is an exchange interaction between two localized spin $\vec{S}_i = (S_i^x, S_i^y, S_i^z)$ and $\vec{S}_j$ in a real space (see Fig. 2.1).

We use Green function technique for studying the Heisenberg system, where the definition for a time-dependent spin Green function is the following Zubarev [1960]:

$$G_{ij}(t) = -\imath\theta(t)\langle[S_i^+(t); S_j^-(0)]\rangle, \tag{2.2}$$

where the spin operator $S_i^\sigma(\sigma = +, -)$ is

$$S_i^\sigma = S_i^x + \sigma\imath S_i^y, \tag{2.3}$$

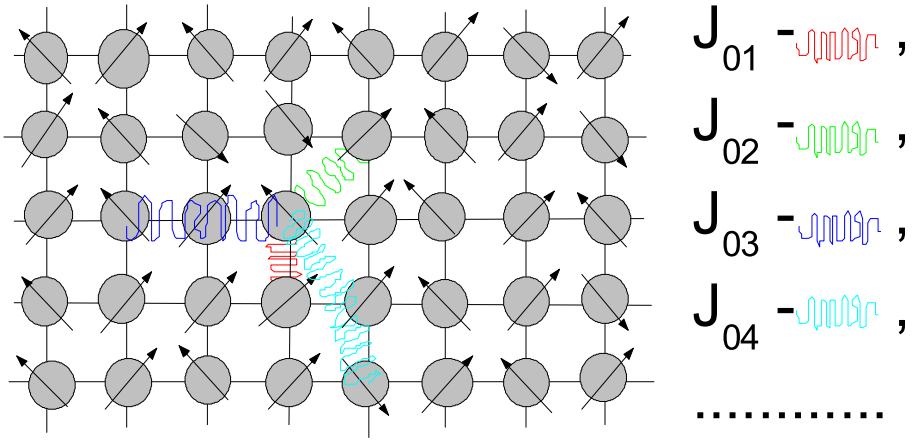

Abbildung 2.1.: There is a schematic presentation of the crystal lattice Heisenberg model. A circle in the lattice node shows an atom. An arrow on an atom means the magnetic moment. There are magnetic interaction between any two magnetic atoms. On the figure the interaction between nearest-neighbor, next-nearest-neighbor, ... atoms are shown by red, green, ... colors.

the time dependent $S_i^\sigma(t)$ spin operator is

$$S_i^\sigma(t) = e^{\imath Ht} S_i^\sigma e^{-\imath Ht}, \tag{2.4}$$

the time dependent function $\theta(t)$ is

$$\theta(t) = \begin{cases} 1, & t > 0 \\ 0, & t < 0, \end{cases} \tag{2.5}$$

the brackets from two operators $[A, B]$ is a commutator

$$[A, B] = AB - BA, \tag{2.6}$$

and the right left brackets $\langle ... \rangle$ means thermodynamical average.

We can write the direct and inverse Fourier transformations $\langle\langle S_i^+ | S_j^- \rangle\rangle_E$ for the time-dependent Green function $G_{ij}(t)$ in the following form, respectively:

$$\langle\langle S_i^+ | S_j^- \rangle\rangle_E = \int e^{\imath Et} G_{ij}(t) dt \tag{2.7}$$

$$G_{ij}(t) = \frac{1}{2\pi} \int e^{-\imath Et} \langle\langle S_i^+ | S_j^- \rangle\rangle_E dE \tag{2.8}$$

So, now using the technique of an equation of motion for the Green function $G_{ij}(t)$

$$E\langle\langle S_i^+ | S_j^- \rangle\rangle_E = \langle [S_i^+, S_j^-] \rangle + \langle\langle [S_i^+, H] | S_j^- \rangle\rangle_E, \tag{2.9}$$

and the Bogolyubov-Tyablikov method of decoupling for the high spin Green function Bogoliubov and Tyablikov [1959]:

$$\langle\langle S_l^z S_i^+ | S_j^- \rangle\rangle_E = \langle S_l^z \rangle \langle\langle S_i^+ | S_j^- \rangle\rangle_E, \tag{2.10}$$

we find the the spin Green function in the following form:

$$G_{ij}(E) = \frac{1}{2\pi N} \sum_{\vec{k}} e^{\imath \vec{k}(\vec{R}_j - \vec{R}_i)} G(\vec{k}, E), \tag{2.11}$$

where

$$G(\vec{k}, E) = \frac{2\langle S_l^z \rangle}{E - \varepsilon_{\vec{k}}}, \tag{2.12}$$

$$\varepsilon_{\vec{k}} = \langle S_l^z \rangle (J(0) - J(\vec{k})), \tag{2.13}$$

$$J_{ij} = \frac{1}{2\pi N} \sum_{i,j} e^{\imath \vec{k}(\vec{R}_j - \vec{R}_i)} J(\vec{k}). \tag{2.14}$$

Using the spectral theorem for the Green function $G(\vec{k}, E)$:

$$\langle S_i^- S_i^+ \rangle = \frac{1}{N} \sum_{\vec{k}} \int dE \frac{-\frac{1}{\pi} ImG(\vec{k}, E)}{e^{\beta E} - 1}, \tag{2.15}$$

we calculate the average $\langle S_i^- S_i^+ \rangle$:

$$\langle S_i^- S_i^+ \rangle = \frac{2\langle S_l^z \rangle}{N} \sum_{\vec{k}} \frac{1}{e^{\beta\varepsilon_{\vec{k}}} - 1}. \tag{2.16}$$

From other hand, using a equation for a full quadratic spin

$$S_l^- S_l^+ + (S_l^z)^2 - S_l^z = S(S+1) \tag{2.17}$$

we have the following correlation at the case $S = \frac{1}{2}$

$$S_l^- S_l^+ = \frac{1}{2} - S_l^z. \tag{2.18}$$

And we write the following equation for finding the average magnetization $\langle S_l^z \rangle$:

$$\langle S_l^z \rangle \frac{1}{N} \sum_{\vec{k}} cth \frac{\beta\varepsilon_{\vec{k}}}{2} = \frac{1}{2}. \tag{2.19}$$

From this equation we also find Curie-temperature $\langle S_l^z \rangle (T_c) = 0$:

$$\beta_c = \frac{1}{T_c} = \frac{3}{2S(S+1)} \frac{1}{N} \sum_{\vec{k}} \frac{1}{\varepsilon_0 - \varepsilon_{\vec{k}}}. \tag{2.20}$$

For the case $S > \frac{1}{2}$, using the same technique it is possible to write, so-called, the Callen equation for the average magnetization Callen [1963]:

$$\langle S^z \rangle = \frac{(S-\phi)(1+\phi)^{2S+1} + (S+1+\phi)\phi^{2S+1}}{(1+\phi)^{2S+1} - \phi^{2S+1}}, \tag{2.21}$$

where

$$\phi = -\frac{1}{\pi} \frac{1}{N} \sum_{\vec{k}} \int_0^\infty \frac{ImG_{\vec{k}}(E)}{e^{\beta E} - 1} dE. \tag{2.22}$$

2.2. Disordered HM

Suppose that we start to destroy the crystal lattice presented on the Fig. 2.1 by throwing out certain magnetic atoms from the crystal lattice nodes. We obtain a random crystal lattice which is shown on Fig. 2.2.

Let us consider a disordered crystal lattice that have only N_M magnetic atoms and $N - N_M$ empty nodes(non-magnetic). So, now we have a structurally disordered system of $N_M = xN$ spins which is described by the isotropic Heisenberg Hamiltonian

$$\hat{H} = -\sum_{ij} J_{ij} X_i^M X_j^M \left(S_i^z S_j^z + S_i^+ S_j^- \right), \tag{2.23}$$

where in order to introduce the disorder into a random lattice crystal of the

$A_{1-x}M_x$ type, we introduce projection operators

$$X_i^M = \begin{cases} 1, & -if\ site\ i\ is\ M \\ 0, & -otherwise. \end{cases} \tag{2.24}$$

After the transformation

$$X_i^M \vec{S}_i \to \vec{\tilde{S}}_i \tag{2.25}$$

the disordered model (Eq. 2.23) is become a regular one with fluctuated spins. So, we can use the equation of motion techniques for the Green function in order to investigate of the spin excitations in the regular Heisenberg model and standard commutator rules for the spin operator:

$$\begin{array}{c} \left[S_l^+, S_k^-\right] = 2\delta_{lk} S_l^z, \\ \left[S_l^z, S_k^\sigma\right] = \sigma\delta_{lk} S_l^\sigma. \end{array} \tag{2.26}$$

The Green function for the regular Heisenberg model within Tyablikov approximation satisfies the equation of motion

$$\begin{array}{l} E\left\langle\left\langle \tilde{S_l^+} | \tilde{S_k^-} \right\rangle\right\rangle_E = 2\delta_{lk}\left\langle \tilde{S_l^z} \right\rangle + \\ 2\sum_j J_{lj}\left\langle\left\langle \left\langle \tilde{S_j^z} \right\rangle \tilde{S_l^+} - \left\langle \tilde{S_l^z} \right\rangle \tilde{S_j^+} | \tilde{S_k^-} \right\rangle\right\rangle_E. \end{array} \tag{2.27}$$

This microscopic equation 2.27 with the fluctuated spins is a very complicated one but we can reduce the problem after using the following reasonable assumptions:

$$\begin{array}{c} \left\langle \tilde{S_l^z} \right\rangle \approx X_l^M \left\langle S^z \right\rangle, \\ \left\langle\left\langle \tilde{S_l^+} | \tilde{S_k^-} \right\rangle\right\rangle_E \approx \left\langle\left\langle S_l^+ | S_k^- \right\rangle\right\rangle_E, \end{array} \tag{2.28}$$

which mean that we neglect some structure fluctuations in the magnetization.

Then we can write the equation of motion for the disorder Heisenberg model (Eq. 2.23) in the following form:

$$\begin{array}{l} E\left\langle\left\langle S_l^+ | S_k^- \right\rangle\right\rangle_E = 2\delta_{lk} X_l^M \left\langle S_l^z \right\rangle + \\ 2\sum_j J_{lj}\left\langle\left\langle X_j^M \left\langle S_j^z \right\rangle S_l^+ - \left\langle S_l^z \right\rangle X_l^M S_j^+ | S_k^- \right\rangle\right\rangle_E. \end{array} \tag{2.29}$$

First, we multiply from left and right sides of the equation of motion (2.29) on $1/\sqrt{N} exp(-\imath\vec{q}\vec{R}_l)$ and $1/\sqrt{N} exp(-\imath\vec{q'}\vec{R}_k)$, respectively, and then we take sum on every l and k nodes in the lattice. After introducing the following definitions:

$$\begin{array}{c} \left\langle\left\langle S_{\vec{q}}^+ | S_{\vec{q'}}^- \right\rangle\right\rangle_E = \sum_{l,k} \frac{1}{\sqrt{N}} exp(-\imath\vec{q}\vec{R}_l)\left\langle\left\langle S_l^+ | S_k^- \right\rangle\right\rangle_E \frac{1}{\sqrt{N}} exp(-\imath\vec{q'}\vec{R}_k), \\ X_{\vec{q}} = \frac{1}{\sqrt{N}} \sum_l X_i^M e^{-i\vec{q}\vec{R}_l}, \\ \Delta X_{\vec{q}} = X_{\vec{q}} - x\sqrt{N}\delta(\vec{q}), \end{array} \tag{2.30}$$

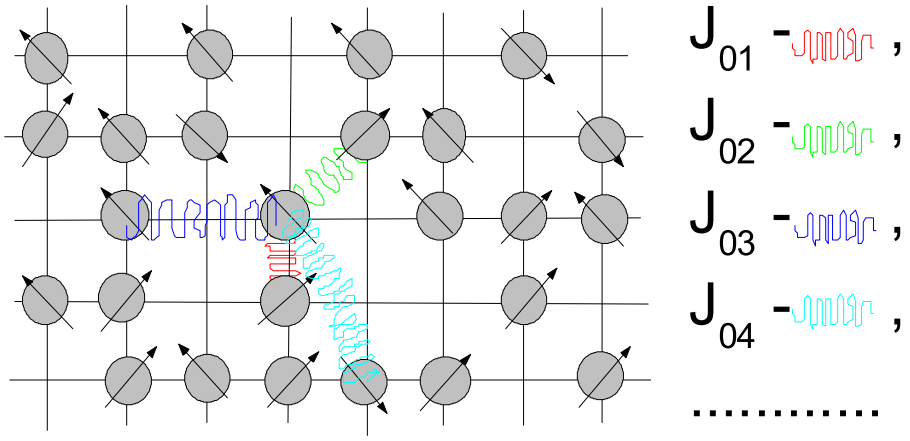

Abbildung 2.2.: There is a schematic presentation of the disorder crystal lattice Heisenberg model. A circle in the lattice node is shown an atom. An arrow on an atom is shown the magnetic moment. There are magnetic interaction between any two magnetic atoms. On the figure the interaction between nearest-neighbor, next-nearest-neighbor, ... atoms are shown by red, green, ... colors.

we can write the Eq. (2.29) in the following form:

$$\begin{aligned}&\left(E - x\left\langle S^z\right\rangle E_0(\vec{q})\right)\left\langle\left\langle S^+_{\vec{q}}|S^-_{\vec{q}'}\right\rangle\right\rangle_E = \\ &2x\left\langle S^z\right\rangle\delta(\vec{q}+\vec{q}') + 2\left\langle S^z\right\rangle\frac{1}{\sqrt{N}}\Delta X_{\vec{q}+\vec{q}'} + \\ &2\left\langle S^z\right\rangle\sum_{\vec{k}}\left(J(\vec{q}-\vec{k}) - J(\vec{k})\right)\frac{1}{\sqrt{N}}\Delta X_{\vec{q}-\vec{k}}\left\langle\left\langle S^+_{\vec{k}}|S^-_{\vec{q}'}\right\rangle\right\rangle_E,\end{aligned} \tag{2.31}$$

where we have used

$$\begin{aligned}E_0(\vec{q}) &= 2(J(0) - J(\vec{q})), \\ J(\vec{q}) &= \frac{1}{N}\sum_{l,j} J_{lj}e^{-\imath\vec{q}(\vec{R}_l - \vec{R}_j)}.\end{aligned} \tag{2.32}$$

2.3. Configurational average

So, we have two microscopic equations of motion (Eq. 2.29 and Eq. 2.31) for finding the spectrum $\left\langle\left\langle S^+_l|S^-_k\right\rangle\right\rangle_E$ and $\left\langle\left\langle S^+_{\vec{q}}|S^-_{\vec{q}'}\right\rangle\right\rangle_E$, respectively, in the disorder Heisenberg model, but both of them are not enough in the such presentation that were done in theses equations.

The microscopic equation (2.29) is strong singular and demands a solution for the every site in a crystal lattice. What is not possible from a technique point of view, at leas for an analytical solution.

The solution of the microscopic equation (2.31) which is a transformation of Eq. (2.29) by used the definition of the Eq. (2.30), demands a some additional assumption about the $\Delta X_{\vec{q}}$ operator. The $\Delta X_{\vec{q}}$ operator is a value of deviation of $X_{\vec{q}}$ from the average value. The $X_{\vec{q}}$ (Eq. 2.30) operator is called a collective

variable of a full system because it consists with the microscopic X_l^M operators in every lattice's nodes and their sum characterizes some collective properties of the such disordered system Yukhnovskii [1987], Yukhnovskii and Gurskii [1991].

The $X_{\vec{q}}$ (Eq. 2.30) is a more suitable variable for funding the spectrum of the disorder Heisenberg model than the projective operator X_i^M because this variable is a regular one but its has very strong oscillations in a **k**-space. Theses oscillations are connected with micro-peculiarities structure in the system. If we make a compare the spectrum of excitations for random and regular Heisenberg model which are have done by Eq. (2.31), and Eq. (2.12), respectively, we see that the $\Delta X_{\vec{q}}$ deviation serves as a perturbation in the model.

If we could find a such procedure that can reduce the high-oscillation behaviour in the $\Delta X_{\vec{q}}$ then we solve the equation of a motion (Eq. 2.30) in the same technique as was done for the regular Heisenberg model (Eq. 2.12).

There is a such procedure that can help in this problem. It calls a configurational average procedure. It means than we have to do a some additional average in the equation of motion (Eq. 2.30) for the Green function $\left\langle\left\langle S_{\vec{q}}^+ | S_{\vec{q}'}^- \right\rangle\right\rangle_E$ which is characterized a micro-peculiarities structure of the disodered system. After the such average procedure we loss theses micro-peculiarities in the solution for the magnon Green function of the random crystal, and the such collective functions, like to $\Delta X_{\vec{q}}$, also reduce their oscillation properties in a **k**-space.

Suppose, that we know how is distributed magnetic atoms in a lattice. So, it means that the configrational average on the projective X_i^M variables gives the concentration of the magnetic atoms x.

$$\overline{(X_i^M)_{\vec{R_1},\vec{R_2},\ldots\vec{R_i},\ldots,\vec{R_N}}} = x, \tag{2.33}$$

where the configurational average procedure is defined as the overline near the X_i^M.

In the same manner we can take the configurational average from every function f which is depended on the X_i^M variables:

$$\overline{f(X_i^M, X_l^M)_{\vec{R_1},\vec{R_2},\ldots,\vec{R_i},\ldots\vec{R_l},\ldots,\vec{R_N}}} = \overline{f}. \tag{2.34}$$

If we take the configurational average from $\Delta X_{\vec{q}}$ operator we find the following:

$$\begin{aligned}&\overline{\Delta X_{\vec{q}}} = \overline{X_{\vec{q}} - x\sqrt{N}\delta(\vec{q})} = \overline{\tfrac{1}{\sqrt{N}}\textstyle\sum_l X_l^M e^{-i\vec{q}\vec{R}_l}} - x\sqrt{N}\delta(\vec{q}) = \\ &\tfrac{1}{\sqrt{N}}\textstyle\sum_l \overline{X_l^M} e^{-i\vec{q}\vec{R}_l} - x\sqrt{N}\delta(\vec{q}) = 0.\end{aligned} \tag{2.35}$$

This propertie of the $\Delta X_{\vec{q}}$ operator are very important and means that the configurational average from the deviation of the collective variable $X_{\vec{q}}$ in the disordered system is zero. Nevertheless the configurationel average from a quadratic fluctuation $\overline{[\Delta X_{\vec{q}}]^2}$ is not zero, and gives us a structure factor of the disorder Heisenberg model.

Now, we can back to the assumption in the Eq. (2.28). After the configura-

tional average procedure we have the following:

$$\begin{array}{c} \overline{\left\langle \tilde{S}_l^z \right\rangle} = x \left\langle S^z \right\rangle \\ \overline{\langle\langle \tilde{S}_l^+ \mid \tilde{S}_k^- \rangle\rangle_E} = \overline{\left\langle\left\langle S_l^+ \mid S_k^- \right\rangle\right\rangle_E}, \end{array} \tag{2.36}$$

which means the total average magnetization of the disordered system is decreased on the concentration factor x comparing to a non-disordered case.

We use the two-time temperature Green function method for investigation of the spin excitations. The Green function within Tyablikov approximation satisfies the equation of motion (2.31). Averaging over all thinkable realization of atomic position configurations from left and right sides of the equation (2.31) give the following:

$$\begin{array}{l} (E - x\left\langle S^z\right\rangle E_0(\vec{q}))\,\overline{\left\langle\left\langle S_{\vec{q}}^+ | S_{\vec{q}'}^-\right\rangle\right\rangle}_E = 2x\left\langle S^z\right\rangle \delta(\vec{q}+\vec{q}') + \\ 2\left\langle S^z\right\rangle \sum_{\vec{k}} \left(J(\vec{q}-\vec{k}) - J(\vec{k})\right) \frac{1}{\sqrt{N}} \overline{\Delta X_{\vec{q}-\vec{k}} \left\langle\left\langle S_{\vec{k}}^+ | S_{\vec{q}'}^-\right\rangle\right\rangle}_E. \end{array} \tag{2.37}$$

The equation contains a higher-order averaged Green function $\overline{\Delta X G}$. One can write the equation of motion for this function, multiplying by ΔX and performing configurational averaging.

$$\begin{array}{l} \left(E - x\left\langle S^z\right\rangle E_0(\vec{k})\right) \overline{\frac{1}{\sqrt{N}} \Delta X_{\vec{q}-\vec{k}} \left\langle\left\langle S_{\vec{k}}^+ | S_{\vec{q}'}^-\right\rangle\right\rangle}_E = 2\left\langle S^z\right\rangle \overline{\frac{1}{N} \Delta X_{\vec{q}-\vec{k}} \Delta X_{\vec{k}-\vec{q}'}} + \\ 2\left\langle S^z\right\rangle \sum_{\vec{k}'} \left(J(\vec{k}-\vec{k}') - J(\vec{k}')\right) \frac{1}{\sqrt{N}} \overline{\Delta X_{\vec{q}-\vec{k}} \Delta X_{\vec{k}-\vec{k}'} \left\langle\left\langle S_{\vec{k}'}^+ | S_{\vec{q}'}^-\right\rangle\right\rangle}_E. \end{array} \tag{2.38}$$

These equations include $\overline{\Delta X \Delta X G}$. In order to solve these equations the following decoupling of configurational averages is used

$$\overline{\Delta X_{\vec{q}-\vec{k}} \Delta X_{\vec{k}-\vec{k}'} \left\langle\left\langle S_{\vec{k}'}^+ | S_{\vec{q}'}^-\right\rangle\right\rangle} \approx \overline{\Delta X_{\vec{q}-\vec{k}} \Delta X_{\vec{k}-\vec{k}'}}\, \overline{\left\langle\left\langle S_{\vec{k}'}^+ | S_{\vec{q}'}^-\right\rangle\right\rangle}, \tag{2.39}$$

where

$$\overline{\Delta X_{\vec{q}-\vec{k}} \Delta X_{\vec{k}-\vec{k}'}} = \delta(\vec{q}-\vec{k}')\, \overline{\Delta X_{\vec{q}-\vec{k}} \Delta X_{\vec{k}-\vec{q}}}. \tag{2.40}$$

The equation exploits translation symmetry.

The equation (2.38) is transformed into the following form:

$$\begin{array}{l} \left(E - x\left\langle S^z\right\rangle E_0(\vec{k})\right) \overline{\frac{1}{\sqrt{N}} \Delta X_{\vec{q}-\vec{k}} \left\langle\left\langle S_{\vec{k}}^+ | S_{\vec{q}'}^-\right\rangle\right\rangle}_E = \\ 2\left\langle S^z\right\rangle \delta(\vec{q}-\vec{q}') \overline{\frac{1}{N} \Delta X_{\vec{q}-\vec{k}} \Delta X_{\vec{k}-\vec{q}'}} + \\ 2\left\langle S^z\right\rangle \left(J(\vec{k}-\vec{q}) - J(\vec{q})\right) \overline{\frac{1}{\sqrt{N}} \Delta X_{\vec{q}-\vec{k}} \Delta X_{\vec{k}-\vec{q}}} \overline{\left\langle\left\langle S_{\vec{q}}^+ | S_{\vec{q}'}^-\right\rangle\right\rangle}_E. \end{array} \tag{2.41}$$

So, put this expression into (Eq. 2.37) without the $\overline{\Delta X G}$ term.

$$\begin{array}{l} (E - x\left\langle S^z\right\rangle E_0(\vec{q}))\,\overline{\left\langle\left\langle S_{\vec{q}}^+ | S_{\vec{q}'}^-\right\rangle\right\rangle}_E = 2x\left\langle S^z\right\rangle \delta(\vec{q}+\vec{q}') + \\ 4[\langle S^z\rangle]^2 \delta(\vec{q}+\vec{q}') \sum_{\vec{k}} \frac{J(\vec{q}-\vec{k}) - J(\vec{k})}{E - x\langle S^z\rangle E_0(\vec{q})} \overline{\frac{1}{\sqrt{N}} \Delta X_{\vec{q}-\vec{k}} \Delta X_{\vec{k}-\vec{q}}} + \\ 4[\langle S^z\rangle]^2 \overline{\left\langle\left\langle S_{\vec{q}}^+ | S_{\vec{q}'}^-\right\rangle\right\rangle}_E \sum_{\vec{k}} \frac{(J(\vec{q}-\vec{k}) - J(\vec{k}))(J(\vec{k}-\vec{q}) - J(\vec{q}))}{E - x\langle S^z\rangle E_0(\vec{q})} \overline{\frac{1}{\sqrt{N}} \Delta X_{\vec{q}-\vec{k}} \Delta X_{\vec{k}-\vec{q}}}. \end{array} \tag{2.42}$$

Thus, for the averaged Green function $\overline{\left\langle\left\langle S^+_{\vec{q}}|S^-_{\vec{q'}}\right\rangle\right\rangle}_E$ in the momentum space we eventually get

$$\begin{aligned}
&\overline{\left\langle\left\langle S^+_{\vec{q}}|S^-_{\vec{q'}}\right\rangle\right\rangle}_E = \delta(\vec{q}+\vec{q'})\tfrac{2x\langle S^z\rangle+P(\vec{q};E)}{E-E_0(\vec{q})-\Sigma(\vec{q};E)},\\
&P(\vec{q};E) = \tfrac{1}{N}\textstyle\sum_{\vec{k}}\tfrac{J(\vec{q}-\vec{k})-J(\vec{k})}{E-E_0(\vec{k})}S(\vec{q}-\vec{k}),\\
&\Sigma(\vec{q};E) = \tfrac{1}{N}\textstyle\sum_{\vec{k}}\tfrac{(J(\vec{q}-\vec{k})-J(\vec{q}))(J(\vec{q}-\vec{k})-J(\vec{k}))}{E-E_0(\vec{k})}S(\vec{q}-\vec{k}),
\end{aligned} \tag{2.43}$$

where we have introduced the structure factor for the random distribution of magnetic atoms

$$S(\vec{q}) = [\langle S^z\rangle]^2\overline{\Delta X_{\vec{q}}\Delta X_{-\vec{q}}}. \tag{2.44}$$

Virtual Crystal Approach

This is the simplest approximation for the magnon Green function. If we neglect all scattering processes ($P = 0, \Sigma = 0$) in Eq. (2.43) we obtain the following expression for the magnon Green function:

$$\overline{\left\langle\left\langle S^+_{\vec{q}}|S^-_{\vec{q'}}\right\rangle\right\rangle}_E = \delta(\vec{q}+\vec{q'})\frac{2x\,\langle S^z\rangle}{E-E_0(\vec{q})}. \tag{2.45}$$

Low Quadratic Approximation

The next simple approach for the structure factor $S(\vec{k})$, where is included scattering processes ($P \neq 0, \Sigma \neq 0$), can be obtained applying the cumulant technique (Refs. Edwards and Jones [1971],Matsubara and Yonezawa [1966]). Using of the definition (2.30) of $X_{\vec{k}}$ variables

$$\overline{\Delta X_{\vec{k}}\Delta X_{-\vec{k}}} = \frac{1}{N}\sum_{i,j}e^{\vec{k}(\vec{R}_i-\vec{R}_j)}(\overline{X^M_iX^M_j}-x^2), \tag{2.46}$$

and the cumulant formula for finding the average of the product of X^M_i variables.

$$\overline{X^M_iX^M_j} = \delta_{ij}P_2(x) + [P_1(x)]^2. \tag{2.47}$$

where $P_2(x) = x(1-x), P_1(x) = x$ are second and first cumulants, respectively.

Then, we can use as approximation for the structure factor $S(\vec{k})$.

$$S(\vec{k}) \to S^{eff} = [\langle S^z\rangle]^2(1-x)x. \tag{2.48}$$

It leads to the expression for the magnon Green function of the Low Quadratic Approximation(LQA) of Ref. Dvey-Aharon and Fibich [1978].

$$\begin{aligned}
&\overline{\left\langle\left\langle S^+_{\vec{q}}|S^-_{\vec{q'}}\right\rangle\right\rangle}_E = \delta(\vec{q}+\vec{q'})\tfrac{2x\langle S^z\rangle+S^{eff}\frac{1}{N}\sum_{\vec{k}}P(\vec{k};E)}{E-E_0(\vec{q})-S^{eff}\frac{1}{N}\sum_{\vec{k}}Q(\vec{k};E)},\\
&P(\vec{k};E) = \tfrac{J(\vec{k}-\vec{q})-J(\vec{k})}{E-E_0(\vec{k})}\\
&Q(\vec{k};E) = \tfrac{(J(\vec{k}-\vec{q})-J(\vec{k}))(J(\vec{k}-\vec{q})-J(\vec{q}))}{E-E_0(\vec{k})}.
\end{aligned} \tag{2.49}$$

2.4. Thermodynamics of disorder Heisenberg model

Currently there is no such solid-state theory which would allow the prediction of all properties of a substance from its chemical composition. All phase transformation theories designed for the phase description center on the thermodynamic potential and vary in the form of writing this potential in terms of the theory. Clearly, the extent to which any such theory approaches ideality is determined by the minimum number of phenomenological parameters needed to describe all interparticle interactions.

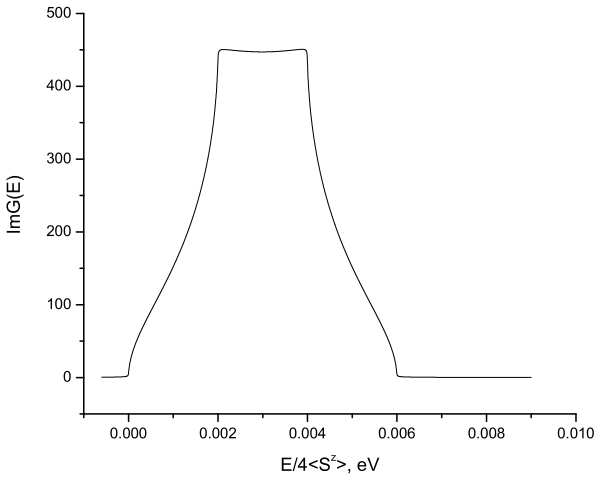

Abbildung 2.3.: The magnetic density of states (DOS) in a simple cubic lattice for the Heisenberg model (Eq. 2.11) for a case only short range interaction $J_1 = 0.001eV$ at $T = 0$, $S = 1/2$.

So, we try to find thermodynamical properties (a dependence of a magnetization on a temperature) of materials without considering a partition function of system. Our theory bases only on a possibility to find a magnetization if we can find the magnetic quasi-particle spectrum of a system. For example, in the case of the regular Heisenberg model we can calculate the Green function $G_{ii}(E) = G(E)$ (Eq. 2.11) and then solving equation (2.19) for $S = 1/2$ or (2.21) for a higher spin we find the dependence of a magnetization on temperature (see. Figs. 2.3,2.4). It is a self-consistency mean field method. For detailed technique about numerical methods of this calculation please see App. A.

Of course, we can use similar technique for the Random Heisenberg model (Eq. 2.23). We calculated first the quasimagnon excitation function $\overline{G_{ij}(E)}$ after the configurational averaging using the Eq. (2.43). And second, we find the dependence of the magnetization on a temperature by solving in self-consistent way the Callen equation (2.21) for magnetization.

For finding the magnon Green function $\overline{G_{ij}(E)}$ for a disordered crystal we must evaluate complicated functions $P(\vec{q}; E)$ and $Q(\vec{q}; E)$ (see. Eq. 2.43) that due with a scattering of magnons on disordered structure of the magnetic

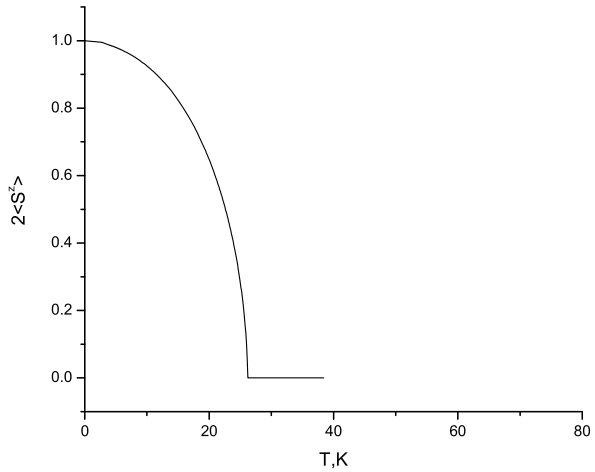

Abbildung 2.4.: The dependence of magnetization on temperature for the Heisenberg model that was obtained from the DOS presented on the Fig. 2.3.

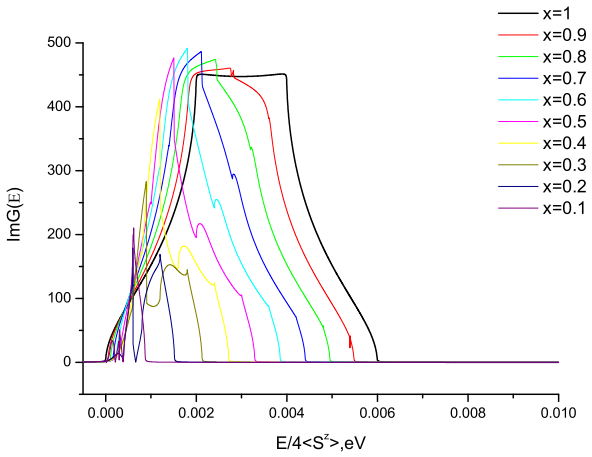

Abbildung 2.5.: Quasiparticle magnon DOS at fixed model parameters $S = 1/2$, $T = 0$ for different values of the concentrations of magnetic atoms x, and additional assumption about magnetic interaction in the crystal lattice $J_1 = 1meV; J_2 = 0.01meV; J_3 = 0.001meV$.

subsystem. For this we used a technique for the standard finite lattice system Lavis and Bell [1999] that is detailed described in App. A.

Other very important aspect of the system is a magnetic interaction J_{ij} in the finite lattice system. In such analytical model like HM we must know a value of J_{ij} or at least a tendency in changing the interaction for a different distance between two atoms in the finite lattice. If this is system with a short-range interaction, like the perovskite manganese oxides, where we can consider only a first shell with an interaction J_1 for nearest-neighbor atoms only (see. Fig. 2.2), or if this is a material which has long-range interaction between

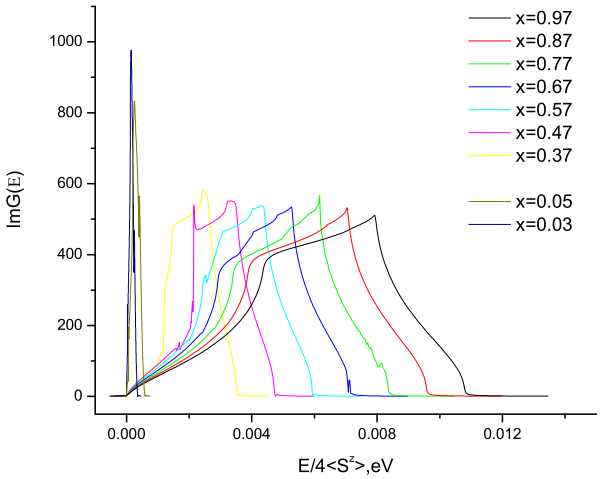

Abbildung 2.6.: Quasiparticle magnon DOS at fixed model parameters $S = 1/2$, $T = 0$ for different values of the concentrations of magnetic atoms x, and additional assumption about magnetic interaction in the crystal lattice $J_1 = 1meV; J_2 = 0.5meV; J_3 = 0.1meV$.

magnetic atoms where is important many shell $J_1, J_2, J_3, J_4, ...$, like in the metallic case $Cu_{1-x}Mn_x$. We propose a self-consistent approximate solution of the HM to get the interconnected electronic and magnetic properties of 'local-moment' systems like diluted ferromagnetic semiconductors. Aiming at $(A_{1-x}M_x)$ compounds, where magnetic (M) and non-magnetic (A) atoms are distributed randomly over a crystal lattice, we present a theory which treats the subsystems of itinerant charge carriers and localized magnetic moments in a homologous manner. The coupling between the localized moments J_{ij} due to the itinerant electrons is treated by a modified RKKY-theory which maps the electronic subsystem onto an effective HM. The exchange integrals turn out to be functionals of the electronic selfenergy guaranteeing selfconsistency of our theory. The disordered electronic and magnetic moment systems are both treated by CPA-type methods. But now, for testing the disorder HM, we show several quasiparticle magnon DOSs at the fixed magnetic interaction in the different shell $J_1, J_2, J_3, ...$ for the finite simple cubic lattice.

In Fig. 2.5 is shown what happens with the quasiparticle magnon DOS for the disorder HM in a regime with short-range interaction. For the magnetic concentration x less than critical percolation $x_c \sim 0.3$ we have the magnon DOS like to two different picks, which are due to different cluster contribution. A ground state of such system is not ferromagnetic. But if we turn on interaction in higher shell $J_2, J_3, ...$ the picture is drastically can change (see Fig. 2.6). If the exchange interaction is increased in the higher shell, which means long-range interaction between two magnetic model in the system, the ferromagnetic state is stabilized even for small concentration x of magnetic atoms. It is that for smaller $x < x_c$ we have a ferromagnetic ground state (see. Fig. 2.7).

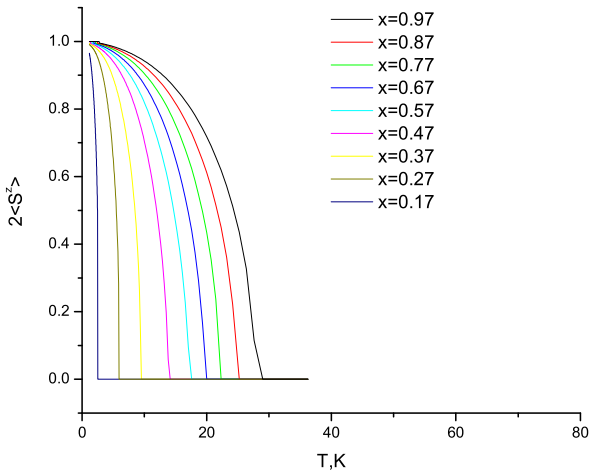

Abbildung 2.7.: The dependence of magnetization on temperature for the disordered HM that was obtained from the DOS presented on the Fig. 2.6

Another important question that can solve our ansatz of finding directly magnetization from Eq. 2.21 without the thermodynamic potential, it is a conclusion about a kind of phase transition from a paramagnetic to ferromagnetic state. Typically for the regular HM, there is a second kind phase transition (see. Fig. 2.7). For a disordered and nonstoichiometric system there are both the second and first kind ones. In our calculation that is based on the disorder HM we can obtain also both kind of phase transition. The kind of phase transition depends on the value and character of the exchange interaction J_{ij} between two atoms in the system.

The important problem of disordered ferromagnetic alloys is also treat the dynamics of the disordered spin system, such as the spin-wave excitations that the system can sustain. In the long-wave limit $\vec{k} \to 0$ its was found for disordered systems an bound to the excitation energy which has the form $D(x)k^2$ where $D(x)$ is a nearly linear function, and also was also found a higher contribution to the energy, like to $\gamma(x)k^3$ which is comparable with the quadratic term. This is a reason of a metastable character of the such system. And a question how to stabilize the ferromagnetic state here is very important for a practical using such alloys.

So, first of all for continuing our ansatz we have to look for a method that can evaluate the exchange interaction J_{ij} in direct space. It will be have done in the next chapter of this thesis.

3. Electronic structure of disorder materials

One of the central issues of basic and applied physics is to understand the relation between the electronic structure or composition of a given material and its different electronic, transport and magnetic properties. The methods that are applied may be either experimental or theoretical, but ultimately only through a combination of both these approaches one can achieve a detail understanding of such a relationship. In experimental situation the specific class of materials are studied within precise measurements of their various physical properties while the same is calculated in theory based on model Hamiltonian by making use of the parameters which are in close proximity to the experimental ones.

In the field of applied solid state theory, out of the various physical properties the calculation of quasi-particle bandstructure of bulk, thin films and surfaces of real substances have always been of great interest since they can be directly compared with experimental studies and can provide a lot of physical insight into the underlying basic mechanism concerning electronic correlation. But for the derivation of the electronic structure one must have already an idea of a relative arrangement of energy levels.

The DMS materials based on III-V and II-VI semiconductors exhibit a very striking correlation between the transport and magnetic properties (see Ref.Jungwirth et al. [2006]). Ideally, each Mn dopant atom represents an acceptor that introduces a local spin and a hole carrier. The ferromagnetism is driven by a charge-carrier mediated mechanism as a consequence of an interband exchange interaction between the localized magnetic moments and the carrier(hole) spins. Experimentally, the Curie temperature T_c of the DMS is enhanced by postgrowth annealing of the samples, which changes positions of defects and the hole concentration Jungwirth et al. [2006]. So the magnetism in the DMS is heavily depending on the impurity (Mn ion) disorder and dilution, carrier concentration and compensation, and the coupling mechanism between the localized Mn spins and the itinerant holes. Therefore, it is very hard to study these materials without some approximations. There are many theoretical approaches attempting to understand DMS physics Zhou et al. [2004], Tang and Nolting [2007], Bryksa and Nolting [2008a], Bouzerar and Bruno [2002], Nolting et al. [2004], Hilbert and Nolting [2004], Kudrnovsky et al. [2004], Bouzerar et al. [2003, 2006a], Subrat and Singh [2005], Singh et al. [2003], Takahashi [2004], Priour and Sarma [2006]. However, the mutual influence of interband-coupling effects and disorder effects with respect to the ferromagnetic phase transition have not been completely understood so far. So we propose first of all to study the ferromagnetic properties of the ideal alloy

$A_{1-x}M_x$ system Tang and Nolting [2007], Bryksa and Nolting [2008a], where A is a non magnetic atom and M is a magnetic atom.

Such an alloy model may exhibit very rich magnetic properties, due to the exchange interaction between localized moments of the magnetic atom M and conduction electron spin in the host of A atoms. For example, in the metallic case $Cu_{1-x}Mn_x$ (many carriers) we can study the Ruderman-Kittel-Kasuya-Yosida(RKKY) interaction and the Kondo effect Mydosh [1993]. In the dielectric case $Ga_{1-x}Mn_xAs$ (few carriers) we have a diluted magnetic semiconductors(DMS) Jungwirth et al. [2006], Potashnik et al. [2002].

The advantage of such theoretical studies as compared to the experimental ones is that the systems are well defined. Therefore, the results are not doubtful because of unwanted effects like impurities, inhomogeneities, etc. Furthermore, in certain cases the theoretical studies provide much more information beyond the reach of experiments. While on the other hand, the biggest drawback is that in almost all cases one has to study idealized systems which have less relation with reality. Since in some cases the above mentioned unwanted effects are very much desirable but due to their complexity it is quite difficult to treat them theoretically. Therefore, an interconnection between experiments and theory is quite important to get a thorough understanding of the new or existing materials.

More or less realistic electronic structure calculations based on density functional theory (DFT) or simulation methods as classical Quantum Monte Carlo investigations for standard models like the Heisenberg Hilbert and Nolting [2004] one were used. However, the disadvantage of the realistic DFT-calculations come from their strong material dependence Kudrnovsky et al. [2004]. Therefore, they do not explain the basic physics of disordered local-moment systems in a simple way. The better results in this respect are obtained from model study of the disordered Kondo lattice.

It is also important to consider short-range and long-range atom distributions as one element of such disorder system. Short-rang order characterizes only the radial atomic distribution, i.e. fluctuations of atomic concentrations in various coordination spheres. In contrast long-range order includes in addition the angular distribution and thus it is possible to determine which atomic species occupies a particular site of the crystal lattice. It is very important to consider short-range order when long-range order is absent i.e. when the mutualarrangement of atoms is correlated. The correlations found relate to the difference in the interaction energies of like and unlike atoms. And the structure of a solid solution, i.e. the mutual arrangement of atoms of different species on crystal lattice sites is described by short-range order parameters.

3.1. Theoretical techniques

As mentioned, a very important aspect of these alloys is the disorder, the magnetic and non-magnetic atoms are distributed randomly over the crystal lattice. The magnetic exchange interactions are to be taken into account for all distances between the different moments. This defines an effective Heisenberg

model for the magnetic moments. The concentration x controls the average distance between two magnetic atoms. On the other hand, the effective Heisenberg interaction also depends on x. The same holds for interband-coupling effects Nolting et al. [1996b], Liechtenstein et al. [1987]. Both effects are important for understanding the ferromagnetic transition in such component Tang and Nolting [2007], Bryksa and Nolting [2008a].

The most developed approach for incorporation of the carrier disorder is the coherent potential approximation Matsubara and Yonezawa [1966], Elliott et al. [1974], Bouzerar and Bruno [2002], Takahashi [2004], Tang and Nolting [2007], Nolting et al. [2001, 2004], Bryksa and Nolting [2008a]. However, there are many indications that this method is not sufficient for the explanation of certain properties of the disordered ferromagnetic semiconductors Elliott et al. [1974], Butler [1972]. For example, the CPA does not incorporate the electron scattering on the crystal field fluctuations, which are important and can change the Curie temperature very drastically Jungwirth et al. [2006]. One attempt of treating the crystal field fluctuation in the DMS systems using numerical simulation for finite systems has recently been used in ref. Bouzerar et al. [2006b]. However, the authors use only the effect of chemical substitution that accompanies the presence of the magnetic atom.

A special challenge when treating the random Kondo-lattice model arises with the fact that both the electron and the spin subsystem have to be considered simultaneously and on the same level. Most of the KLM investigations are focused on the electronic Takahashi [2004], Blackman et al. [1971] or magnetic Theumann and Tahir-Kheli [1975], Dvey-Aharon and Fibich [1978], Harris et al. [1974], Bouzerar and Bruno [2002], Hilbert and Nolting [2004], Bouzerar et al. [2006a] subsystem only. A special goal of our study is the homologous treatment of the electronic and magnetic properties of the random KLM, which mutually condition each other and, therefore, should be determined self-consistently.

Nevertheless, we are forced to apply different methods to study the influence of the disorder and dilution of the magnetic moments subsystem on the properties of these two aforementioned subsystems. For the itinerant electron system a proper alloy analogy with the respective coherent potential approximation (CPA) Elliott et al. [1974] may be used. For the random spin system, for which the situation is not so clear, an equivalent ansatz must be found. As it was done successfully for the periodic KLM Nolting et al. [1996b] (*'modified' RKKY (MRKKY)*) one can map the KLM-interband exchange on an effective and random Heisenberg model. The resulting effective exchange integrals between the localized spins will be long range and complicated functionals of the electronic self-energy. The conventional RKKY, resulting from second order perturbation theory may be insufficient even with a phenomenological damping factor Kudrnovsky et al. [2004], Bouzerar et al. [2006a]. Higher order conduction electron self-energy effects, being taken into account by *'modified' RKKY* but neglected by conventional $RKKY$, provide the self-consistency of the full KLM. They drastically influence the magnetic properties such as the Curie temperature.

3.2. Theoretical Model

The correlated KLM-Hamiltonian can be written in second quantized form as the sum of a kinetic energy, an exchange interaction, and a Hubbard-type Coulomb interaction

$$\hat{H}^K = \sum_{i,j,\sigma} t_{ij} a^+_{i\sigma} a_{j\sigma} + \frac{U}{2} \sum_{i\sigma} n_{i\sigma} n_{i,-\sigma} - \frac{J}{2} \sum_{i\sigma} \left\{ z_\sigma S^z_i a^+_{i\sigma} a_{i\sigma} + S^\sigma_i a^+_{i,-\sigma} a_{i\sigma} \right\}, \quad (3.1)$$

with abbreviations

$$z_\sigma = \delta_{\sigma\uparrow} - \delta_{\sigma\downarrow}, S^\sigma_i = S^x_i + i z_\sigma S^y_i. \quad (3.2)$$

$a^+_{i\sigma}$ ($a_{i\sigma}$) is the creation (annihilation) operator for the Wannier electron with the spin σ ($\sigma = \uparrow, \downarrow$) at the site $\vec{R}_i$, J is an exchange coupling , t_{ij} is an electron hopping integral between lattice sites, U is the Coulomb interaction, and N is the total number of crystal sites.

In order to introduce the disorder into KLM of the $A_{1-x}M_x$ type, we introduce projection operators

$$X^A_i = \begin{cases} 1, & \text{- } \textit{if site } i \textit{ is } A \\ 0, & \text{- } \textit{otherwise,} \end{cases} \quad (3.3)$$

$$X^M_i = \begin{cases} 1, & \text{- } \textit{if site } i \textit{ is } M \\ 0, & \text{- } \textit{otherwise.} \end{cases} \quad (3.4)$$

Using these definitions we can change the notations in the Hamiltonian (3.1) for the disorder in hopping and exchange coupling terms, respectively:

$$\begin{array}{c} t_{ij} \to \sum_{k,\acute{k} \in A,M} t^{k\acute{k}} X^k_i X^{\acute{k}}_j, \\ J \to \sum_{k \in A,M} J^k X^k_i, \end{array} \quad (3.5)$$

where top indices are $k, \acute{k} \in A, M$, hopping parameters $t^{AA} = t^{MM} = t^{AM} = t^{MA} = t = W/6$ are the same for the different kind of atoms and are equivalent to a half band width W for the case of a simple cubic lattice, and exchange couplings are $J^M = J, J^A = 0$ for magnetic and nonmagnetic atoms, respectively.

After configurational averaging these operators are simply expressed by the concentration x of magnetic atoms M.

$$\begin{array}{l} \left\langle X^A_i \right\rangle_c = 1 - x, \\ \left\langle X^M_i \right\rangle_c = x. \end{array} \quad (3.6)$$

To study conduction-electron properties, we use the configurationally averaged single-electron Green function

$$G_{ij\sigma}(E) = \overline{\left\langle\left\langle a_{i\sigma} | a^+_{j\sigma} \right\rangle\right\rangle_E}. \quad (3.7)$$

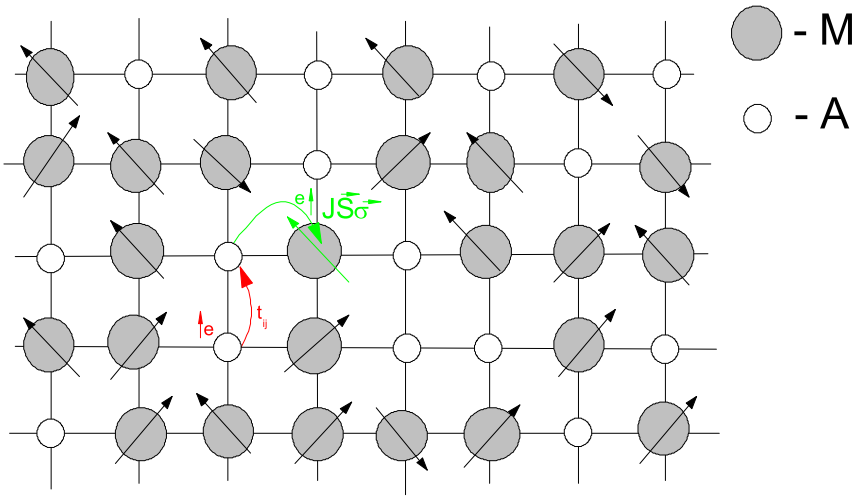

Abbildung 3.1.: There is a schematic presentation of the the disordered Kondo-lattice model.

The relation between the band occupation n and the chemical potential μ is as follows:

$$n = n_\uparrow + n_\downarrow = -\frac{1}{\pi}\sum_\sigma \int_{-\infty}^{\infty} \frac{ImG_{ii,\sigma}(E)}{e^{\beta(E-\mu)}+1} dE, \tag{3.8}$$

with $\beta = 1/kT$ is the inverse temperature.

The main idea of this paper is to map the disordered KLM on an effective random spin Heisenberg Hamiltonian:

$$\hat{H}^{RH} = -\frac{1}{2}\sum_{ij} J_{ij} X_i^M X_j^M \left(S_i^z S_j^z + S_i^+ S_j^-\right), \tag{3.9}$$

where J_{ij} is an effective interaction between localized magnetic moments. If we assume that we can calculate the effective interaction J_{ij} using the MRKKY method Nolting et al. [1996b, 2001], Nolting and Oles [1980]

$$J_{\vec{q}} = \frac{I^2}{4\pi}\int_{-\infty}^{\infty} \frac{dE}{e^{\beta(E-\mu)}+1} \frac{1}{N}\sum_{\sigma,\vec{k}} Im\left[G^0_{\vec{k}}(E)\, G_{\vec{k}+\vec{q},\sigma}(E)\right], \tag{3.10}$$

where $J_{\vec{q}}$ is the Fourier-transform of J_{ij}, then we get the full self-consistent loop for a finite temperature calculation (see next chapter). Now we discuss these approximations in more detail.

3.2.1. Electron Subsystem: Zero-bandwidth limit of the correlated KLM

The total Hamiltonian of the correlated KLM model is given by (3.24).

The zero-bandwidth limit Nolting and Oles [1980] is defined by

$$t_{ij} \to 0. \tag{3.11}$$

In this approximation the excitation spectrum consists of the following four poles

$$\begin{array}{ll} \epsilon_1 = -\frac{1}{2}JS, & \epsilon_2 = \frac{1}{2}J\left(S+1\right), \\ \epsilon_3 = U + \frac{1}{2}JS, & \epsilon_4 = U - \frac{1}{2}J\left(S+1\right). \end{array} \tag{3.12}$$

It means that the single electron spectral density $A_\sigma\left(E\right)$ must be a four-pole function

$$A_\sigma\left(E\right) = \sum_{m=1}^{4} \alpha_{m\sigma}\delta\left(E - \epsilon_m\right). \tag{3.13}$$

The temperature- and concentration-dependent coefficients $\alpha_{m\sigma}$ have the physical meaning of spectral weights for the corresponding excitation energies. The expressions for these weight-factors are Nolting and Oles [1980]:

$$\begin{array}{l} \alpha_{1\sigma} = \frac{1}{2S+1}\left(S + 1 + z_\sigma\left\langle S^z\right\rangle - \left(S+1\right)n_{-\sigma} + \Delta_{-\sigma}\right), \\ \alpha_{2\sigma} = \frac{1}{2S+1}\left(S - z_\sigma\left\langle S^z\right\rangle - Sn_{-\sigma} - \Delta_{-\sigma}\right), \\ \alpha_{3\sigma} = \frac{1}{2S+1}\left(\left(S+1\right)n_{-\sigma} + \Delta_{-\sigma}\right), \\ \alpha_{4\sigma} = \frac{1}{2S+1}\left(Sn_{-\sigma} - \Delta_{-\sigma}\right), \end{array} \tag{3.14}$$

where $\Delta_\sigma = \left\langle S^\sigma a^+_{-\sigma}a_\sigma\right\rangle + z_\sigma\left\langle S^z n_\sigma\right\rangle$ is a mixed spin-electron correlation function.

The term Δ_σ can be expressed by the single-electron Green function Nolting [1979]:

$$\Delta_\sigma = -\frac{1}{\pi}\frac{1}{N}\sum_{\vec{k}}\int \frac{dE}{e^{\beta(E-\mu)}+1}\left(E - t_{\vec{k}}\right) ImG_{\vec{k}\sigma}\left(E\right). \tag{3.15}$$

A propagating σ electron will meet at a certain lattice site $\vec{R}_i$ the atomic level ϵ_1 with probability $\alpha_{1\sigma}$, the level ϵ_2 with probability $\alpha_{2\sigma}$ and so on, if there is no correlation between sites. This leads to the four-component alloy.

It is easy to generalize this alloy analogy to a disordered KLM. We have to take into consideration as the fifth alloy constituent the non-magnetic sites $\epsilon_5 = \epsilon_A$ with the spectral weight $1 - x$. The excitation spectrum is then:

$$\begin{array}{lll} \epsilon_m & \to & \tilde{\alpha}_{m\sigma} = x\alpha_{m\sigma}, \\ \epsilon_5 = 0 & \to & \tilde{\alpha}_{5\sigma} = 1 - x. \end{array} \tag{3.16}$$

This zero-bandwidth alloy analogy is the frame for applying CPA to get the electron selfenergy.

$$\Sigma_\sigma(E) = \sum_{m=1}^{5} \tilde{\alpha}_{m\sigma}\frac{\epsilon_m}{1 - (\epsilon_m - \Sigma_\sigma(E))G_0(E - \Sigma_\sigma(E))}. \tag{3.17}$$

Therewith we can write the electron Green function:

$$G_{\vec{k},\sigma}(E) = \frac{1}{E - \Sigma_\sigma(E) - t_{\vec{k}}}, \tag{3.18}$$

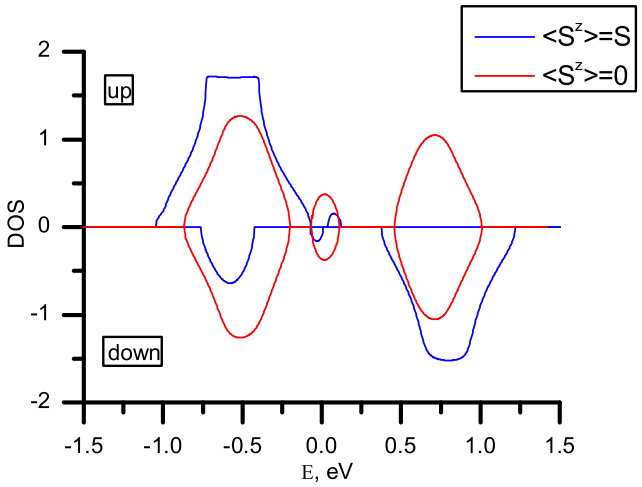

Abbildung 3.2.: Density of electron states for the disordered KLM at $x = 0.95$, $U = \infty$, $n = 0.06$, $S = 5/2$, $J = 0.4$ for ferromagnetic $\langle S^z \rangle = S$ and paramagnetic $\langle S^z \rangle = 0$ cases

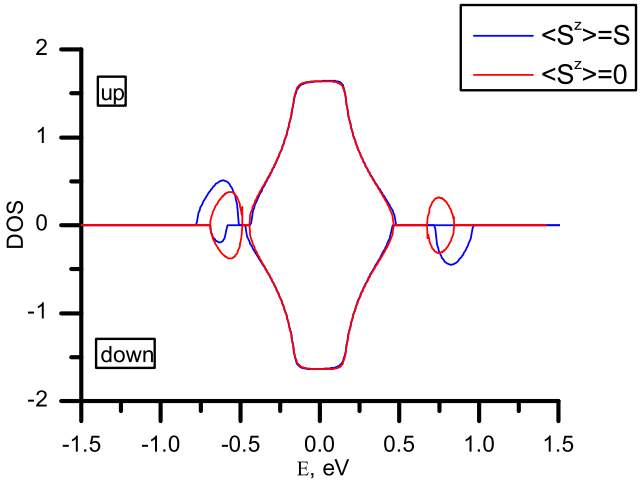

Abbildung 3.3.: Density of electron states for the disordered KLM at $x = 0.1$, $U = \infty$, $n = 0.06$, $S = 5/2$, $J = 0.4$ for ferromagnetic $\langle S^z \rangle = S$ and paramagnetic $\langle S^z \rangle = 0$ cases

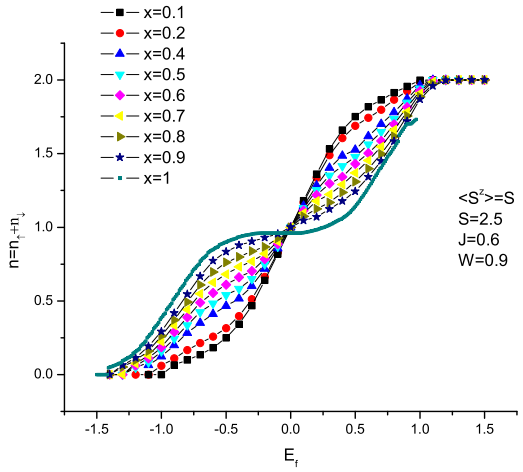

Abbildung 3.4.: Dependence of the total band occupation $n_\uparrow + n_\downarrow$ on the position of the Fermi edge at $T = 0$, $S = 5/2$, $J = 0.6$, $W = 0.9$ for a different value of concentration of the magnetic atoms.

where $t_{\vec{k}}$ is the Fourier transform of the hopping integral t_{ij}. The quasiparticale density of states (DOS) is derived essentially from imaginary part of the Green function:

$$\rho_\sigma(E) = -\frac{1}{\pi N} \sum_{\vec{k}} ImG_{\vec{k},\sigma}(E). \tag{3.19}$$

Fig. 3.2 and Fig. 3.3 present the quasiparticale density of states for large and small concentrations x of A atoms in full saturation $\langle S^z \rangle = S$ and paramagnetic $\langle S^z \rangle = 0$ limits, respectively. In the case of strong Coulomb interaction($U \to \infty$), the DOS consists in general of three subbands. For $\langle S^z \rangle = S(T = 0)$ the spin up electron density is absent for energies around $J(S + 1)/2$, while the spin down density is finite there.

A very interesting quality of the atomic limit approximation is a dependence of the DOS on the total band occupation n (see Fig. (3.4,3.5)). This property is important special for a high band occupation ($n > 0.2$). But for such regime is also important to include the Coulomb interaction, which is not considered here. First of all, we are interested in the exchange ferromagnetic interaction between localized magnetic moments with a free electron spin and an influence of disorder on this interaction but not the itinerant band-ferromagnetism. This is a reason why we don't consider the Coulomb interaction. Another reason why we didn't include Coulomb interaction because we are interested to consider such disorder system for only the small band occupation regime which is a more suitable for an explanation of the ferromagnetic properties of semiconductor materials.

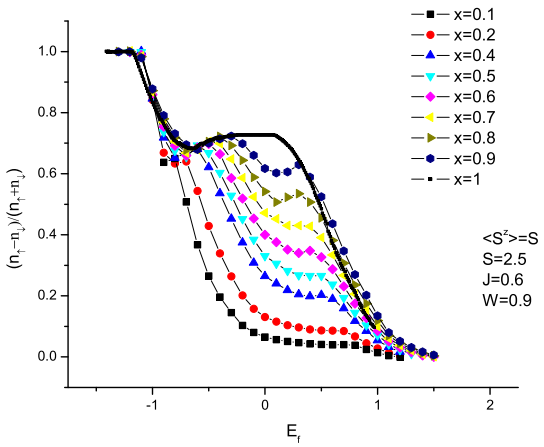

Abbildung 3.5.: Dependence of the electron polarization on the position of the Fermi edge at $T = 0$, $S = 5/2$, $J = 0.6$, $W = 0.9$ for a different value of concentration of the magnetic atoms.

3.2.2. Electron Subsystem: Interpolating self-energy approach

The electronic part of the many-body problem is solved as soon as the single-electron Green function $G_{\vec{k},\sigma}(E)$ is available. For this electron propagator we have the Dyson equation:

$$G_{\vec{k},\sigma}(E) = \frac{1}{E - t(\vec{k}) - \Sigma_\sigma(E)}, \tag{3.20}$$

where the self-energy $\Sigma_\sigma(E)$ describes the electronic properties of the itinerant electron subsystem.

The approximate expression for the electronic self-energy $\Sigma_\sigma(E)$ of the low-density KLM using here is the following:

$$\begin{aligned}
&\Sigma_\sigma^{ISA}(E) = -\tfrac{1}{2} J z_\sigma \langle S^z \rangle + \tfrac{1}{4} J^2 \frac{a_\sigma G_0(E - \frac{1}{2} J z_\sigma \langle S^z \rangle)}{1 - \frac{1}{2} J G_0(E - \frac{1}{2} J z_\sigma \langle S^z \rangle)}, \\
&G_0(E) = \tfrac{1}{N} \textstyle\sum_{\vec{k}} \frac{1}{E - \epsilon(\vec{k})}, \\
&a_\sigma = S(S+1) - z_\sigma \langle S^z \rangle (z_\sigma \langle S^z \rangle + 1), \\
&z_\sigma = \delta_{\sigma\uparrow} - \delta_{\sigma\downarrow}.
\end{aligned} \tag{3.21}$$

This result fulfills the zero-bandwidth limit for all temperatures T and arbitrary coupling strengths J, as well as the exact $T = 0$ result for arbitrary bandwidths and couplings(Ref. Nolting et al. [2001]). Exact high-energy expansions help to fix the parameters a_σ.

In the diluted ferromagnetic alloy $A_{1-x}M_x$ we can use a standard CPA formalism Nolting [2005] for finding the electronic selfenergy in diluted system

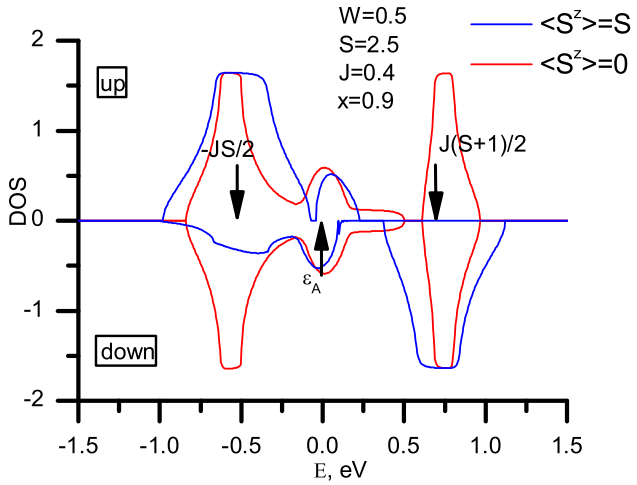

Abbildung 3.6.: Density of electron states for the disordered KLM at $x = 0.9$, $S = 5/2$, $J = 0.4$ for ferromagnetic $\langle S^z \rangle = S$ and paramagnetic $\langle S^z \rangle = 0$ cases

$\Sigma_\sigma^{dis}(E)$:

$$0 = (1-x)\frac{-\Sigma_\sigma^{dis}(E)}{1+G_\sigma(E)\Sigma_\sigma^{dis}(E)} + x\frac{\Sigma_\sigma^{ISA}(E)-\Sigma_\sigma^{dis}(E)}{1-G_\sigma(E)(\Sigma_\sigma^{ISA}(E)-\Sigma_\sigma^{dis}(E)}. \qquad (3.22)$$

The limiting cases $x = 0(\Sigma_\sigma^{dis}(E) = 0)$ and $x = 1(\Sigma_\sigma^{dis}(E) = \Sigma_\sigma^{ISA}(E))$ are obviously fulfilled for the non-magnetic system and the concentrated KLM, respectively. It means that the local self-energy is approximately negligible for non-magnetic atoms($k = A$), and contains two electron spin scattering parts(Ising and spin-flip parts) for magnetic atoms ($k = M$).

The single-particle properties can then be derived from the propagator:

$$G_\sigma(E) = \frac{1}{N}\sum_{\vec{k}}\frac{1}{E - t(\vec{k}) - \Sigma_\sigma^{dis}(E)} = \int_{-\infty}^{\infty}\frac{\rho_0(\epsilon)}{E-\epsilon-\Sigma_\sigma^{dis}(E)}d\epsilon, \qquad (3.23)$$

where $\rho_0(\epsilon)$ is the Bloch-density of the non-interacting electrons.

In the Fig. (3.6,3.7) are showed the DOS for the same parameters as are for the atomic limit on the Fig. (3.2,3.3).

So, now we can compare these two approximations: the atomic alloy analogy and the Interpolating self-energy approach (ISA) ones. First of all the ISA approach is valid for a low band occupation n and the DOS don't depend on the last. There is also valid the spin-polaron limit which means that for the full spin saturation case the DOS of the down spin electrons is not zero at any Fermi position in the first correlated sub-band of the up electron Green function (Fig. 3.7). In the atomic alloy analogy approach (Fig. 3.3) there is a some critical value of the Fermi position till which the DOS of the down spin

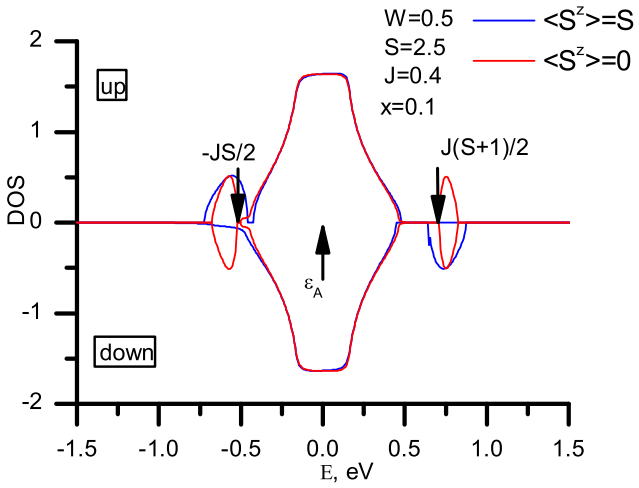

Abbildung 3.7.: Density of electron states for the disordered KLM at $x = 0.1$, $S = 5/2$, $J = 0.4$ for ferromagnetic $\langle S^z \rangle = S$ and paramagnetic $\langle S^z \rangle = 0$ cases.

electrons is zero. This situation with the spin polaron limit is a very important and special for the disordered system. For a finite temperature the spin polaron states start to destroy drastically and the both models predict approximately the same properties of the electron Green function.

3.3. Electron Subsystem: Cluster CPA treatment

The Hamiltonian of the disordered Kondo-lattice model (KLM) for the $A_{1-x}M_x$ alloy can be written in second quantized form as a sum of a kinetic energy, an exchange interaction, and a crystal field energy:

$$\hat{H} = \sum_{i,j,\sigma} t_{ij} a^+_{i\sigma} a_{j\sigma} + \sum_i \hat{H}_i, \tag{3.24}$$

where the single site part $\hat{H}_i$ has the following form;

$$\hat{H}_i = \sum_{\sigma} \epsilon_i n_{i\sigma} + \sum_{\sigma,\acute{\sigma}} J_i (\vec{S}_i \vec{\sigma})_{\sigma\acute{\sigma}} a^+_{i\sigma} a_{i\acute{\sigma}} + \sum_{\sigma} \delta L_i n_{i\sigma}. \tag{3.25}$$

$a^+_{i\sigma}$ ($a_{i\sigma}$) is the creation (annihilation) operator for the Wannier electron with the spin σ ($\sigma = \uparrow, \downarrow$) at the site $\vec{R}_i$. In order to introduce the disorder into the $A_{1-x}M_x$ KLM, we introduce projection operators $X^k (k = A, M)$(Eq. 3.3,3.4).

The energy and exchange coupling constants are written as:

$$\begin{aligned} \epsilon_i &= \textstyle\sum_{k \in A,M} \epsilon^k X^k_i, \\ J_i &= \textstyle\sum_{k \in A,M} J^k X^k_i, \end{aligned} \tag{3.26}$$

where chemical energy parameters $\epsilon^A = \epsilon^M = 0$ are equivalent, and exchange couplings are $J^M = J, J^A = 0$ for magnetic and nonmagnetic atoms, respectively.

The crystal field energy is given by;

$$\begin{array}{c} \delta L_i = \sum_{k\in A,M} \sum_{l\in A,M} \sum_{j\neq i} X_i^k \lambda_{ij}^{kl} X_j^l, \\ \lambda_{ij}^{kl} = \int \varphi_{ki}^*(\vec{r}) U_l(\vec{r} - \vec{R}_j) \varphi_{ki}(\vec{r}) d\vec{r}, \end{array} \tag{3.27}$$

where the $U_l(\vec{r} - \vec{R}_j)$ term is the potential energy of the electron at the point $\vec{r}$ near the site defined by the radius-vector $\vec{R}_j$. The cluster wave functions φ_{ki} are constructed from the atomic functions of an i-site of k type.

The transfer matrix is written as

$$t_{ij} = \sum_{k,\acute{k}\in A,M} t^{k\acute{k}} X_i^k X_j^{\acute{k}}, \tag{3.28}$$

where hopping parameters $t^{AA} = t^{MM} = t^{AM} = t^{MA} = t$ are the same for the different kind of atoms and $6t = W$, where W is the half band width of a free electron band for the case of simple cubic lattice.

Rewrite the Hamiltonian (3.24) to the form of

$$\hat{H} = \hat{H}_0 + \hat{H}_{int}, \tag{3.29}$$

where the $\hat{H}_0$ term represents a singe site part and $\hat{H}_{int}$ is an interaction part

$$\hat{H}_{int} = \sum_{\sigma} \delta L_i \tilde{a}_{i\sigma}^+(\tau) \tilde{a}_{j\sigma}(\tau) + \sum_{i,j,\sigma} t_{ij} \tilde{a}_{i\sigma}^+(\tau) \tilde{a}_{j\sigma}(\tau). \tag{3.30}$$

The operator is given by

$$\tilde{a}_{j\sigma}(\tau) = e^{\imath\tau\hat{H}_0} a_{j\sigma} e^{-\imath\tau\hat{H}_0}. \tag{3.31}$$

In order to find the Green's function the average like the

$$\langle ... \rangle_a = Z^{-1}(X) Tr_a(...e^{-\beta\hat{H}}) \tag{3.32}$$

has to be calculated (Ref. Zubarev [1960], Nolting [2005]). The technique similar to that developed in Ref. Matsubara and Yonezawa [1966], Elliott et al. [1974] is used for calculation of the Green's function

$$G_{ij\sigma}(\tau) = -\langle T_\tau \tilde{a}_{j\sigma}(0) \tilde{a}_{i\sigma}^+(\tau) \rangle_a = -\langle \sigma(\beta, X) \rangle_{0a}^{-1} \langle T_\tau \tilde{a}_{j\sigma}(0) \tilde{a}_{i\sigma}^+(\tau) \sigma(\beta, X) \rangle_{0a}, \tag{3.33}$$

with

$$\sigma(\beta, X) = T_\tau exp\{-\int_0^\beta \hat{H}_{int}(\tau) d\tau\}, \tag{3.34}$$

and where $\tilde{a}_{j\sigma}$,$\tilde{a}_{i\sigma}^+$ are written in the interaction presentation, and the average $\langle ... \rangle_0$ is done with the $\hat{H}_0$ hamiltonian (Ref. Nolting [2005]).

In the equations (3.32,3.33) we write in the partion function also the X variables, because this microscopic Green function depends on them. By using

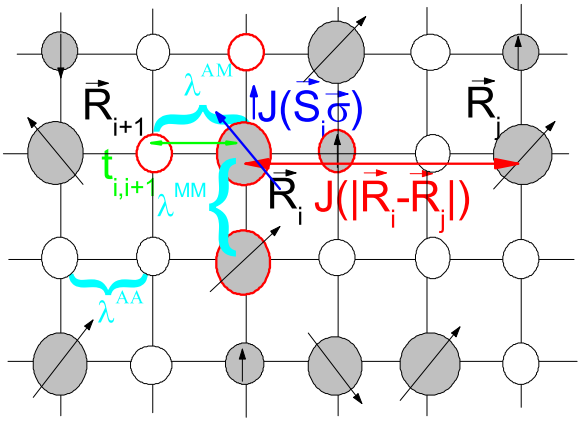

Abbildung 3.8.: Schematic picture of the lattice and the electron processes.

the same technique of the configurational average which was done previously in the section (2.3) we have to rewrite the equation for the Green function (3.33).

So, after configurational averaging procedure X operators are simply expressed by the concentration x of magnetic atoms M.

$$\begin{aligned} \overline{\langle X_i^A \rangle} &= 1 - x, \\ \overline{\langle X_i^M \rangle} &= x. \end{aligned} \tag{3.35}$$

And to study conduction-electron properties, we use the configurationally averaged single-electron Green function Matsubara and Yonezawa [1966], Elliott et al. [1974]

$$G_{ij\sigma}(E) = \overline{\left\langle\left\langle a_{i\sigma} | a_{j\sigma}^{+} \right\rangle\right\rangle_E}, \tag{3.36}$$

where the symbol $\overline{(\ldots)}$ is the configurational ensemble average (Eq. 2.34).

Since the introduction of diagrammatic notation by Edwards (Ref. Edwards [1958]) for classifying and collecting the terms in the perturbation expansion of the electronic properties of alloys, many authors have extensively used such diagrams to study many properties of disordered systems (Ref. Elliott et al. [1974]), and they have been useful in seeing what sorts of scattering are physically important.

We shall use this method to obtain the CPA equations as a self-consistent scattering problem, but shall begin our description by writing the series of diagrams for the Green function (Eq. 3.33) before the configurational ensemble average procedure (Eq.3.36). For the alloy $A_{1-x}M_x$, the perturbations are the interatomic hopping t_{ij} and crystal field coupling δL_i (see. Eqs.3.29,3.30). If the Green function (Eq. 3.33) expands the $\sigma(\beta, X)$ in the power series with respect to this interaction, using the Hubbard-I approximation (Refs. Izyumov [1995, 1997], the graphical equation for the Green's function can be written

follows:

$$\left\langle\left\langle a_{i\uparrow}|a^{+}_{j\uparrow}\right\rangle\right\rangle_{E} =$$

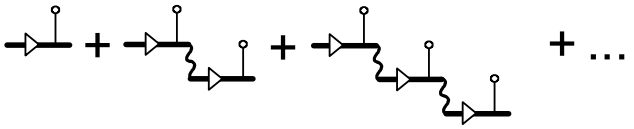

(3.37)

where every horizontal line is already renormalized by the crystal field effects in the following manner:

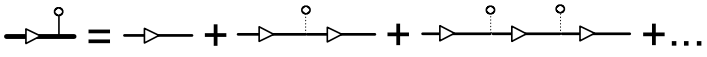

(3.38)

The graphical symbols refer to:

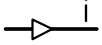

$$\equiv \delta_{ij} g_{i\uparrow}(E) = \delta_{ij} \sum_{k} g^{k}_{i\uparrow}(E) X^{k}_{i} \tag{3.39}$$

the local electron propagator near the site i for the spin $\uparrow$;

$$\equiv \delta L_i \tag{3.40}$$

the crystal field perturbation on the site i from the neighbor atoms;

$$\equiv t_{ij} \tag{3.41}$$

the transfer matrix between two neighbor sites i and j.

An open arrow (full arrow) on the horizontal electron line means an electron with spin up (down). The same we can write down for the $\downarrow$ Green function $\left\langle\left\langle a_{i\downarrow}|a^{+}_{j\downarrow}\right\rangle\right\rangle_{E}$. The hopping and crystal field perturbations don't change the spin quantum number σ in the electron scattering.

For the electron local propagator $g^{k}_{i\sigma}(E)$ we have the Dyson equation:

$$g^{k}_{i\sigma}(E) = \frac{1}{E - \epsilon^{k} - \Sigma^{k}_{\sigma}(E)}, \tag{3.42}$$

where the self-energy $\Sigma^{k}_{\sigma}(E)$ describes the electronic properties of the itinerant electron subsystem in the diluted ferromagnetic alloy $A_{1-x}M_x$. The local self-energy is almost negligible for non-magnetic atoms ($k = A$), and contains two electron spin scattering parts(Ising and spin-flip parts) for magnetic atoms ($k = M$). The local electronic self-energy $\Sigma^{k}_{\sigma}(E)$ becomes the central quantity of the many-body problem. For finite temperatures and arbitrary band occupations, an exact expression of $\Sigma^{k}_{\sigma}(E)$ is not available and one needs to apply an approximation. In this paper, we use the interpolating self-energy ap-

proach (ISA) Nolting et al. [2001], which results in a wave-vector independent self-energy $\Sigma_\sigma^k(E)$, and is already used in (3.21).

$$\Sigma_\sigma^k(E) = \begin{cases} 0, & \text{if } k = A \\ \Sigma_\sigma^{ISA}(E), & \text{if } k = M \end{cases} \tag{3.43}$$

After summation the set of diagrams (3.38) reduces to the electron local propagator renormalized by the crystal field effect;

$$\begin{aligned} &= \delta_{ij} g_{i\uparrow}(E) + \delta_{ij} g_{i\uparrow}(E) \textstyle\sum_m \delta L_m \delta_{mj} g_{m\uparrow}(E) + \\ &\delta_{ij} g_{i\uparrow}(E) \textstyle\sum_m \delta L_m \delta_{mn} g_{m\uparrow}(E) \sum_n \delta L_n \delta_{nj} g_{n\uparrow}(E) + ... \\ &= \delta_{ij} \textstyle\sum_k \frac{X_i^k}{[g_{i\uparrow}^k(E)]^{-1} + \delta L_i^k} \end{aligned} \tag{3.44}$$

In order to perform the averaging over the X operator or the configurational average in the Green function $\left\langle\left\langle a_{i\sigma} | a_{j\sigma}^+ \right\rangle\right\rangle_E$ (Eq. 3.36) or any other functions (Eq. 2.34) the density operator $\hat{\rho_X}$ can be written as

$$\hat{\rho_X} = \prod_i \rho_X^i = \prod_i [(1-x) X_i^A + x X_i^M]. \tag{3.45}$$

We can check that this function is normalezed for one

$$Tr_X(\hat{\rho_X}) = (1-x) Tr_X(X_i^A) + x Tr_X(X_i^M) = 1. \tag{3.46}$$

So now, for example, using this density operator, one gets the averaged $\left\langle X_i^k \right\rangle$ operators in more detail and then the electron local propagator $\langle g_{\sigma i} \rangle_X$ also:

$$\begin{aligned} &\left\langle X_i^A \right\rangle_X = Tr_X(X_i^A \hat{\rho}_X) = Tr_X(X_i^A \textstyle\prod_l [(1-x) X_l^A + x X_l^M]) = \\ &(1-x) Tr_X([X_i^A]^2) = 1 - x, \end{aligned} \tag{3.47}$$

$$\begin{aligned} &\left\langle X_i^M \right\rangle_X = Tr_X(X_i^M \hat{\rho}_X) = Tr_X(X_i^M \textstyle\prod_l [(1-x) X_l^A + x X_l^M]) = \\ &x Tr_X([X_i^M]^2) = x. \end{aligned} \tag{3.48}$$

Here we used the following properties of the X operators:

$$X_i^k X_j^m = \delta_{ij} \delta k m X_i^k, \tag{3.49}$$

where $k, m = A, M$.

And the same for the first diagram in the Eq. (3.38) by using the Eq. (3.39):

$$\langle g_{\sigma i} \rangle_X = Tr_X(g_{\sigma i} \hat{\rho}_X) = (1-x) g_{\sigma i}^A + x g_{\sigma i}^M. \tag{3.50}$$

For averaging of the Green's function (Eq. 3.37), we use the standard cumulant decompositions Matsubara and Yonezawa [1966], Elliott et al. [1974] (see also appendix B). The cumulants of two random variables $g_{\sigma i}$, δL_i are defined

by

$$S^{\sigma}(\zeta_1;\zeta_2) = \left\langle e^{\zeta_1 g_{\sigma i}+\zeta_2 \delta L_i}\right\rangle_X = exp(\sum_{n,m;n+m>0} \frac{[\zeta_1]^n[\zeta_2]^m}{n!m!} M^{\sigma}_{nm}), \tag{3.51}$$

where ζ_1, ζ_2 are infinitesimal variables.

From that it follows the cumulant expression Matsubara and Yonezawa [1966];

$$M^{\sigma}_{nm} = \frac{\partial^n}{\partial\zeta_1^n}\frac{\partial^m}{\partial\zeta_2^m} S^{\sigma}(\zeta_1 \to 0;\zeta_2 \to 0). \tag{3.52}$$

In the graphical presentation, the cumulant is shown as oval near given site. For example, the first electron cumulant near one local electron line $g_{\uparrow i}$, and one crystal field point δL_i and the second electron cumulant near two local electron lines gathers one and two separate parts, respectively:

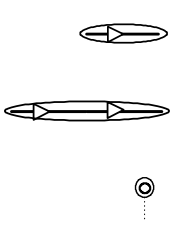

$$\equiv M^{\uparrow}_{10} = (1-x)g^A_{\sigma i} + x g^M_{\sigma i}$$

$$\equiv M^{\uparrow}_{20} = -(M^{\uparrow}_{10} - g^A_{\uparrow i})(M^{\uparrow}_{10} - g^M_{\uparrow i}) \tag{3.53}$$

$$\equiv M^{\uparrow}_{01} = M^{\downarrow}_{01} = \langle \delta L_i \rangle_X .$$

We also show the configurational average procedure the first two diagrams in the electron Green function in the Eq. 3.37.

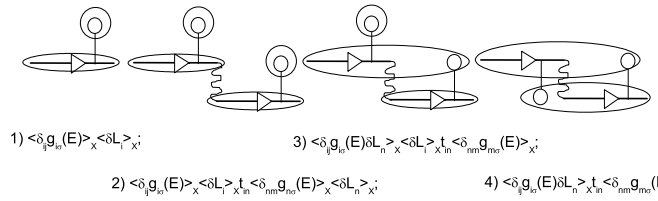

(3.54)

In this study we consider solely the diagrams for which the configuration averaging embraces the electron propagators and the crystal field separately. And it means that we neglect contributions like to diagrams 3),4) in the Eq. (3.54). Such averaging is equivalent to the statement of the coherent potential to be independent of the crystal field. The local Green's functions (3.38) become renormalized by crystal field, but new poles do not arise. Therefore, it is appropriate to introduce a special notation of such renormalized Green's function (first diagram in the expression (3.37));

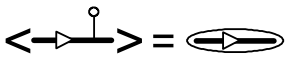

$$\equiv \delta_{ij}\sum_k \left\langle \frac{1}{[g^k_{\sigma i}(E)]^{-1} - \delta L^k_i}\right\rangle^{crys} X^k_i, \tag{3.55}$$

where $\langle ... \rangle^{crys}$ means an average procedure over atom configurations on other nodes than i. The configuration averaging of each vertical lines in (3.38,3.55) can be performed in different ways Gusev et al. [2001], Ziman [1979] but in this paper we use the cluster approximation Gusev et al. [2001](see also Refs. Dzyub

[1973, 1974a,b]). In the cluster approach one has:

$$D^k_{i\sigma}(E) \equiv \left\langle \frac{1}{[g^k_{\sigma i}(E)]^{-1} - \delta L_i} \right\rangle^{crys} = \sum_{r=0}^{z} \frac{w(r)}{[g^k_{\sigma i}(E)]^{-1} - (z-r)\lambda^{kk}_{ij} - r\lambda^{k\acute{k}}_{ij}}, \tag{3.56}$$

where $w(r) = z!/(r!(z-r)!)(1-x)^r x^{z-r}; \acute{k} \neq k$; z is the number of nearest neighbors; i, j denote nearest-neighbors sites in the crystal lattice.

Now we see that this cluster crystal field average technique implies that every energy level multiplet of the local propagator $D^k_{i\sigma}(E)$ enters the averaged Green's function on equal footing, but with different probability $w(r)$ which depends on the number of the nearest host atoms around a given one.
The further averaging over the full Green function $\overline{\left\langle\left\langle a_{i\uparrow} | a^+_{j\uparrow} \right\rangle\right\rangle}_E$ in the Eq. (3.37) leads to the equation for the averaged Green's function,

$$G_{\sigma;ij}(E) = \Xi_{\sigma;ij}(E) + \sum_{i_1,j_1} \Xi_{\sigma;ii_1}(E) t_{i_1 j_1} G_{\sigma;j_1 j}(E). \tag{3.57}$$

Here the $\Xi_{\sigma;ij}$ term is the self-energy part of the averaged Green's function in the Larking presentation for whole crystal and is irreducible by the transfer. It is called the locator in ref. Elliott et al. [1974] and has the following diagram representation:

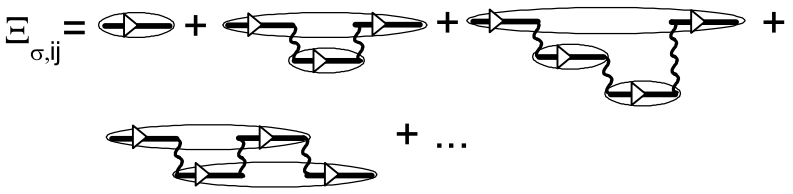

(3.58)

Let us restrict ourselves to single-site diagrams in the expression (3.58) for $\Xi_{\sigma;ij}$ (e.g. $1, 2, 3$, and so on), i.e. to the single-site approximation

$$\Xi_{\sigma;ij}(E) = \delta_{ij} \Xi_\sigma(E). \tag{3.59}$$

Then equation (3.58) can be rewritten in the form;

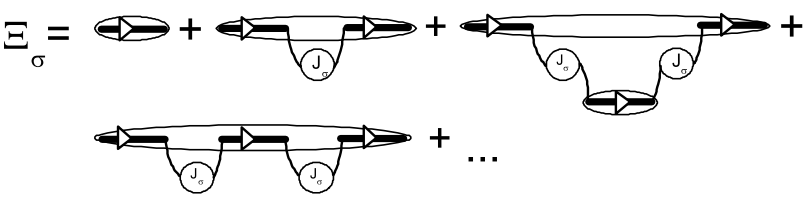

(3.60)

where $J_\sigma(E)$ is the sum of all diagrams beginning and terminating at the

same site and having no common cumulants.

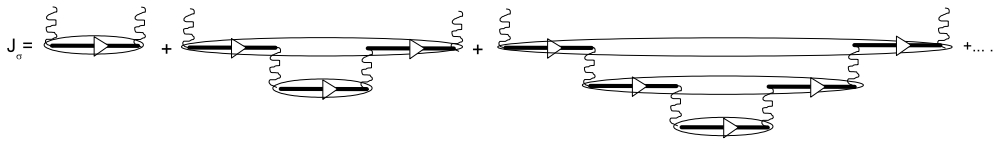

(3.61)

The set (3.60) can be calculated using the technique of ref. Elliott et al. [1974].

$$\Xi_\sigma(E) = \frac{(1-x)D^A_\sigma(E) + xD^M_\sigma(E) - D^A_\sigma(E)D^M_\sigma(E)J_\sigma(E)}{1-(xD^A_\sigma(E)+(1-x)D^M_\sigma(E))J_\sigma(E)}. \tag{3.62}$$

On the other hand, the sum $J_\sigma(E)$ can be determined if one finds the sum of all diagrams beginning and terminating at the same site and having the common cumulants(ovals):

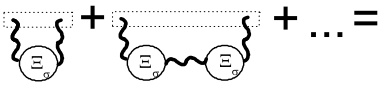

(3.63)

$$\frac{1}{N}\sum_{\vec{k}} t_{\vec{k}}\Xi_\sigma + \frac{1}{N}\sum_{\vec{k}} t^2_{\vec{k}}[\Xi_\sigma]^2 + ... = \frac{1}{N}\sum_{\vec{k}} \frac{t^2_{\vec{k}}}{[\Xi_\sigma]^{-1}-t_{\vec{k}}},$$

where $t_{\vec{k}}$ is the Fourier transform of the transfer matrix. It is clear that the sum (3.63) (called the fully renormalized interactor in ref. Elliott et al. [1974]) is equal to

$$\frac{1}{N}\sum_{\vec{k}} \frac{t^2_{\vec{k}}}{[\Xi_\sigma(E)]^{-1}-t_{\vec{k}}} = \frac{J_\sigma(E)}{1-\Xi_\sigma(E)J_\sigma(E)}. \tag{3.64}$$

Let us rewrite the expressions (3.57),(3.63),(3.64) in the form of the equations for the coherent potential as follows:

$$G_{\sigma;ii}(E) = \frac{1}{N}\sum_{\vec{k}} \frac{1}{[\Xi_\sigma(E)]^{-1}-t_{\vec{k}}}. \tag{3.65}$$

Then the coherent potential $J_\sigma(E)$ takes the form

$$J_\sigma(E) = [\Xi_\sigma(E)]^{-1} - [G_{\sigma,ii}(E)]^{-1}. \tag{3.66}$$

Combining Eqs. (3.62),(3.65) and (3.66) one gets the solution of the self-consistent problem for the $A_{1-x}M_x$ crystal lattice.

$$G_{\sigma,ii}(E) = \frac{1-x}{[D^A_\sigma(E)]^{-1}-[\Xi_\sigma(E)]^{-1}+G^{-1}_{\sigma,ii}(E)} + \frac{x}{[D^B_\sigma(E)]^{-1}-[\Xi_\sigma(E)]^{-1}+G^{-1}_{\sigma,ii}(E)}, \tag{3.67}$$

where the disorder in the first coordination sphere(red atoms in the Fig. 3.8) is included in the local propagators $D^A_\sigma(E), D^M_\sigma(E)$ which can be evaluated by

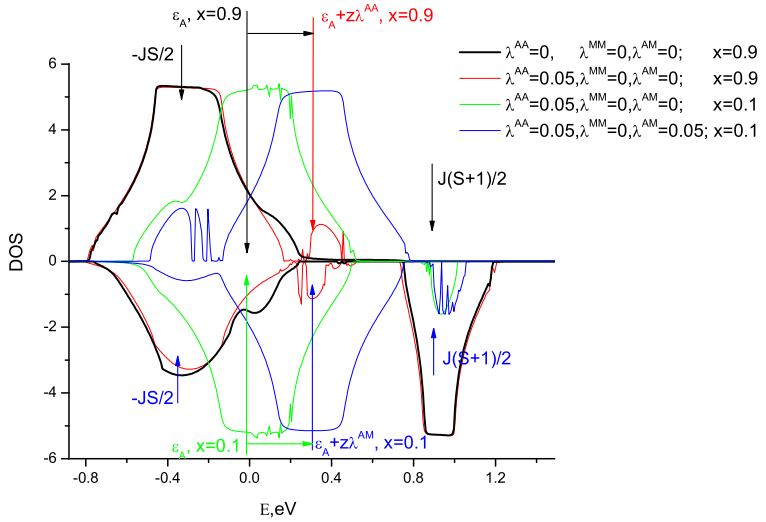

Abbildung 3.9.: Density of electron states in the cluster approximation for the disordered KLM at $S = 1/2$, $J = 1$, $W = 0.5$ for ferromagnetic $\langle S^z \rangle = S$ case at the different crystal field parameters

using the cluster approach (Eq. 3.56).

The figure 3.9 shows the quasiparticle DOS of the conduction band at $T = 0$ for two different case: switch off ($\lambda^{AA} = 0, \lambda^{AM} = 0, \lambda^{MM} = 0$) and switch on ($\lambda^{AA} \neq 0, \lambda^{AM} \neq 0, \lambda^{MM} \neq 0$) the crystal field effects. In the first case the properties of the disordered Kondo-lattice are absolutely the same as was discussed in the earlier chapter for the atomic limits approximation and the ISA.

The DOSs consist of two correlated and one non-correlated band per spin direction. The correlated bands correspond to the magnetic atoms M, with the spectral weight $\sim x$ and the center of gravity ϵ_M. The non-correlated band stems from non-magnetic atoms A with the spectral weight $\sim (1 - x)$ and the center of gravity ϵ_A. The DOS of the correlated bands for $\langle S^z \rangle = S(T = 0)$ and a large enough interband exchange coupling J consists in general of two subbands centered near the atomic energies: $-JS/2$ and $J(S + 1)/2$. For the spin up electrons at $T = 0$ there is no DOS for energies around $J(S + 1)/2$, while the spin down density is finite there (magnetic polaron states). For weak couplings ($J < 0.2$) correlated and uncorrelated bands are mixed preventing a clear interpretation of the various influences.

For the electron DOS with the crystal field effects included, these two bands are built-up by seven mini-bands which correspond to the cluster types presented in Fig. 3.10,3.11 with band width proportional to λ. The denominator of the local Green function (3.56) controls the center of gravity of every miniband and the numerator controls the shape of the minibands. Fig. 3.9 presents the influence of different crystal field parameters ($\lambda^{AA}, \lambda^{AM}, \lambda^{MM}$) on the electron DOS. At very low or very high x, for example $x = 0.1$ or $x = 0.9$ the crystal field between two neighbor non-magnetic atoms λ^{AA} cannot change(shift) the

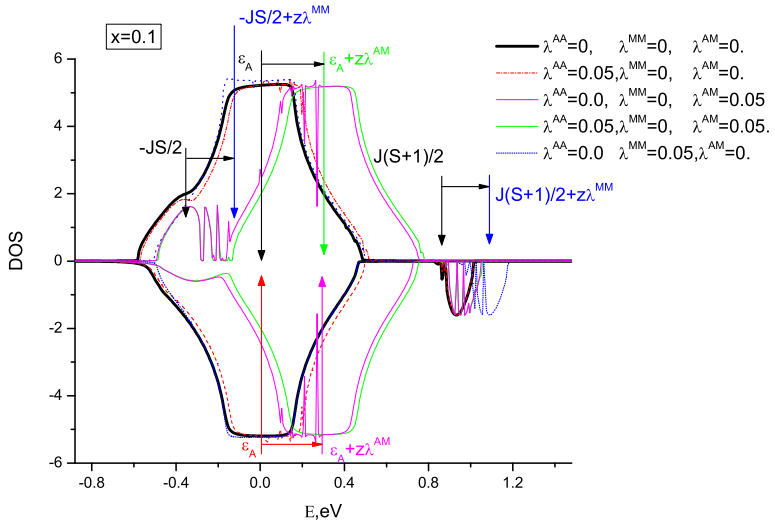

Abbildung 3.10.: Density of electron states in the cluster approximation for the disordered KLM at $S = 1/2$, $J = 1$, $W = 0.5$ for ferromagnetic $\langle S^z \rangle = S$ case at the different crystal field parameters

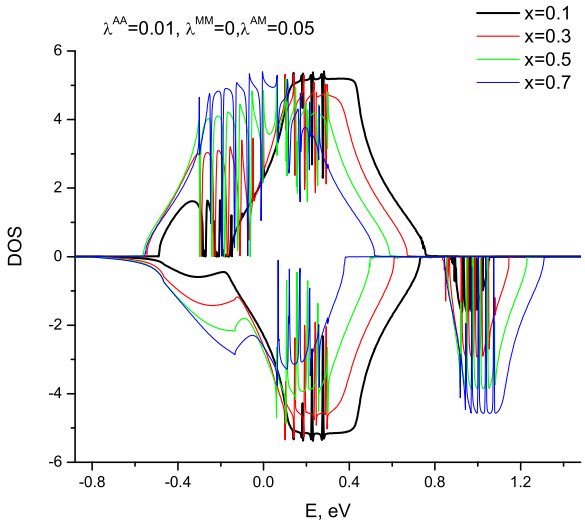

Abbildung 3.11.: Density of electron states in the cluster approximation for the disordered KLM at $S = 1/2$, $J = 1$, $W = 0.5$ for ferromagnetic $\langle S^z \rangle = S$ case at the different crystal field parameters

DOS very drastically and the electron DOS(green vertical line with arrow on the Fig. (3.9)) is approximately the same as the DOS without the crystal field effects(black vertical line with an arrow on the Fig. (3.9)). The same conclusion we can do for the correlated subband (black vertical short line with an arrow on the Fig. (3.9) near the energy position $-JS/2$ and $J(S+1)/2$). Increasing the crystal field parameter λ^{AA} for the case where the matrix consist with approximately fully magnetic atom M (for $x \sim 1$) or increasing the crystal field parameter λ^{AM} between magnetic and non-magnetic atoms change the center of gravity on the value $6\lambda^{AA}$ (horizontal black line with an arrow on the Fig. (3.9)) or the value $6\lambda^{AM}$ (horizontal green line with an arrow on the Fig. (3.9)) and don't change the center of gravity for the correlated bands.

Increasing the crystal field parameter λ^{MM} between two magnetic atoms the center of gravity of the correlated subband monotonically shifts to higher energy hardly changing the non-correlated bands (horizontal black line with an arrow between center of gravity of the correlated subbands on the Fig (3.10)). The crystal field between magnetic and non-magnetic atoms λ^{AM} plays the role of a hybridization between correlated and non-correlated subbands (horizontal black line with an arrow between center of gravity of the non-correlated subbands on the Fig (3.10)).

At finite temperature all mini-subbands are mixed. Finally, the spectrum of up and down electrons from the correlated and non-correlated bands becomes symmetric at $T > T_c$, where bands are equally populated and spin-polarization disappears Bryksa and Nolting [2008a], Tang and Nolting [2007], Nolting et al. [2001, 2004].

For performing the investigation of the mutual influence of magnetic correlations and disorder effects in diluted local-moment systems we introduced phenomenological crystal field parameters $(\lambda^{AA}, \lambda^{AM}, \lambda^{MM})$. These parameters are acting on of the electronic subsystem of the disordered Kondo-lattice. In principle, they must be calculated by a self-consistent procedure. But the complexity of the problem did not yet allow us to realize this strategy. So, in these calculation we take such $\lambda^{AA}, \lambda^{AM}, \lambda^{MM}$ which are at least less then the hoping parameter t $(0.1 < t < 0.2)$.

4. Self-Consistent Task

4.1. Direct and Indirect mechanisms

The exchange interactions represents a characteristic quantum effect having no analog in classical mechanics and its main goal being in determining the spontaneous magnetization for a system having permanent magnetic moments. This phenomenon of collective magnetism Mattis [1965] is a part of one of the oldest and basic problems in solid state physics. Due to the lack of its complete understanding, it is currently one of the very hot topic in fundamental research. The main weakness being the absence of a unified theory which would be able to explain the rich diversity of the subject within the framework of one and the same theoretical model. The different types of magnetic materials (metals, non-metals) fulfills different models descriptions, each of them having a fairly restricted regime. Thus, while studying their magnetic properties one should specify the model under consideration.

The simplest model of magnetism in solids is the following : electrons in well localized magnetic d or f states interact with one another via a Heisenberg nearest neighbor exchange mechanism Heisenberg [1928], Slater [1930]. The direct overlap of wave functions belonging to neighboring spins leads to a magnetic interaction which can be of either sign- ferromagnetic or antiferromagnetic. But, in many metals or non-metals calculations suggest that the direct exchange between the nearest neighbors in a localized spin model is itself not responsible for ferromagnetism because the distance between the nearest neighbors is too great for there to be appreciable overlap of the wave functions.

The general idea of the exchange interaction have therefore been extended by the concept of ïndirect exchange"which was first suggested by Kramers Kramers [1934]. The principle involved in this interaction is that exchange between two magnetic ions does not occur directly but it is maintained via an intermediatory diamagnetic ion. In the simplest terms exchange alignment occurs between an electron on the magnetic ion and one on the diamagnetic ion and the latter then interacts with the next magnetic ion so producing a further alignment. The net effect is therefore an exchange coupling between the two magnetic ions.

When applied to non-metals it is termed as *superexchange* Anderson [1930, 1961] by Anderson. In his treatment he assumes that the d states of the magnetic ions will be modified by the presence of the nearby diamagnetic p states so that they will have some p admixture. The new wave functions of the magnetic ions will have much more overlap than did the original simple d functions because now they each have some of the p character of the diamagnetic ions. He then calculates the direct exchange between two magnetic ions using the modified wave functions. Such calculations as have been made suggest that

this is a satisfactory approach to the problem of the exchange mechanism in insulators.

While the same principle from that of Kramer's has been extended by Zener Zener [1951] to conductors within the so-called *double exchange* phenomenon. He proposed that the interaction between the localized $3d$ or $4f$ electrons on different ions arose by means of a coupling via the conduction electrons instead of via the diamagnetic ions as was discussed earlier.

And an equivalent treatment exist for metals where the exchange interaction results in oscillatory function as a consequence of the sharp Fermi surface. In such systems there is an important contribution to the spin- spin interaction due to the polarization of the itinerant electrons and their interaction with localized spins. Originally ascribed to Ruderman and Kittel Ruderman and C.Kittel [1954], the interaction was proposed as a means of explaining unusually broad nuclear spin resonance lines that had been observed in natural metallic silver. It was long ranged and decreased only as the inverse cube of the distance at large separation. Kasuya Kasuya [1956] later proposed that a similar indirect exchange coupling could be applied to localized d electron spins interacting via conduction electrons. A subsequent modification by Yosida Yosida [1957] even further increased the range and thereafter this indirect mechanism is termed as the *RKKY interaction*.

Bloembergen and Rowland Bloembergen and Rowland [1955] adapted the same concept to nonmetals and found qualitatively the same oscillatory behavior but a range reduced by "tunneling".

Apart from the above explained exchange interactions there are a multitude of possible other interactions like biquadratic superexchange Huang and Orbach [1964], triple exchange Carr [1953], some explaining exchange mechanisms in magnetic semiconductors Nagaev [1979], Bastard and Lewiner [1979] while others in diluted magnetic semiconductors Singley et al. [2002], Dietl et al. [2000]. A point which has to be stressed out is that in any particular material these indirect exchange couplings may or may not be comparable in energy to the direct coupling and the two mechanisms doubtless can coexist in the same substance.

In the next section, we try to formulate one of the indirect exchange mechanisms for the case of disorder Kondo lattice model.

4.2. Exchange interaction in the disorder KLM

Here we are interested mainly how the disorder influences the characteristic properties of local-moment systems such as the DMS, where magnetic (M) and non-magnetic (A) atoms are distributed randomly over a crystal lattice ($A_{1-x}M_x$) with a given concentration of magnetic atoms x. In order to answer this question different approaches were proposed Theumann and Tahir-Kheli [1975], Harris et al. [1974], Dvey-Aharon and Fibich [1978], Kudrnovsky et al. [2004], Jones [1971], Bouzerar and Bruno [2002].

The problem of adequate description of disordered correlated electron sys-

tems has been studied intensively during the last decade, especially in context of the physics of magnetism in the DMS systems. The understanding of the true nature of electronic states and their quasiparticle dynamics is one of central topics of the current experimental and theoretical studies in the field. A plenty of experimental and theoretical results show that this many-body quasiparticle dynamics is quite nontrivial. A vast amount of theoretical searches for a suitable description of disorder DMS system deal with simplified model Hamiltonians. These include, as workable patterns, the disordered Heisenberg model and the disorder KLM. In spite of certain drawbacks, these models exhibit the key physical feature: the competition and interplay between kinetic energy and potential energy (localized) effects. A fully consistent theory of quasiparticle dynamics of both the models is believed to be crucially important for a deeper understanding of the true nature of electronic states in the above-mentioned class of materials. In spite of experimental and theoretical achievements, it remains still much to be understood concerning such systems.

Recent theoretical investigations of the disordered systems have brought forth a significant variety of the approaches to solve these controversial problems. There is an important aspect of the problem under consideration, namely, how to take adequately into account the lattice (qusilocalized) character of charge carriers, contrary to simplified theories of the type of a weakly interacting localized spins. To match such a trend, we need to develop a systematic theory for the random Kondo-lattice model arises with the fact that both the electron and the spin subsystems have to be considered simultaneously and on the same level, to describe, from the first principle of the condensed matter theory and statistical mechanics, the physical properties of this class of materials. Most of the KLM investigations are focused on the electronic Takahashi [2004], Blackman et al. [1971] or magnetic Theumann and Tahir-Kheli [1975], Harris et al. [1974], Dvey-Aharon and Fibich [1978], Bouzerar et al. [2006a], Hilbert and Nolting [2004], Bouzerar and Bruno [2002] subsystem only. A special goal of our study is the homologous treatment of the electronic and magnetic properties of the random KLM, which mutually condition each other and, therefore, should be determined self-consistently (see Fig. 4.1).

In previous chapters, we set up the practical technique of the method of finding the spin and electron Green functions for the disordered medium, like to the binary alloy $A_{1-x}M_x$, on the base of disorder Heisenberg and KLM models, respectively. As it was done successfully for the periodic KLM Nolting et al. [1996b] (*'modified' RKKY (MRKKY)*) one can map the KLM-interband exchange on an effective and random Heisenberg model. The resulting effective exchange integrals between the localized spins will be long range and complicated functionals of the electronic self-energy.

This technique was described in recent papers Bryksa and Nolting [2008a,b] and is schematically illustrated in Fig. 4.1. and proceeds as follows. For the zero temperature and for the saturated magnetization $\langle S^z \rangle = S$, the electronic part of the model Hamiltonian is solved by using a single-particle Green function in several different approximations, as explained in Chapter 3. For the zero-bandwidth limit of the correlated KLM, the Interpolating self-energy approach and the cluster CPA we used following self-energy expressions: (3.17), (3.22),

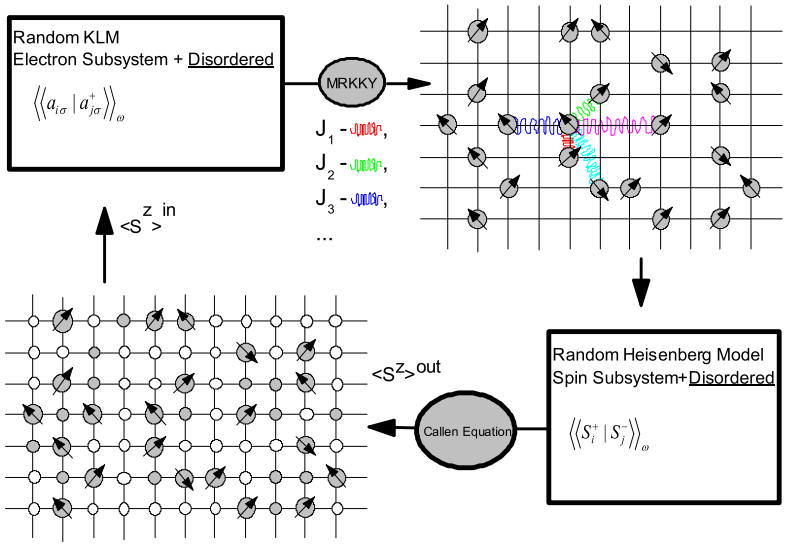

Abbildung 4.1.: Flowchart exhibiting the self consistent determination of the magnetization $\langle S^z \rangle$. The terminologies are as explained in the text.

and (3.67), where the crystal field parameters $(\lambda^{AA}, \lambda^{AM}, \lambda^{MM})$ are included in the average local Green's function (3.56), respectively. The result provides the configurational average single-site electron Green function $G_{ij\sigma}(E)$ for a given band occupation of the conduction band n (Eq. 3.8), concentration of the magnetic atoms x, and exchange coupling constant J. In order to study the magnetic properties (finite temperature), we use the modified RKKY(MRKKY) theory that results from mapping the $s-f$ interaction onto an effective Heisenberg model. Getting effective exchange integrals J_j (Esq. 3.10) mainly determined by the electronic self-energy. Finally, considering random distribution of the magnetic ions, the effective Heisenberg model (Chapter 2.3) is solved in the cluster CPA framework (Refs. Bryksa and Nolting [2008a,b]) self-consistently and new magnetization $\langle S^z \rangle$ can be derived from the mignon Green function in the VCA (2.45) or LQA approximation (2.49) and the Callen equation (2.21). The entire procedure is repeated until the solution of $\langle S^z \rangle$ is self-consistent. Furthermore, one can change the temperature and repeat the entire $\langle S^z \rangle$ self-consistent calculation until one gets T_c ($\langle S^z \rangle = 0$).

Let us discuss the results found for the self-consistent calculation according to the procedure sketched in (Fig. 4.1).

Fig. 4.2 presents the distance-dependence of the effective (MRKKY) exchange integrals for different values of the interband exchange parameter J of the Kondo-lattice model. For the concentrated case $x = 1$ and in the low coupling regime $J \to 0$ the MRKKY interaction agrees with the conventional RKKY Nolting et al. [1996b], Santos and Nolting [2002a]:

$$J^{RKKY}(R) = 6\pi J^2 \frac{\rho^2(E_F)}{E_F} \left(\frac{sin(2k_F R)}{(2k_F R)^4} - \frac{cos(2k_F R)}{(2k_F R)^3} \right), \qquad (4.1)$$

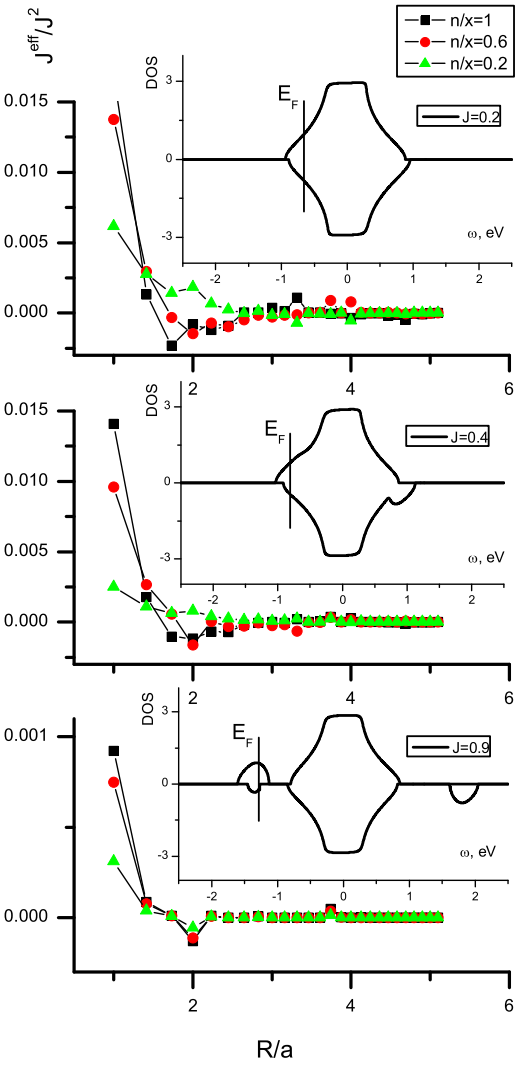

Abbildung 4.2.: Dependence of the MRKKY interaction (Eq. 3.10) on the distance R between magnetic atoms in a simple cubic lattice ($R = 1$ is a first shell(nearest-neighbors atoms),$R = \sqrt{2}$ is a second shell(next nearest-neighbors atoms) and so on) at fixed parameters $W = 0.9, S = 5/2, x = 0.1, T = 0, \langle S^z \rangle = S$ of the model for three different coupling $J = 0.2, J = 0.4, J = 0.9$ and three different values of a small electron concentration $n/x = 1, n/x = 0.6, n/x = 0.2$. In the inset is the electron DOS for the same parameters. The Fermi edge is indicated for the band occupation $n/x = 0.6$.

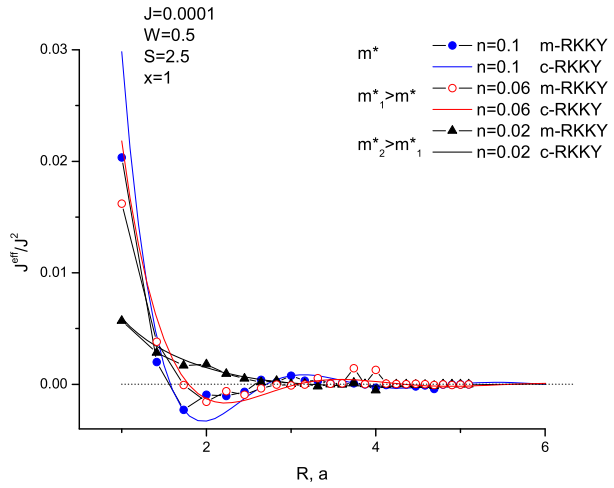

Abbildung 4.3.: Dependence of the conventional RKKY interaction (Eq. 3.10) and MRKKY on the distance R between magnetic atoms in a simple cubic lattice ($R = 1$ is a first shell(nearest-neighbors atoms),$R = \sqrt{2}$ is a second shell(next nearest-neighbors atoms) and so on) at fixed parameters $W = 0.5, S = 5/2, x = 1, T = 0, \langle S^z \rangle = S, J = 0.0001$ of the model for three different values of a small electron concentration $n = 0.02, n = 0.06, n = 0.1$. The terminologies are as explained in the text.

where $k_F = \sqrt{2m^* E_F}$, $\rho(E_F)$ is a DOS on the Fermi edge and m^* is an effective quasiparticle mass.

In this situation the effective exchange constant has a long-range character with strong oscillations in the direct space (see Fig. 4.3). However, with increasing J the MRKKY interaction looses the long range character and transforms into a fairly short-range interaction (like double exchange), where only the first few effective exchange parameters Santos and Nolting [2002a] turn out to be important. We recognize the same behavior for diluted systems $x < 1$. For better comparison with the conventional RKKY, Figs. 4.2,4.3 show only the oscillation part of the MRKKY interaction J^{eff}/J^2.

The conventional RKKY interaction is a continuous function of distance R, while the MRKKY approach can provide only discrete results. The magnetic neighbors of a given magnetic ion are considered as ordered in *'shells'*. The larger the shell number L the larger the distance to the given magnetic ion. The L-th shell is built up by the L-th next-nearest neighbors. Each point in Fig. 4.2 corresponds to a certain shell demonstrating the distance-dependence of the effective exchange parameter J_{ij}^{eff}. Generally, there are two contributions to the effective exchange interaction, namely a Kondo-scattering of electrons J by magnetic impurities and in addition the scattering of the electrons by the random distribution of magnetic atoms with the concentration x. It is not possible to separate these two contributions which both play an important role.

In the Fig. 4.3 we also show a tendency of changing of the conventional RKKY interaction at decreasing of a carrier concentration n, where the solid line means a curve by used Eq. (4.1) with the fitting parameter of the effective mass m^*. We see that the quasiparticle becomes a more heavy one at decreasing of a carrier concentration, what is showed in the Fig. 4.3 by used the different parameters of the effective mass. The same conclusion we can do for the MRKKY interaction. If we increase the exchange coupling J, the quasiparticle became a more heavy one or a more localized one (Fig. 4.2).

Another factor that can change very drastically a character of the exchange interaction between magnetic atoms are crystal field effects as a element of a short-range order. Let us consider a binary solid $A_{1-x}Mn_x$ alloy, where the atomic concentration of the component Mn is x, while the total number of atoms equals N. Assume that the coordinate number of the $n-$th coordination sphere is z_n (see Appendix A). In this case the number of atoms of species Mn is Nx and the total number of atoms in the $n-$th coordination sphere of any atomic species Mn is Nz_nx. Denote the number of atoms of species Mn and A in the n coordination spheres as N^n_{Mn} and N^n_A. Then the relative number of atoms of a particular species in the $n-$th coordination sphere becomes $n^n_{Mn} = N^n_{Mn}/Nz_nx$ and $n^n_A = N^n_A/Nz_nx$. If the atoms are distributed statistically, the number of atoms of species A located in the $n-$th coordination sphere relative to the number of species Mn atoms is $Nz_nx(1-x)$. If any short-range order is present, i.e. if the mutual arrangement of atoms is correlated, then $N^n_{Mn} \neq Nz_nx(1-x)$. Therefore a quantity, which characterizes the relative deviation of the atomic distribution in the $n-$the coordination sphere from the statistical value,

$$\alpha_n = \frac{Nz_nx(1-x) - N^n_A}{Nz_nx(1-x)} = 1 - \frac{n^n_A}{1-x} \tag{4.2}$$

is introduced as the short-range order parameter. If the atoms are distributed statistically, the order parameter α_n is zero. If the correlations are present and if the $n-$th coordination sphere of the A atom of a particular species hosts mostly atoms of the other species the short-range parameter becomes negative: $\alpha_n <= 0$. Otherwise, if the the relative fraction of atoms of other species in th $n-$th coordination sphere of the A atom of a particular species is less then in the case of the statistical distributed: $\alpha_n >= 0$.

So, now we have question how a theory is for the calculation of electron or spin Green function for the binary $A_{1-x}Mn_x$ alloy a sensitive to the short-order parameter α_n?

For the spin configurational average Green function we have the Eq. (2.43) with the structure factor $S(\vec{q})$ for a random distributed the Mn atoms. We can also derive from this equation at some simplification conditions: the VCA (Eq. 2.45) and the LQA (Eq. 2.49). And we see that the VCA equation for the spin configurational average Green function is not a sensitive one to the order parameter α_n. The LQA equation is an equation where $\alpha_n = 0$ which means the A and Mn atoms are distributed statistically. And in order to include the order parameter we have to consider the general equation (2.43).

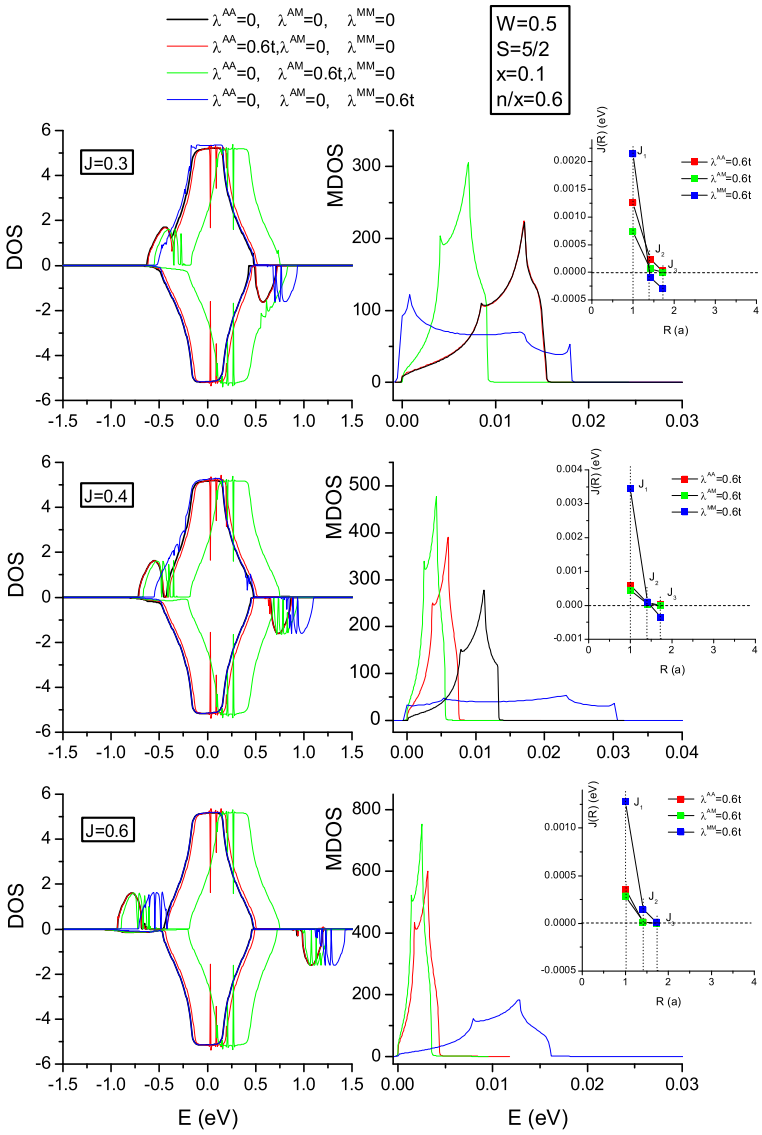

Abbildung 4.4.: Quasiparticle electron(left column) and magnon (right column) density of states(DOS) at fixed model parameters $W = 0.5, S = 5/2, x = 0.1, n/x = 0.6$ for three different couplings and for different values of the crystal field parameters. The inset shows dependence of the MRKKY interaction on the distance R between magnetic atoms in simple cubic lattice($R = 1$ is a first shell, $R = t\sqrt{2}$ is a second shell, and $R = \sqrt{3}$ is a third shell).

With respect to the disorder problem of the electron subsystem there are many papers Elliott et al. [1974], Nolting et al. [2001], Bouzerar and Bruno [2002], Tang and Nolting [2007], Bryksa and Nolting [2008a], Takahashi [2004], Nolting et al. [2004] using the CPA technique to find the electron spectrum for a random crystal. But the CPA has only simple clusters contribution, like to the VCA equation for the spin configurational average magnon Green function (Eq.2.45). The idea to include crystal field effects ($\lambda^{AA}, \lambda^{AM}, \lambda^{MM}$) into the Hamiltonian (Eq. 3.24) can improve this CPA ansatz and it means we have only the short-range order parameter in the first coordination sphere α_1. It is clear that we have to use the cluster CPA technique for the disordered electronic part as was described in the Chapter 3.3.

For performing the investigation of the mutual influence of magnetic correlations and disorder effects in diluted local-moment systems we introduced phenomenological crystal field parameters ($\lambda^{AA}, \lambda^{AM}, \lambda^{MM}$). These parameters have influence on the electronic subsystem of the disordered Kondo-lattice as the different A and Mn atom clusters contribution in the first coordination sphere for the simple cubic lattice. In principle, they must be calculated by a self-consistent procedure together with the effective exchange Heisenberg constants, for example. But the complexity of the problem did not yet allow us to realize this strategy. From the magnon DOS (Fig. 4.4) we can conclude that for better fitting of our results to the Quantum Monte Carlo calculation Hilbert and Nolting [2004] it is necessary to support large values of the crystal field between two magnetic atoms λ^{MM}.

The effects of the crystal field from the only magnetic atom was recently discussed in ref. Bouzerar et al. [2006b] for the DMS system. There was considered a correlation between the on-site crystal field potential V_i and the exchange constants in the effective Heisenberg model Liechtenstein et al. [1987] J_{ij}.

Another important method to introduce the crystal field effects is based on a non-diagonal hopping term between the different kind of atoms and a matrix technique of ref. Blackman et al. [1971]. But this technique is more complicated to apply than our one. We reformulated the crystal field potential energy into a single-site problem, which makes the problem diagonal and gives a possibility to apply CPA technique, where are included the crystal field effects and their fluctuations in the binary alloy $A_{1-x}Mn_x$ for the first coordination shell only.

Fig. 4.5 represents the dependencies of the nearest-neighbor and the next-nearest-neighbor effective exchange interaction (J_1, J_2) on the interband exchange coupling J, and that for different concentrations x and for two different spin values $S = 5/2$ and $S = 1/2$. In the strong coupling regime ($J > 0.8$) of the concentrated system ($x = 1$) only the short-range interaction (J_1) is important, the other interactions are small ($J_2, J_3, ...$) Santos and Nolting [2002a]. In the diluted and strong coupling case, however, the next-neighbor interaction J_1 becomes smaller (Fig. 4.5) than for $x = 1$. In the low coupling regime ($J < 0.1$) the results of the modified RKKY coincide with those of the conventional RKKY ($J_1 \sim J^2$) (Fig. 4.5) being hardly x-dependent. The situation is much more complicated and non-monotonic in the intermediate coupling regime. Dilution may even lead to an enhanced value for the nearest-neighbor localized moment interaction J_1 compared with that for $x = 1$ (Fig. 4.5).

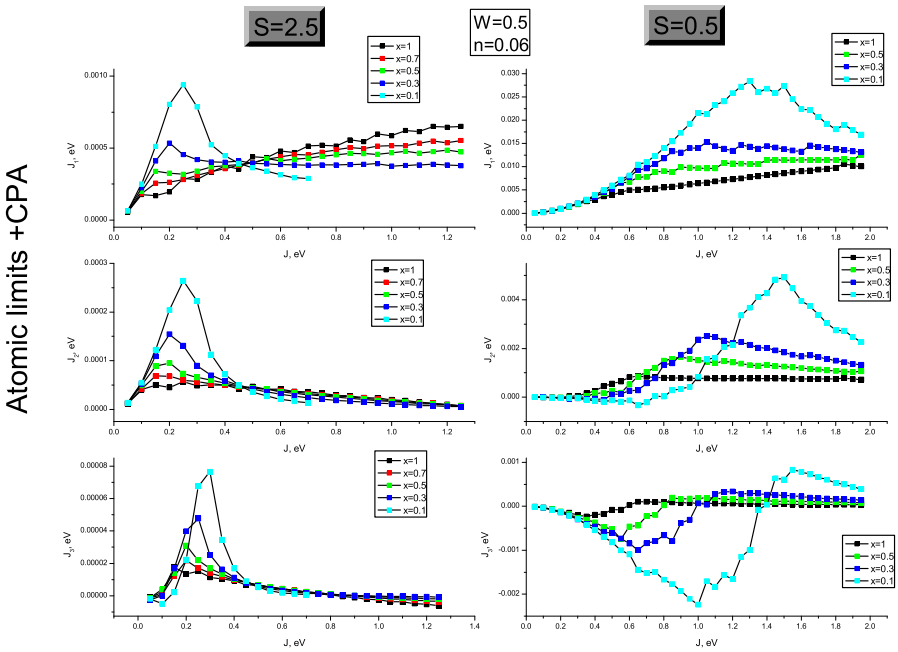

Abbildung 4.5.: Dependence of the nearest-neighbor effective exchange integral J_1, the next-nearest-neighboring one J_2 and J_3 on the exchange coupling J at $W = 0.5, n = 0.06, T = 0$, for different values of concentration x and two value of $S = 1/2, S = 5/2$ which were calculated by using of the zero-bandwith limit (the atomic limit) of the correlated KLM.

Fig. 4.6 shows the influence on the method of calculation (AL and ISA) on the the exchange coupling J_1. We see that both methods give similar results, but the ISA gives a little high a value of the interaction.

Fig. 4.7 represents the dependencies of the nearest-neighbor effective exchange interaction J_1 on the interband exchange coupling J, and that for full concentrated system $x = 1$ and for very small concentration $x = 0.1$ and for different values of the band occupation. In the strong coupling regime of the concentrated system ($x = 1$) the short-range interaction (J_1) is more then for the disordered case ($x < 1$). Increasing the coupling J we obtain some saturation value of J_1 that depends on the value of the band occupation. However, in the intermediate coupling regime the behavior of J_1 is same complicated as on Fig. 4.5 and depends on the band occupation. So, we see the same effect of an enhanced value for the nearest-neighbor localized moment interaction J_1 compared with that for $x = 1$ but for different band occupations n.

Fig. 4.8 shows the influence of the crucial field effects on the exchange couplings J_1, J_2 of the effective Heisenberg model for low concentration. We see that the biggest influence of the first exchange constant of the effective Heisenberg model appears for the intermediate regime of the interband exchange coupling. The low coupling regime and the strong coupling regime are absolutely the same as for the situation where all crystal field effects are neglected. The crystal field λ^{AM} reduces the value of J_1. The crystal field between two

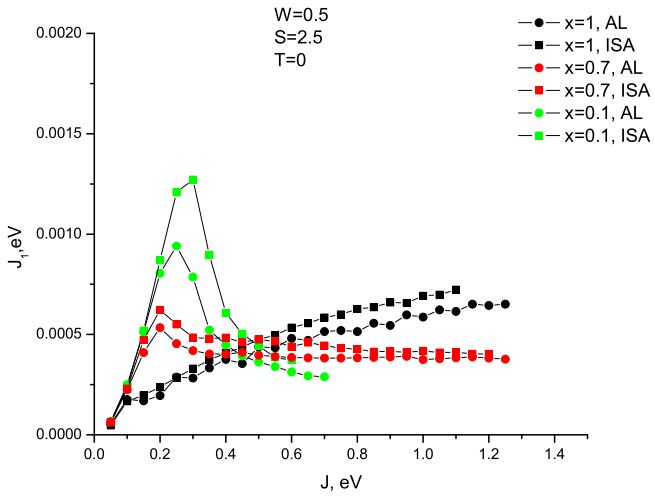

Abbildung 4.6.: Dependence of the nearest-neighbor effective exchange integral J_1 on the exchange coupling J at $W = 0.5, n = 0.06, S = 5/2, T = 0$, for different values of concentration x using two method of calculation for the electron spectrum of the disorder KLM. In the labels we use AL and ISA which mean that the results were calculated by used the zero-bandwidth atomic analogy limit and the Interpolating self-energy approach, respectively.

non-magnetic atoms λ^{AA} doesn't play any role. And increasing the crystal field between the two magnetic atoms we can drastically increase the value of the exchange coupling in the effective Heisenberg model.

4.3. Ferromagnetism in the disorder KLM

The electronic quasiparticle-DOS versus x is shown in Fig. 4.9. There are two parts with different physical meanings. One part consists of correlated bands centered at $-JS/2$ and $J(S+1)/2$ due to the exchange interaction with magnetic atoms. The spectral weights of the two subbands are strongly temperature-dependent. In the case of $T = 0$ the spectral weight of the upper $\uparrow$ subband disappears being, however, present in the $\downarrow$ spectrum. The second part around $\epsilon_A = 0$ represents a non-correlated band being connected to the non-magnetic atoms (Fig. 3.2,3.3,3.6,3.7). This part of the spectrum is practically temperature independent.

Fig. 4.10 shows the magnon DOS in the VCA approximation (2.45) for the saturated ferromagnetic ground state. We see a typical consequence of dilution: a shift to the low energy side with decreasing concentration x of magnetic atoms. The same is valid for the magnon DOS in the low quadratic approximation (2.49) but there are some differences (Fig. 4.11). Usually, in the weak magnon interaction case (Fig. 4.10), the magnon DOS near zero energy can be expressed as $DOS(E) = DE^2$, where D is a stiffness parameter Moto-

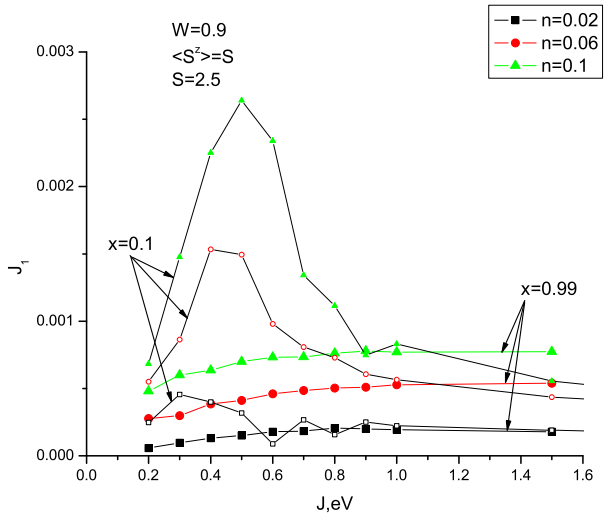

Abbildung 4.7.: Dependence of the nearest-neighbor effective exchange integral J_1 on the exchange coupling J at $W = 0.9, S = 5/2, T = 0$, for different values of concentration x and different values of a band occupation $n = 0.02, n = 0.06, n = 0.1$.

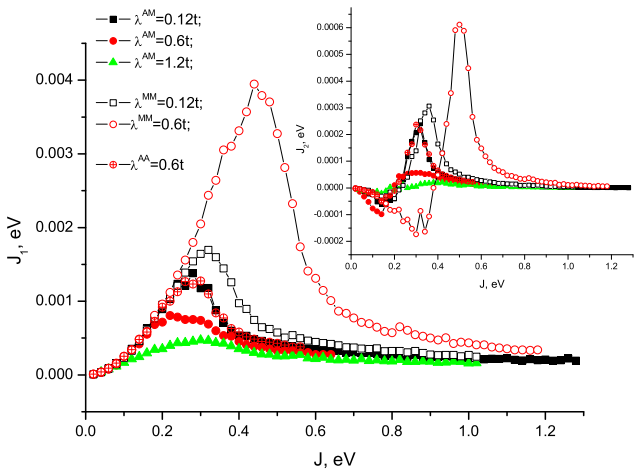

Abbildung 4.8.: Dependence of the nearest-neighbor effective exchange integral J_1 and the next-nearest-neighboring one J_2 on the exchange coupling J at $W = 0.9eV, S = 5/2, T = 0$ for different values of moment-concentration x without crystal field effects.

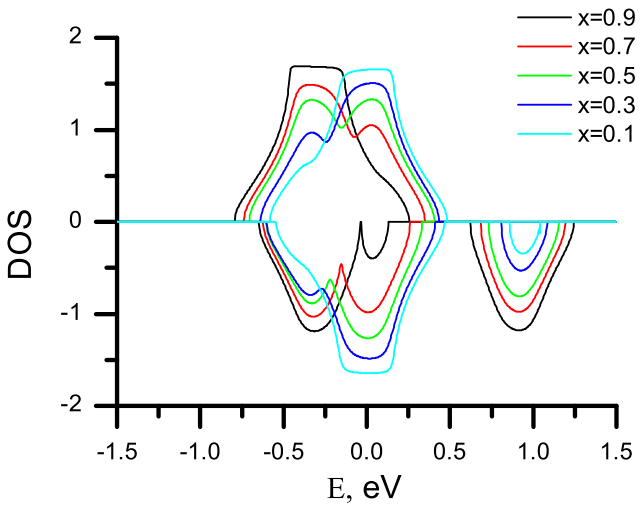

Abbildung 4.9.: Electron DOS calculated with $W = 0.5, J = 1.2, S = 1/2, n = 0.6, T = 0$ for different values of the concentration x.

me and Furukawa [2005]. But for the strong magnon interaction, due to the disorder, the magnon DOS near zero energy has higher contributions, like as $DOS(E) = DE^2 + KE^3$, where K is the disorder parameter. These contributions are strongly modifying the magnon stiffness. For example, the huge low-energy part for low concentrations x can be observed only for strong magnon interaction (inset of Fig. 4.11). But in the VCA we have the normal $DOS(E) = DE^2$ behavior (inset of Fig. 4.10). We conclude the same as in ref. Motome and Furukawa [2005], that the disorder is strongly influencing the low energy magnon DOS.

After the self-consistent calculation for finite temperatures (see. Fig. 4.1) we obtain the dependence of the magnetization on temperature and the resulting value of the Curie temperature (Fig. 4.12, Fig. 4.13). In Fig. 4.12 the results for the magnetization are plotted which are gained within the VCA for the magnon subsystem (2.45). We see that the Curie temperature decreases with increasing dilution $1 - x$. The same holds for the electron polarization (inset of Fig. 4.13): $(n_\uparrow - n_\downarrow)/n$.

The magnetization in Fig. 4.13 being found by the low quadratic approach (2.49) was determined by using the same parameters as for VCA in Fig. 4.13. Since this approach includes more realistically magnon scattering processes than the VCA, the Curie temperature for the same concentration x of magnetic ions is smaller than that of VCA. For small x the low quadratic approximation predicts first order ferromagnetic-paramagnetic transitions Gusev et al. [2001] (dotted lines in Fig. 4.13). The explanation of this fact is connected with the different predictions of the different approximations for the low energy part of the magnon DOS (see Fig. 4.10,4.11).

In Fig. 4.14 is a dependence of the nearest-neighbor effective exchange integral on the temperature T which we obtained solving by used the self-consistency method for the loop presented on the Fig. 4.1. The effective ex-

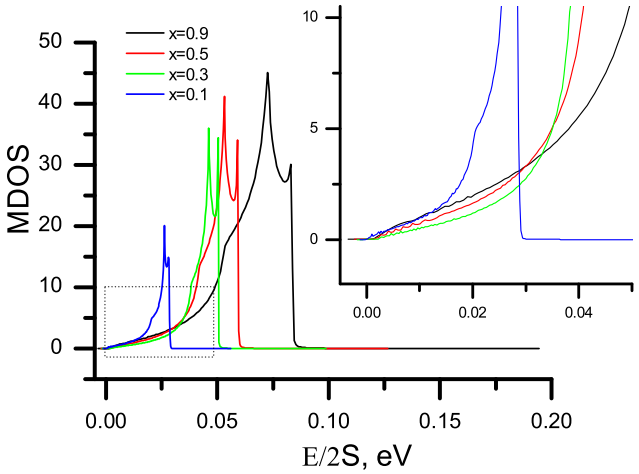

Abbildung 4.10.: Magnon DOS calculated self-consistently by use of the VCA with the same parameters as those in Fig. 4.9 for different values of the concentration x.

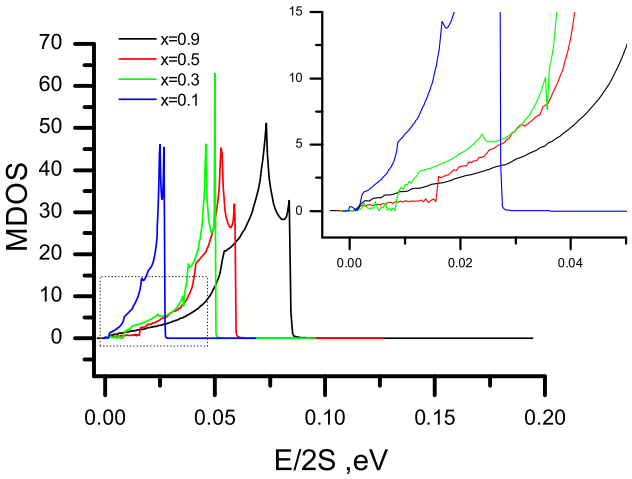

Abbildung 4.11.: Magnon DOS calculated self-consistently by use of the Low Quadratic Approximation with the same parameters as those in Fig. 4.9 for different values of the concentration x.

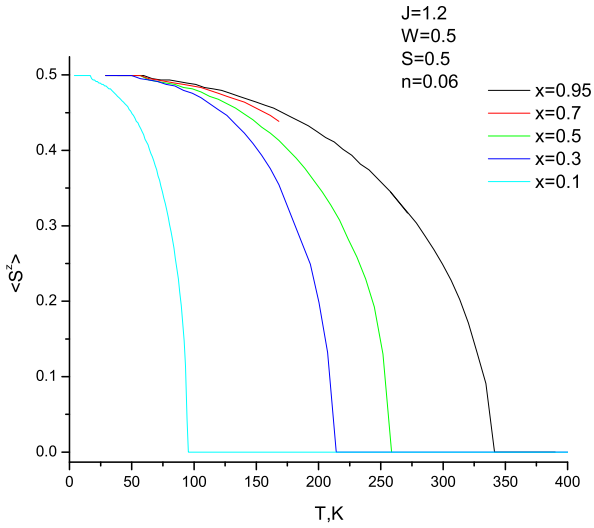

Abbildung 4.12.: Self-consistent calculation of the dependence of the magnetization $\langle S^z \rangle$ on temperature by use of the VCA approximation with the same parameters as those in Fig. 4.9 for different values of the concentration x.

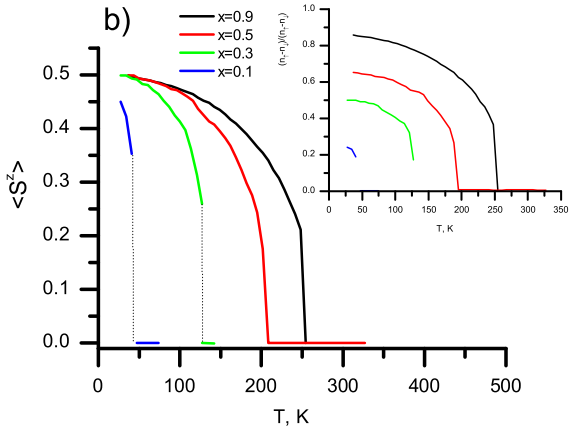

Abbildung 4.13.: Self-consistent calculation of the dependence of the magnetization $\langle S^z \rangle$ on temperature by use of the Low Quadratic Approximation with the same parameters as those in Fig. 4.12 for different values of the concentration x.

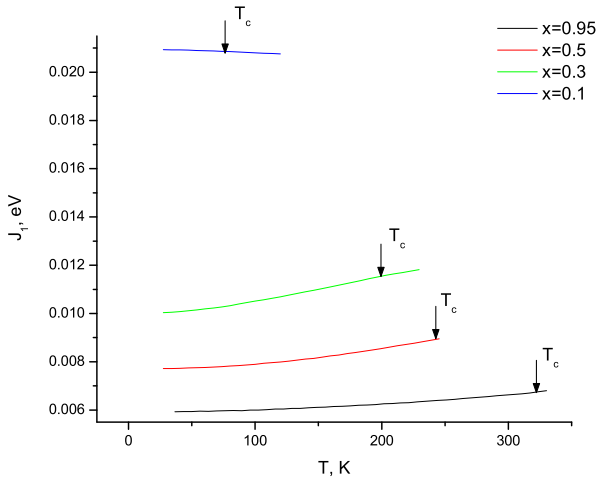

Abbildung 4.14.: Dependence of the nearest-neighbor effective exchange integral J_1 on the temperature T with the same parameters as those in Fig. 4.10 for different values of the concentration x.

change parameters $J_1, J_2, J_3, ..$ yield only a slight temperature-dependence of order 0.01 meV or even less. We see that the nearest-neighbor effective exchange integral J_1 can increase or decrease with a temperature. It is depends on the parameters of the model.

The magnetization in Fig. 4.15 being found by the low quadratic approach (Eq. 2.49). Since this approach includes more realistically magnon scattering processes than the VCA, the Curie temperature for the same concentration x of magnetic ions is smaller than that of VCA. For small x the low quadratic approximation predicts first order ferromagnetic-paramagnetic transitions Gusev et al. [2001] (in Fig. 4.15 is showed stable and metastable parts of the magnetization). It could indicate that in the system there is possibility for reconstruction, specially for a high temperature, for example, to form the Mn clusters in the non-magnetic matrix of the A atoms.

The crystal field effects play a critical role for understanding and controlling the ferromagnetic key-properties such as the Curie temperature. Figs. 4.16,4.17 show the change of the Curie temperature as function of the interband exchange coupling in the Kondo lattice model.

Comparing with the concentrated Kondo lattice model Santos and Nolting [2002a] ($x = 1$) we realize a strong non-monotonic change of the Curie temperature by a variation of the interband exchange coupling Tang and Nolting [2007] J (Figs. 4.16,4.17). This is due, first of all, to the effective exchange coupling in the effective Heisenberg model (Fig. 4.8). But even for an extremely low carrier concentration there is an induced ferromagnetism. The exchange coupling J must exceed a critical value J_c to get a finite T_c. For $J < J_c$ the system has paramagnetic properties ($T_c = 0$). For the strong coupling regime the Curie temperature is saturated to some constant value (Fig. 4.16). It turns out that a realistic effective occupation parameter of the correlated subbands for the diluted Kondo lattice is the value n/x rather than n. There is also a

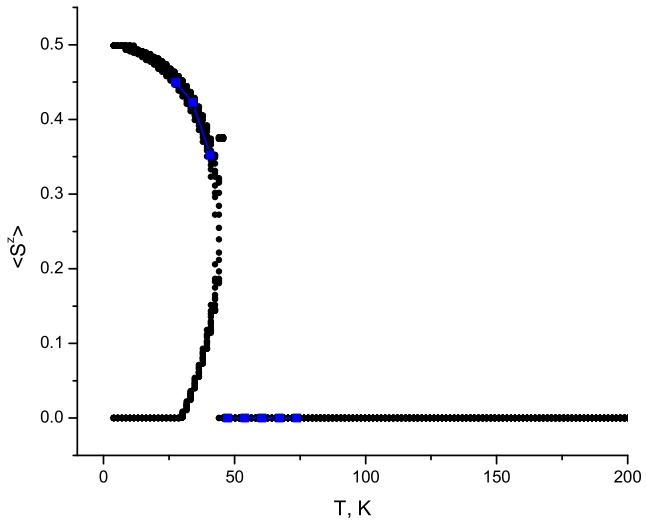

Abbildung 4.15.: Self-consistent calculation of the dependence of the magnetization $\langle S^z \rangle$ on temperature by use of the Low Quadratic Approximation with the same parameters as those in Fig. 4.12 for the concentration $x = 0.1$.

non-monotonic shift to higher values of the critical exchange coupling J_c when increasing the electron band occupation n/x as in the concentrated Kondo lattice model Santos and Nolting [2002a].

Fig. 4.17 shows the dependence of the Curie temperature on the interband exchange coupling constant J, with included crystal field effects in the first environment shell(see Fig. 4.1). We see that the crystal field effects don't change drastically the Curie temperature in low and strong coupling regimes compared to the case without crystal field effects. But there is a drastic change in the intermediate region of the interband exchange coupling ($0.3 < J < 0.7$). Specially, increasing the crystal field parameter between two magnetic atoms λ^{MM} can lead to a very drastic change of the Curie temperature (Fig. 4.17).

Fig. 4.18 shows a dependence of the magnetization on a temperature with including the crystal field effects. So, we see that the crystal field effects play a crucial role for understanding and controlling key-properties such as the Curie temperature. We have seen that disorder effects in the first environment shell change very drastically the Curie temperature.

In Fig. 4.18 we show by triangle with the same color as the magnetization also a value of the self-consistent Curie T_c temperature on the every calculation point of the magnetization (see Fig. 4.1). It could be seen that the dependence of the reduced value of the magnetization $\langle S^z \rangle / S$ as a long-range order parameter on the reduced temperature T/T_c for various values of x do not fall on a single universal curve what is predicting in the scale theory; for lower the concentration x, the more rapid is the decrease in $\langle S^z \rangle / S$.

Efforts to describe critical phenomena in terms of the mean field representation were made before Gusev et al. [2001], Ziman [1979], Krivoglaz and Smirnov [1964]. Atomic ordering takes place at thermodynamic equilibrium. Therefore

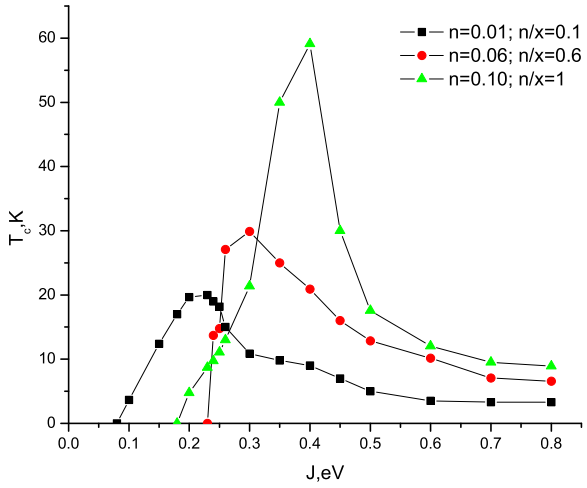

Abbildung 4.16.: Dependence of the Curie temperature T_c on the exchange coupling J at $W = 0.5eV, S = 5/2, x = 0.1$ and tree different value of a small electron concentration $n/x = 0.1, n/x = 0.6, n/x = 1$ without crystal field parameters influence.

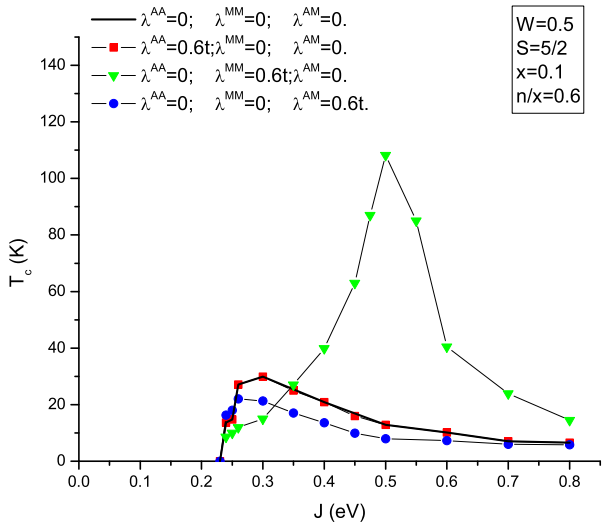

Abbildung 4.17.: Dependence of the Curie temperature T_c on the exchange coupling J at $W = 0.5eV, n = 0.06, x = 0.1, S = 5/2$ for the case of finite crystal field parameters.

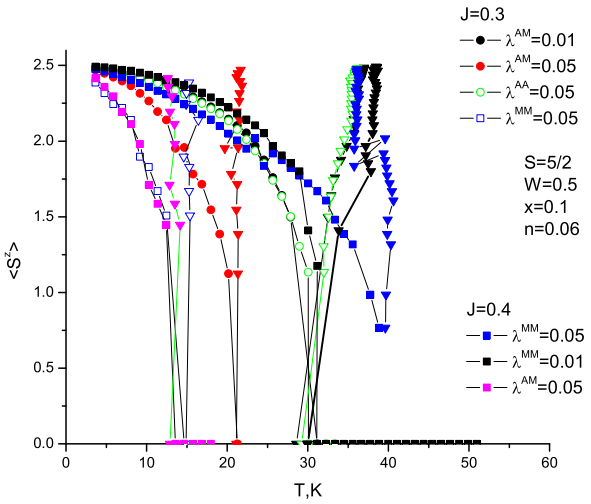

Abbildung 4.18.: Self-consistent calculation of the dependence of the magnetization $\langle S^z \rangle$ on temperature by use of the VCA approximation with the same parameters as those in Fig. 4.17 for different values of the concentration x.

a correct mean field value can can be obtained by minimizing the system's free energy with respect to the order parameter that characterizes the mean field. The order parameter not only characterizes changes in the degree of order during a transition, but also describes most crucial properties of the final ordered state. The thermodynamic approach, which involves minimization of the free energy with respect to order parameters, differs from the first method.

To determine equilibrium properties of an ordering crystal $A_{1-x}B_x$ at a given temperature T and preset component concentration x, it is necessary to find the statistical sum

$$Z = \sum_n exp(-E_n/T), \tag{4.3}$$

where E_n is the crystal energy in a state n.

If n stands for states with different mutual arrangements of atoms, the expression $-T \ln Z$ expresses the configuration part of the free energy. The configuration energy E_n can be presented as the energies of interaction between pairs of atoms located at different distances ρ_l (ρ_l is the radius of the $l-$th coordination sphere). For a binary solution $A-B$, the configuration energy is

$$E_n = -\sum_l [N^l_{AA}\epsilon_{AA}(\rho_l) + N^l_{BB}\epsilon_{BB}(\rho_l) + N^l_{AB}\epsilon_{AB}(\rho_l)], \tag{4.4}$$

where $\epsilon(\rho_l)$ denotes the energies of corresponding paired interatomic interactions at distances ρ_l and N^l is the number of corresponding pairs of these atoms. In the approximation allowing for the interaction of nearest neighbors only, E_n has the form

$$E_1 = -(N_{AA}\epsilon_{AA} + N_{BB}\epsilon_{BB} + N_{AB}\epsilon_{AB}). \tag{4.5}$$

If a crystal comprises N_A atoms of species A and N_B atoms of species B, while

the number of pairs of unlike atoms in the first coordination sphere is N_{AB}, then the number of pairs of like atoms will be

$$\begin{aligned} N_{AA} &= (zN_A - N_{AB})/2, \\ N_{BB} &= (zN_B - N_{AB})/2. \end{aligned} \tag{4.6}$$

And then we can rewrite the Eq. 4.5 in the following form:

$$E_1 = -\frac{1}{2}(z(N_A\epsilon_{AA} + N_B\epsilon_{BB}) + VN_{AB}), \tag{4.7}$$

where $V = 2\epsilon_{AB} - \epsilon_{AA} - \epsilon_{BB}$ is the mixing energy. (We use for the $A_{1-x}M_x$ alloy in the local propagator (Eq. 3.56) the same configuration cluster energy, where are $\epsilon_{AA} \to \lambda_{AA}$, $\epsilon_{BB} \to \lambda_{MM}$, $V \to \lambda_{AM}$).

For example, the Gorsky-Bragg-Williams theory Krivoglaz and Smirnov [1964] underlying this ordering theory is that probabilities of species A or B atoms occupying a given lattice site are independent of the atomic configuration at the surrounding sites. They are determined only by the concentration of components and the degree of long-range order parameter which is determined as a certain deviation of the probability from its value x of the B atoms in the disordered solution. In other words, the long-range order parameter alone is sufficient for an adequate description of the system in that theory at a given composition of solid solution, while short-range correlations of atoms are disregarded.

However direct application of the Gorsky-Bragg-Williams theory for the description of the ordering in solid solutions, for example, in $CuAu$ structure leads to a qualitatively erroneous conclusion Krivoglaz and Smirnov [1964], Gusev et al. [2001] that the order-disorder transition represents a phase transformation of the second kind. But atomic ordering in solid solutions with this structure proceeds as a phase transformation of the first kind. In this case, the approximation, which disregards correlation, proves to be too rough.

The $A_{1-x}M_x$ theory is more complicated then the Gorsky-Bragg-Williams one. But it is also a mean field theory, where a long-range order parameter is a magnetization $\langle S^z \rangle$ which characters by the indirect $MRKKY$ interaction between the localized spins of two magnetic atoms with a configuration energy of magnons likes to the Eq. (4.4) (many shells) that was gotten by used of the configurational average spin Green function of the Eq. (2.49) and leads to a conclusion about the phase transformation of the first kind. And if we restrict this average magnon Green function to the VCA one (Eq. 2.45) with a configuration energy of magnons likes to the Eq. (4.5) that leads to the order-disorder transition represents a phase transformation of the second kind what is the same in the Gorsky-Bragg-Williams theory of the atomic ordering.

5. Summary & Outlook

In this dissertation, the electronic and magnetic properties of the disorder Kondo lattice model for the $A_{1-x}M_x$ alloy are studied by performing a model calculation followed by its application to real materials like DMS which can be well described within the model under consideration. The generalization of the system is always cross-checked by comparing the results with that of the regular variation and also to other limiting cases of the model. This allows us to systematically study of the disordered effects and the exchange coupling of the system and the nature of its physical origin of the ferromagnetism. The electronic and magnetic sub-systems are treated within certain approximations and an attempt is made in order to understand the properties of the disorder $A_{1-x}M_x$ KLM.

In Chapter 2, we describe the Heisenberg problem. It is governed by the inter-atomic exchange between the two localized moments at each site on a periodic lattice. There is an interaction between not only nearest-neighbor magnetic atoms but also between any two atoms in a certain cavity. In order to solve this model we utilize the Greens function theory and equation of motion method. This chapter deals only with the magnetic properties of the model i.e. calculating the magnon density of states of the magnetic sub-system, and also the magnetization by used the Callen ansatz.

We extend the theory to the disordered situation where the system consists of the magnetic M and nonmagnetic A atoms and thereby propose one technique for studding such alloy systems. In the disorder model we have an additional parameter i.e. concentration of magnetic atoms x apart from the exchange parameters between localized magnetic moments in the different shells which we can get self-consistency from the electronic subsystem.

Chapter 3 deals with the disorder KLM and its electronic properties such as the quasiparticle energy excitations and the temperature dependent correlation effects. Starting from an alloy analogy based on the exactly known zero-bandwidth limit and the interpolating self-energy approach with and without the cluster contribution of the KLM we applied a CPA procedure to find out the reaction of the electronic spectrum on the random mixture of magnetic and nonmagnetic atoms. The analytical expression for the electronic selfenergy has been used then to get the effective exchange integrals of the modified RKKY theory.

In order to apply the disorder KLM theory which might be helpful in explaining the basic mechanism of ferromagnetism in $Ga_{1-x}Mn_xAs$, we concentrated more our calculations on the low x regime ($x < 0.2$). For the realistic input parameters in the theory we obtained the similar Curie temperature as are the experimental results.

In Chapter 4, we develop the disorder KLM which treats the subsystems

of itinerant charge carriers and localized magnetic moments in a homologous manner. It concerns with configurational averaging out the electronic charge degrees of freedom thereby mapping the disorder Kondo lattice model onto an effective disorder Heisenberg exchange model. The exchange integrals are temperature dependent due to the fact that they depend on the electronic self-energy which in turn is governed by the temperature dependence of magnetization. Thus, both the electronic and magnetic sub-systems are calculated within a self consistent approach.

As a result, we obtain the T_c as a function of intra-atomic exchange J, band occupation n and concentration of the magnetic atoms x. There is no direct interaction between the localized moments. Therefore the collective order is caused by the indirect interaction mediated by the itinerant band electrons. Consequently, the indirect momentum coupling strongly depends on electronic model parameters such as exchange coupling J and band occupation n. A further important parameter is of course the concentration of magnetic atoms x. The interactions found by modified RKKY resemble those of the conventional RKKY only in the low coupling limit ($J \sim 0$). In the large coupling regime the originally long-range interaction transforms into short-range interaction, where only the nearest-neighbor interaction is important. But we found that for intermediate couplings the effective exchange interaction between the localized magnetic moments is strongly non-linear for small concentration x of magnetic atoms. Another important finding is an influence of the disorder on the magnon excitations for small concentrations of magnetic atoms. We found rather different results for the magnetic excitations in, respectively, VCA and the local quadratic approach. It is clear that VCA yields too simple expressions for the magnon Green's function. Our results show that for small concentrations the disorder effects are also very important. Such effects play an important role for the understanding and controlling key-properties such as the Curie temperature. We see that disorder changes very drastically the magnon-DOS in particular for low energy excitations being decisive for the resulting values of the Curie temperature.

So, we have performed a self-consistent model calculation of the electronic and magnetic properties of diluted local-moment systems $A_{1-x}M_x$ described by ferromagnetic Kondo-lattice model ($s-f$ model), where we included disorder in the first environment shell by use of crystal field parameters between two non-magnetic, one magnetic and non-magnetic, and two magnetic atoms, respectively $\lambda^{AA}, \lambda^{AM}, \lambda^{MM}$. The electronic self-energy was derived by a Green's function formalism (Interpolating Self-energy Approach) previously developed and tested for the normal KLM. The CPA treatment had to be generalized to include the crystal fields effects and the resulting self-energy turns out to be dependent on the magnetization of the disordered local-moment system. This quantity was determined by mapping the interband exchange interaction of the KLM on an effective Heisenberg model solved in VCA. Finally we arrived at a closed system of equations which could be solved self-consistently for the electronic and magnetic properties of the diluted local-moment system.

We consider also the self-consistent model calculation of the electronic and magnetic properties of diluted local-moment systems $A_{1-x}M_x$ model system,

where we included disorder in the first environment shell by use of crystal field parameters between two non-magnetic, one magnetic and non-magnetic, and two magnetic atoms, respectively $\lambda^{AA}, \lambda^{AM}, \lambda^{MM}$. In principle, they must be calculated by a self-consistent procedure together with the effective exchange Heisenberg constants, for example. But the complexity of the problem did not yet allow us to realize this strategy. From the magnon DOS we can conclude that for better fitting of our results to the Quantum Monte Carlo calculation it is necessary to support large values of the crystal field between two magnetic atoms λ^{MM}. The crystal field effects play a crucial role for understanding and controlling key-properties such as the Curie temperature. We have seen that disorder effects in the first environment shell change very drastically the Curie temperature.

We find (Refs. Bryksa and Nolting [2008a,b]) a sharp rise of T_c for very low magnetic atoms concentration x which basically highlight their role in stabilizing the T_c . In order to further prove this self-consistent model of DMS and also to understand an anomaly in the low concentration behavior of magnetic atoms, we are planing to consider the DFT calculation for the $III_{1-x}Mn_xV$ semiconductors Müller and Nolting [2002], Schiller [2000], S.Schwieger and W.Nolting [2002]. It helps to clarify three important facts as observed experimentally. First it indicates the presence of impurities existing at the top of the valence band Kikoin and Fleurov [1994], Bhattacharjee [1992], Dietl et al. [2000], secondly it explains the anomalous behavior of the temperature dependent optical conductivity Singley et al. [2002], Craco et al. [2003] and lastly it provides the reason for the experimentally reported wide range of T_c Ohno [1999], Iye et al. [1999], Dietl et al. [2000], Ohno et al. [2002], Wojtowicz et al. [2003], Jungwirth et al. [2006].

Thus the carrier-mediated mechanism (RKKY) is responsible for observed experimental Curie temperature. And according to our theory, the disorder effects have a large influence on the T_c value. This result has to be experimentally verified and has to be evaluated theoretically within a realistic electronic structure calculation which forms the outlook of this thesis.

A. Finite lattice calculation

The functions of $\frac{1}{N}\sum_{\vec{q}} P(\vec{q};E)$, $\frac{1}{N}\sum_{\vec{q}} Q(\vec{q};E)$ (Eq. 2.49) for the magnetic subsystem and $J(\vec{k})$ (Eq. 3.10) for the electronic subsystem are in an unsuitable form for numerical calculations. In this appendix these functions will be expressed in terms of a finite lattice sum of products like $f_i(\vec{k})C_i(E)$. The $f_i(\vec{k})$'s are explicit real functions of $\vec{k}$ and the $C_i(E)$'s are lattice-structure-dependent, complex functions of E, which are dependent on a number of the i's shell (see on the inset of Fig. A.1.

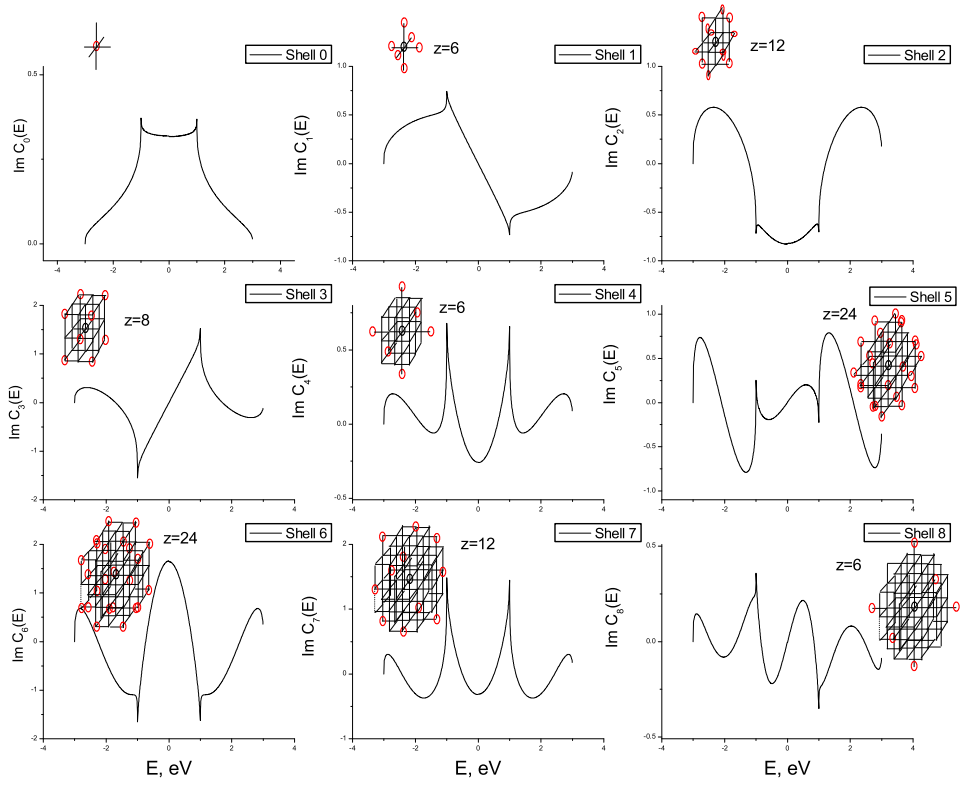

Abbildung A.1.: Dependence of the imagery part of the $C_i(E)$ function (Eq. 3.10) on the energy E in a simple cubic lattice for several shells. In the inset is the shell structure of the given cluster.

We start with function

$$\frac{1}{N}\sum_{\vec{q}} Q(\vec{q};E) = \frac{1}{N}\sum_{\vec{q}} \frac{(J(\vec{k}-\vec{q})-J(\vec{k}))(J(\vec{k}-\vec{q})-J(\vec{q}))}{E-2(J(0)-J(\vec{q}))}, \qquad \text{(A.1)}$$

where $J(\vec{k}) = \sum_{\vec{\rho}} J_{\vec{\rho}} e^{\vec{k}\vec{\rho}}$, $\vec{\rho}$ being the lattice vectors, reduces to $\sum_{\vec{\rho}} J_{\vec{\rho}} cos(\vec{k}\vec{\rho})$ due to the inversion symmetry of the cubic lattices.

Inserting this lattice dispersion into Eq. A.1 one obtains

$$\begin{aligned} \frac{1}{N}\sum_{\vec{q}} Q(\vec{q};E) &= \sum_{\vec{\rho_1},\vec{\rho_2}} J(\vec{\rho_1})J(\vec{\rho_2})[cos(\vec{\rho_1}\vec{k}) - cos((\vec{\rho_1}+\vec{\rho_2})\vec{k})] \\ &\quad \times \frac{1}{N}\sum_{\vec{q}} \frac{cos(\vec{\rho_1}\vec{q}) - cos((\vec{\rho_1}+\vec{\rho_2})\vec{q})}{E - 2(J(0) - J(\vec{q}))}. \end{aligned} \tag{A.2}$$

First of all, it is useful to introduce the following notation for the q'sum in Eq. A.2;

$$C_{\vec{\rho}}(E) = \frac{1}{N}\sum_{\vec{q}} \frac{cos(\vec{\rho}\vec{q})}{E - 2(J(0) - J(\vec{q}))} \tag{A.3}$$

It is thus convenient to express the sums in Eq. A.3 as sums over shells and over lattice vectors within the shells, i.e.,

$$\sum_{\vec{\rho}} \rightarrow \sum_i \sum_{\vec{a_i}}, \tag{A.4}$$

where $\vec{a_i}$ is a lattice vectors in the ith shell.

The $C_{\vec{\rho}}(E)$ function depends only on the shell in which the lattice vector $\vec{\rho}$ lies and we introduce a new function $C_i(E)$ which is characterized the properties of i's shell.

$$C_i(E) = \frac{1}{N}\sum_{\vec{q}} \frac{\gamma_i(\vec{q})}{E - 2(J(0) - J(\vec{q}))}, \tag{A.5}$$

where

$$\gamma_i(\vec{q}) = \frac{1}{z_i}\sum_{\vec{a_i}} cos(\vec{a_i}\vec{q}) \tag{A.6}$$

is the crystal lattice sum over all z_i sites in the ith shell

Actually we thus obtain the final the $\frac{1}{N}\sum_{\vec{q}} Q(\vec{q};E)$ expression for the numerical calculations:

$$\begin{aligned} \frac{1}{N}\sum_{\vec{q}} Q(\vec{q};E) &= \sum_{i,j} J_i J_j (z_i C_i(E)\gamma_j(\vec{k}) - \frac{1}{z_j}\gamma_j(\vec{k})\sum_m N_{ij}(m) z_m C_m(E) \\ &\quad + \sum_m N_{ij}(m)\gamma_m(\vec{k})[C_m(E) - C_i(E)]) \equiv \sum_i f_i(\vec{k}) C_i(E), \end{aligned} \tag{A.7}$$

where $N_{ij}(m)$ is the number of times the mth shell is covered by all possible combinations of two successive steps, of order i and of order j (Lavis and Bell [1999]). Several values of $N_{ij}(m)$ and other topological parameters for the simple cubic lattices are given in Table A.1.

Similarly one gets for $\frac{1}{N}\sum_{\vec{q}} P(\vec{q};E)$,

$$\frac{1}{N}\sum_{\vec{q}} P(\vec{q};E) = \sum_i J_i (C_i(E) - C_0(E))\gamma_i(\vec{k}). \tag{A.8}$$

$C_i(E)$ at $E + i\epsilon$ is a complex function of E. Its imagery part is nonvanishing only in the interval of E. It is more convenient to calculate $ImC_i(E)$ first and

Tabelle A.1.: Several topological parameters for a simple cubic lattice

i	z_i	$N_{11}(i)$	$N_{12}(i)$	$N_{22}(i)$
Shell	Num.of atoms in i-th shell	Covering factors for the i-th shell		
1	6	0	4	0
2	12	2	0	4
3	8	0	3	0
4	6	1	0	4
5	24	0	1	0
6	24	0	0	2
7	12	0	0	1

then obtained $ReC_i(E)$ by use of the Kramers-Kroning relation,

$$ReC_i(E) = \frac{1}{\pi} P \int_{-\infty}^{\infty} \frac{ImC_i(E_1)}{E - E_1} dE_1. \tag{A.9}$$

Let start with the calculation for $ImC_0(E)$. Using the following relations:

$$i(C_0(E + i\epsilon) - C_0(E - i\epsilon)) = 2ImC_0(E), \tag{A.10}$$

$$\frac{1}{E - x + i\epsilon} - \frac{1}{E - x - i\epsilon} = -2i\pi\delta(E - x), \tag{A.11}$$

we obtain the expression for $ImC_0(E)$:

$$ImC_0(E) = \pi \frac{1}{N} \sum_{\vec{q}} \delta(E - 2(J(0) - J(\vec{q}))). \tag{A.12}$$

For the cubic space groups of a simple cubic lattice the magnon dispersion $J(\vec{q})$ with only nearest-neighbor hopping leads to the wellknown spectra

$$J(\vec{q}) = J_1(cosq_x + cosq_y + cosq_z). \tag{A.13}$$

Setting $l_i = cosq_i$ and observing the symmetry the integral in Eq. A.12 is transformed into

$$ImC_0(E) = 8\pi \int_{-1}^{1} \int_{-1}^{1} \int_{-1}^{1} \frac{\delta(E - 2J_1 - 2J_1(l_1 + l_2 + l_3)) dl_1 dl_2 dl_3}{\sqrt{(1 - l_1^2)(1 - l_2^2)(1 - l_3^2)}}. \tag{A.14}$$

After introducing a new notation for the energy $E \to \frac{E - 2J_1}{2J_1}$ and the integration over l_3, it is easily performed the Eq. A.14 and leads to

$$ImC_0(E) = \frac{4\pi}{J_1} \int \int_L \frac{dl_1 dl_2}{\sqrt{(1 - l_1^2)(1 - l_2^2)(1 - (E + l_1 + l_2)^2)}}, \tag{A.15}$$

where the domain L given by the section of a square of the sides 2, which lies symmetrically to the origin, and the band defined by the inequality $|E + l_1 +$

$l_2| \leq 1$ (see Ref. Jelitto [1969]).

The integration over l_1 and l_2 in the Eq. A.15 may by performed explicitly and leads to complete elliptic integrals of the first kind Jelitto [1969]. The function $ImC_0(E)$ without $2J_1$ scaling is plotted in Fig. A.1.

Similarly one used strategy of the numerical calculation of the higher imagery part $ImC_i(E)$ which are plotted also in Fig. A.1.

So, now we can calculate the such complicated sums as $\frac{1}{N}\sum_{\vec{q}} Q(\vec{q};E)$ and $\frac{1}{N}\sum_{\vec{q}} P(\vec{q};E)$ just put the numerical calculation of the $C_i(E)$ functions into Eq. A.7 and Eq. A.8, correspondingly, with such high precision (many shells) as we want.

Using the same technique we can calculate also the modified RKKY integrals (Eq. 3.10):

$$J_{\vec{q}} = \frac{J^2}{4\pi}\int_{-\infty}^{\infty} \frac{dE}{e^{\beta(E-\mu)}+1} \frac{1}{N}\sum_{\sigma,\vec{k}} Im\left[G^0_{\vec{k}}(E)\, G_{\vec{k}+\vec{q},\sigma}(E)\right]. \tag{A.16}$$

And then using the the inverse Fourier transformation

$$J_{ij} = \frac{1}{N}\sum_{\vec{q}} J_{\vec{q}} e^{-i\vec{q}(\vec{R}_i-\vec{R}_j)} \tag{A.17}$$

in order to obtain the distance dependent MRKKY interaction of the magnetic atoms.

We can write (see Ref. Georges et al. [1996])

$$\sum_{\vec{k}} G^0_{\vec{k}}(E)\, G_{\vec{k}+\vec{q},\sigma}(E) = \sum_{ij} e^{-i\vec{q}(\vec{R}_i-\vec{R}_j)} G^0_{ij}(E)\, G_{ij,\sigma}(E). \tag{A.18}$$

So, now we change the Eq. A.16

$$\begin{aligned} J_{\vec{q}} &= \tfrac{1}{N}\textstyle\sum_{ij}\{\tfrac{J^2}{4\pi}\sum_\sigma Im\int_{-\infty}^{\infty}\tfrac{dE}{e^{\beta(E-\mu)}+1} G^0_{ij}(E)\, G_{ij,\sigma}(E)\} e^{-i\vec{q}(\vec{R}_i-\vec{R}_j)} \\ &= \textstyle\sum_{ij} J_{ij} e^{-i\vec{q}(\vec{R}_i-\vec{R}_j)}, \end{aligned} \tag{A.19}$$

and we have following the equation for J_{ij}:

$$J_{ij} = \frac{J^2}{4\pi}\sum_{\sigma} Im\int_{-\infty}^{\infty} \frac{dE}{e^{\beta(E-\mu)}+1} G^0_{ij}(E)\, G_{ij,\sigma}(E). \tag{A.20}$$

After expressing Eq. A.20 in the shell presentation (see. Eq. A.4)

$$J_n = \frac{J^2}{4\pi}\sum_{\sigma} Im\int_{-\infty}^{\infty} \frac{dE}{e^{\beta(E-\mu)}+1} G^0_{n}(E)\, G_{n,\sigma}(E), \tag{A.21}$$

where n is the shell number and $\vec{a_i}$ is one vector in the nth shell. For the

noninteracting Green function $G_n^0(E)$ we have the following expression:

$$\begin{aligned} G_n^0(E) &= \sum_{\vec{a_i}} \frac{1}{N} \sum_{\vec{k}} e^{i\vec{k}\overrightarrow{R_{n,\vec{a_i}}}} G_{\vec{k}}^0(E) \\ &= \frac{1}{N} \sum_{\vec{k}} \sum_{\vec{a_i}} \int_{-\infty}^{\infty} dx \delta(x - t_{\vec{k}}) e^{i\vec{k}\overrightarrow{R_{n,\vec{a_i}}}} G_x^0(E) = \int_{-\infty}^{\infty} dx \rho_n(x) G_x^0(E), \end{aligned} \tag{A.22}$$

where

$$G_x^0(E) = \frac{1}{E - x + i\epsilon}, \tag{A.23}$$

and $\rho_n(x)$ is the imagery part of the $C_i(E)$ function (see Eq. A.5):

$$\rho_n(x) = \frac{1}{N} \sum_{\vec{k}} \gamma_n(\vec{k}) \delta(x - t_{\vec{k}}). \tag{A.24}$$

And for the interacting Green function $G_{n,\sigma}(E)$ we have the similar expression:

$$G_{n,\sigma}(E) = \int_{-\infty}^{\infty} dx \rho_n(x) G_{x,\sigma}(E), \tag{A.25}$$

where

$$G_{x,\sigma}(E) = \frac{1}{E - x - \Sigma_\sigma(E)}. \tag{A.26}$$

B. Cumulant technique

If we haven't an exact formula for the partition function we have to choose between a compact presentation and a series expansion. The finite sum of this series is usually regular and we can extrapolate this series to infinite ones which is studied in the quantum statistical and thermodynamical theory. For example, a singularity in this infinite sum means a possibility of phase transition.

A presentation of the series coefficients in a form of combinatorial ones which are connected with the enumeration of lattice diagrams is very important aspect of a modern physics of disorder materials.

Let start with the series for a partition function for high temperature case, where β is a small parameter.

$$\begin{array}{l} Z = \langle exp(-\beta\hat{H})\rangle = 1 - \beta\langle\hat{H}\rangle + \\ \frac{1}{2}\beta^2\langle\hat{H}^2\rangle - ... + \frac{1}{n!}(-\beta)^n\langle\hat{H}^n\rangle + ... \end{array} \tag{B.1}$$

Here the brackets $\langle ...\rangle$ can mean the quantum thermodynamical average (the trace of operator) or the the configurational average over every configurational states of system.

For example, for Ising model

$$\beta\hat{H} = -\frac{1}{2}K\sum_{l,l'}\sigma_l\sigma'_l \tag{B.2}$$

the brackets mean a sum over everything value, ± 1, for a every spin of σ_l.

So, now we can calculate every term in the series expansion (Eq. B.1) for the Ising model (Eq. B.2). For example, for the $\langle\hat{H}^n\rangle$ term we would be to have at least the K^n multiplier and the $\langle\sigma_1\sigma_2...\sigma_{2n}\rangle$ average which is a product of the binary multipliers, like to, $\langle\sigma_1\sigma_2\rangle$, $\langle\sigma_3\sigma_4\rangle$, i.e. The spin number $1, 2, 3, 4, ...2n$ in the every products are equivalent of numbered nodes in a lattice which we can only combine in pairs $(1-2, 3-4, ..., 2n-1, 2n)$ because there are interactions between only neighboring atoms in the model.

But there are many topological equivalent diagrams (see, for example, in Fig. B.1) with the same contribution to the $\langle\sigma_1\sigma_2...\sigma_{2n}\rangle$ average and we have to find the number of the equivalent diagrams because it gives an additional combinatorial factor near the spin average (there can be at least $n!$ diagrams totally). In most cases such program of the partition function calculation isn't possible to realize even for not so big n.

But really we look for a free energy that corresponds to one lattice site and

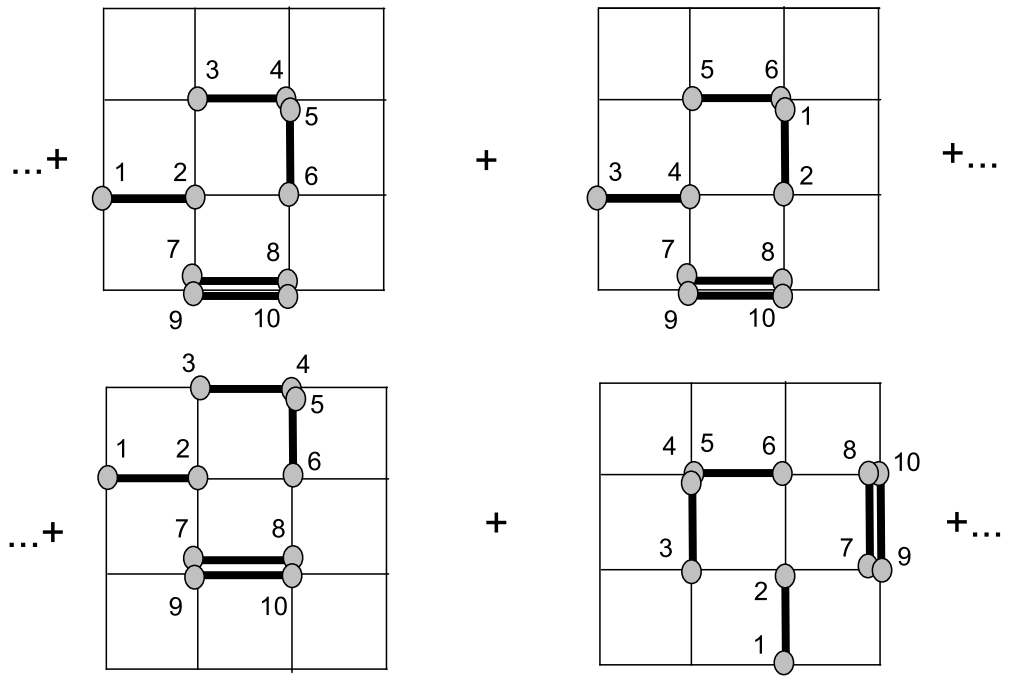

Abbildung B.1.: Binary diagrams on the square lattice and their topological equivalent ones.

which we can present also in a series expansion

$$lim_{N\to\infty}(\frac{1}{N}lnZ_N) = \sum_{(n=1)} \frac{1}{n!}c_n(-\beta)^n. \tag{B.3}$$

A link between the series expansion (Eq. B.3) and the series expansion for moments (Eq. B.1) is called a cumulant expansion and we can write following:

$$c_n \equiv \langle H^n \rangle_c, \tag{B.4}$$

where

$$\begin{aligned} &\langle H \rangle_c = \langle H \rangle, \\ &\langle H^2 \rangle_c = \langle H^2 \rangle - \langle H \rangle^2, \\ &\langle H^3 \rangle_c = \langle H^3 \rangle - 3\langle H \rangle \langle H^2 \rangle + 2\langle H \rangle^3, \\ &.... \end{aligned} \tag{B.5}$$

There is one very useful property of the cumulant expansion: a cumulant of product $\langle XY \rangle_c$ is zero if the X and Y multipliers are statistically independent (Ref. Uhlenbeck [1967], Uhlenbeck and Ford [1962]). For example, there is some contribution from $\langle H^n \rangle_c$, like to $\langle \sigma_1 ... \sigma_s \sigma_{s+1} ... \sigma_{2n} \rangle$ which is corresponded to a non bounding diagram or a non-irreducible one on the Fig (B.2). This contribution is zero. So, the $\langle ... \rangle_c$ cumulant is not zero for only irreducible diagrams or bounding ones. And this is a very big advantage compared to the moment expansion (Eq. B.1) we need calculate a sum for the only irreducible diagrams. A disadvantage of this technique is a multiline structure of high

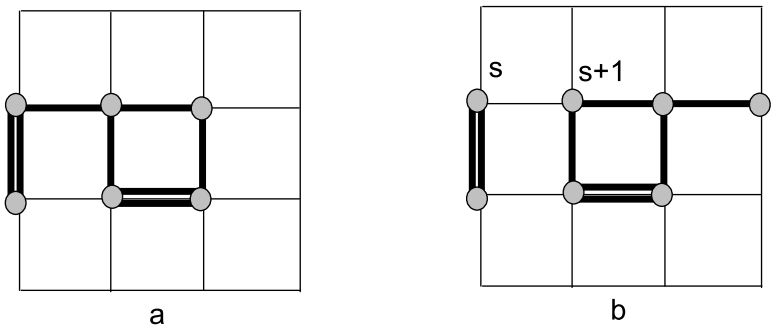

Abbildung B.2.: a) Irreducible diagram, b) Non-irreducible diagram.

cumulants (Fig B.2) which complicates the calculations.

We need mention that the cumulant expansion is a very universal procedure which is valid also for calculation of low temperature properties (Ref. Ziman [1979]).

For example, we need calculate the $\langle exp(\alpha g_i)\rangle_X$, then

$$\begin{array}{l} \langle e^{\alpha g_i}\rangle_X = e^{\sum_n \frac{1}{n!}\alpha^n \langle (g_i)^n\rangle_c}, \\ ln(\langle e^{\alpha g_i}\rangle) = \sum_n \frac{1}{n!}\alpha^n \langle (g_i)^n\rangle_c, \\ \langle (g_i)^n\rangle_c = \frac{d^n}{d\alpha^n}\langle e^{\alpha g_i}\rangle|_{\alpha\to 0}. \end{array} \tag{B.6}$$

At other hand we can write following expression for $\langle (g_i)^n\rangle$ like to the equation B.5:

$$\begin{array}{l} \langle g_i\rangle_X = \langle g_i\rangle_c, \\ \langle (g_i)^2\rangle_X = \langle (g_i)^2\rangle_c + (\langle g_i\rangle_c)^2, \\ \langle (g_i)^3\rangle_X = \langle (g_i)^3\rangle_c + 3\langle (g_i)^2\rangle_c\langle g_i\rangle_c + (\langle g_i\rangle_c)^3, \\ \langle (g_i)^4\rangle_X = \langle (g_i)^4\rangle_c + 4\langle (g_i)^3\rangle_c\langle g_i\rangle_c + 6\langle (g_i)^2\rangle_c\langle (g_i)^2\rangle_c + 6\langle (g_i)^2\rangle_c\langle g_i\rangle_c^2 + \langle g_i\rangle_c^4, \\ ... \end{array} \tag{B.7}$$

It is very useful a graphical presentation of these equations.

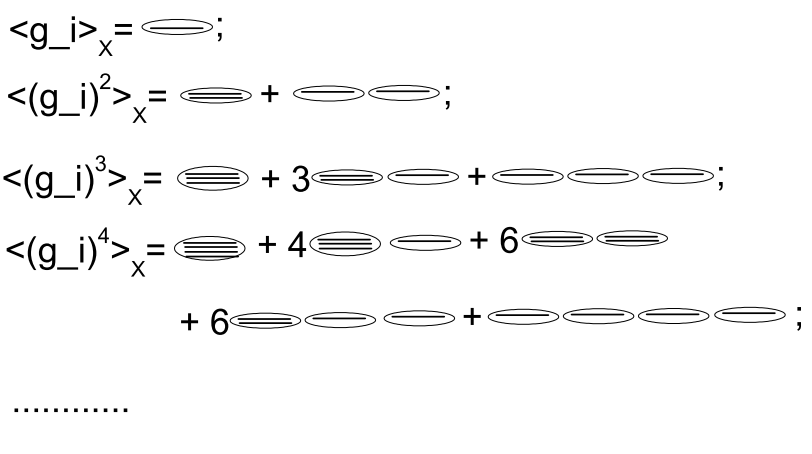

(B.8)

Here we use a horizontal line as the local Green function g_i, and a oval near the

line means a cumulant from this function, near two horizontal lines is a second cumulant and so on ... .The coefficients near the cumulants are obtained by used combinatorial rules, for example, for the third cumulant there are tree ways to gather two and one horizontal lines by two oval, respectively, where the total lines are three. So, there are three equivalent contributions, and we put the coefficient 3.

C. Larking presentation

Let start with a graphical solution of the Dyson equation:

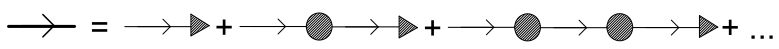

(C.1)

where notations for the full Green function, the zero Green function, a termination of the zero Green function and a full mass operator are given below, respectively:

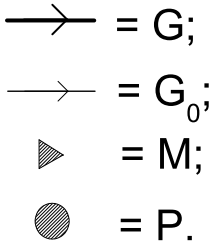

(C.2)

And also the termination M and mass P operators are consisted with the such diagrams which are irreducible in a term of the zero Green function G_0. Such definition means that we cannot split any diagram by two ones by cutting on the zero Green function line. Resulting, we can write the same used by the mathematical symbols:

$$\begin{aligned} &G = G_0M + G_0PG_0M + G_0PG_0PG_0M + ... = \\ &G_0M + G_0P(G_0M + G_0PG_0M + G_0PG_0PG_0M + ...). \end{aligned} \tag{C.3}$$

And the finished graphical and symbolic solutions are following, respectively:

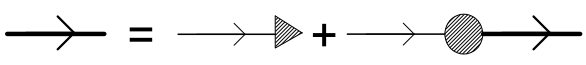

(C.4)

$$G = \frac{M}{(G_0)^{-1} - P}. \tag{C.5}$$

Now suppose that we don't know the zero Green function or there are some other problems with the definition of this zero Green function. But we can do a classification by used of a line of interaction, like to the hopping of an electron t_{ij} or the Heisenberg interaction of two spins J_{ij} in a lattice. And resulting we

have the following equation for finding the full Green function:

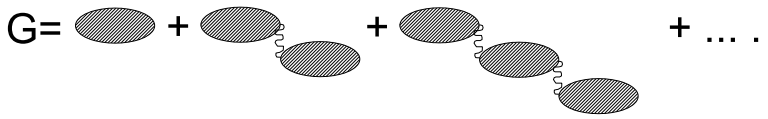

(C.6)

We write the same in the symbolic presentation, where the wave interaction line presents the hopping interaction t and the oval gives the Π operator, respectively:

$$\begin{aligned} G &= \Pi + \Pi t \Pi + \Pi t \Pi t \Pi + \Pi t \Pi t \Pi t \Pi + ... \\ &= \Pi + \Pi t (\Pi + \Pi t \Pi + \Pi t \Pi t \Pi + \Pi t \Pi t \Pi t \Pi + ...). \end{aligned} \tag{C.7}$$

The Π operator consists with the such diagrams which are irreducible in a term of the line of interaction t. What means that we cannot split any diagram in the oval by two ones by cutting on the interaction line. This irreducible is the Larking sense.

We write the solution for the Green function in the Larking presentation:

$$G = \frac{1}{(\Pi)^{-1} - t}. \tag{C.8}$$

There is a link between the Dyson and Larking equations, the Eq. C.1 and Eq. C.7, respectively. We write a solution for the Π operator in the following form:

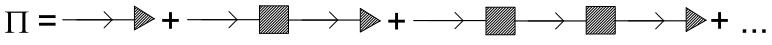

(C.9)

where the self-energy part is next

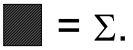

(C.10)

In the symbolic form we have the following

$$\Pi = G_0 M + G_0 \Sigma \Pi \tag{C.11}$$

And

$$\Pi = \frac{M}{(G_0)^{-1} - \Sigma} \tag{C.12}$$

Then we put this solution for Π into the Larking equation (C.8)

$$G = \frac{M}{(G_0)^{-1} - \Sigma + tM}. \tag{C.13}$$

After comparing the Eq. (C.13) and the Eq. (C.5) we have the link between the mass operator in the Dyson equation and the self-energy part of Π:

$$P = \Sigma - tM. \tag{C.14}$$

Acknowledgements

This work would not have been possible without the help of a lot of people and here, i take an opportunity to express my gratitude towards them.

It would have been unmanageable to successfully finish this work without the support of my supervisor, Prof. Wolfgang Nolting. I would like to thank him for giving me an opportunity to work in his group and for providing interesting projects, especially the problem regarding a disorder in alloys. His help has been instrumental in guiding me right from the beginning until the end of this work. I would like to appreciate his careful reading and comments on the initial version of this thesis and of course for translating the abstract in to German language. At various stages of this work, his valuable suggestions were like a strong field acting on my poly-directional thoughts and allowing them to point in the right direction.

I am also grateful to the Humboldt University at Berlin for the financial support throughout this work.

Thank you all.

Literaturverzeichnis

A.A. Abrikosov, A.D. Galanin, L.P. Gorkov, L.D. Landau, I.Ya. Pomeranchuk, and K.A. Ter-Martirosyan. Possibility of formulation of a theory of strongly interacting fermions. *Phys. Rev.*, 111:321–328, 1958.

P.W. Anderson. Antiferromagnetism. theory of superexchange interaction. *Phys. Rev.*, 79:350–356, 1930.

P.W. Anderson. Localized magnetic states in metals. *Phys. Rev.*, 124:41–53, 1961.

G. Bastard and C. Lewiner. Indirect-exchange interactions in zero-gap. *Phys. Rev. B*, 20:4256–4267, 1979.

A.K. Bhattacharjee. Interaction between band electrons and transitions-metal ions in diluted magnetic semiconductors. *Phys. Rev. B*, 46:5266–5273, 1992.

J.A. Blackman, D.M. Esterling, and N.F. Berk. Generalized locator-coherent-potential approach to binary alloys. *Phys. Rev. B*, 4:2412–2428, 1971.

N. Bloembergen and T.J. Rowland. Nuclear spin exchange in solids: tl_20_3 and tl_20_5 magnetic resonance in thallium and thallic oxide. *Phys. Rev.*, 97: 1679–1698, 1955.

N.N. Bogoliubov and S.V. Tyablikov. Retarded and advanced green functions in statistical physics. *Dokl. Akad. Nauk. SSSR*, 126:53–59, 1959.

G. Bouzerar and P. Bruno. Rpa-cpa theory for magnetism in disordered heisenberg binary systems with long-range exchange integrals. *Phys. Rev. B*, 66:014410/1–9, 2002.

G. Bouzerar, J. Kudrnovsky, and P. Bruno. Disorder effects in diluted ferromagnetic semiconductors. *Phys. Rev. B*, 68:205311/1–4, 2003.

R. Bouzerar, G. Bouzerar, and T. Ziman. Why rkky exchange integrals are inappropriate to describe ferromagnetism in diluted magnetic semiconductors. *Phys. Rev. B*, 73:024411/1–8, 2006a.

R. Bouzerar, G. Bouzerar, and T. Ziman. Non-perturbative j_{pd} model and ferromagnetism in diluted magnets. *cond-mat*, 0607640, 2006b.

V. Bryksa and W. Nolting. Disordered correlated kondo-lattice model. *J. Magn. Magn. Mater.*, 320:97–106, 2008a.

V. Bryksa and W. Nolting. Disordered kondo-lattice model: Extension of coherent potential approximation. *Phys. Rev. B*, 78:064417/1–9, 2008b.

W.H. Butler. Self-consistent cluster theory of disordered alloys. *Phys. Lett. A*, 39:203–204, 1972.

H.B. Callen. Green function theory of ferromagnetism. *Phys. Rev.*, 130:890–898, 1963.

W.J. Carr. Use of non-orthogonal wave functions in the treatment of solids, with applications to ferromagnetism. *Phys. Rev.*, 92:28–35, 1953.

L. Craco, M.S. Laad, and E. Muller-Hartmann. Ab initio description of the diluted magnetic semiconductor *gamnas*: ferromagnetic, electronic structure, and optical response. *Phys. Rev. B*, 68:233310/1–4, 2003.

T. Dietl, J. Cibert, P. Kossacki, D. Ferrand, S Tatarenko, Y. Merle A. Wasiela, dAubigne, F. Matsukura, N. Akiba, and H. Ohno. Ferromagnetism induced by free carriers in *p*-type structures of diluted magnetic semiconductors. *Physica E*, 7:967–975, 2000.

H. Dvey-Aharon and M. Fibich. Magnetic properties of a disordered substitutional alloy-heisenberg model. *Phys. Rev. B*, 18:3491–3506, 1978.

I.P. Dzyub. *Cluster theory of spin excitations in a dilute antiferromagnet, application to* $Mn_{1-c}Zn_cF_2$ *system.* Preprint of Institute for Theoretical Physics, Kyiv, 1973. ITP-73-105E.

I.P. Dzyub. *Cluster theory of spin excitations of mixed antiferromagnets, application to* $Mn_{1-c}Co_cF_2$ *and* $KMn_{1-c}Zn_cF_3$. Preprint of Institute for Theoretical Physics, Kyiv, 1974a. ITP-74-49E.

I.P. Dzyub. Cluster theory of a dilute antiferromagnet; application to the $mn_{1-c}zn_cf_2$ system. *Phys. Stat. Sol. (b)*, 61:383–392, 1974b.

D. Edwards, A. Green, and K. Kubo. Electronic structure and resistivity of the double exchange model. *J. Phys. C*, 11(13):2791–2808, Feb 1999.

S.F. Edwards. A new method for the evaluation of electronic conductivity in metals. *Phil. Mag.*, 3:1020–1031, 1958.

S.F. Edwards and R.C. Jones. A green function theory of spin waves in randomly disordered magnetic systems i. the ferromagnet. *J. Phys. C*, 4:2109–2126, 1971.

R.J. Elliott, J.A. Krumhansl, and P.L. Leath. The theory and properties of randomly disordered crystals and related physical systems. *Rev. Mod. Phys.*, 46:465–543, 1974.

J.K. Furdyna. Diluted magnetic semiconductors. *J. Appl. Phys.*, 64:R29–R64, 1988.

A. Georges, G. Kotliar, W. Krauth, and M. J. Rozenberg. Dynamical mean-field theory of strongly correlated fermion systems and the limit of infinite dimensions. *Rev. Mod. Phys.*, 68:13–125, 1996.

A.I. Gusev, A.A. Rempel, and A.J. Magerl. *Disordered and Order in Strongly Nonstoichiometric Compounds*. Springer, Berlin, 2001. ISBN 3-540-41817-2.

A.B. Harris, P.L. Leath, B.G. Nickel, and R.J. Elliott. Excitations in the dilute heisenberg ferromagnet using the coherent potential approximation. *J. Phys. C*, 7:1693–1718, 1974.

W. Heisenberg. Zur theorie des ferromagnetismus. *Zeits. f. Physik*, 49:619–625, 1928.

A.C. Hewson. *The Kondo Problem to Heavy Fermions*. Cambridge University Press, 1997.

T. Hickel. *Theory of many-body effects in the Kondo-lattice model - projection-operator method*. PhD thesis, Humboldt Universität zu Berlin, Germany, 2005. http://edoc.hu-berlin.de/dissertationen/hickel-tilmann-2005-09-23/PDF/hickel.pdf.

T. Hickel and W. Nolting. Proper weak-coupling approach to the periodic $s - d(f)$ exchange model. *Phys. Rev. B*, 69:85110/1–11, 2004.

S. Hilbert and W. Nolting. Disorder in diluted spin systems. *Phys. Rev. B*, 70:165203–165211, 2004.

K. Hirakawa, S. Katsumoto, T. Hayashi, Y. Hashimoto, and Y. Iye. Double-exchange-like interaction in *gamnas* investigated by infrared absorption spectroscopy. *Phys. Rev. B*, 65:193312/1–4, 2002.

W. Hoerstel, W. Kraak, W.T. Masselink, Yu.I. Mazur, G.G. Tarasov, A.E. Belyaev, and E.V. Kuzmenko. Peculiarities of the exchange interaction in narrow-gap *hgcdmnse*. *Semicon. Sci. Technol.*, 14:820–828, 1999.

N.L. Huang and R. Orbach. Biquadratic superexchange. *Phys. Rev. Lett.*, 12: 275–276, 1964.

V. Yu. Irkhin and M. I. Katsnelson. Half-metallic ferromagnets. *Physics-Uspekhi*, 37:705–724, 1994.

V.A. Ivanov, P.M. Krstajic, F.M. Peeters, V.N. Fleurov, and K.A. Kikoin. On the nature of ferromagnetism in diluted magnetic semiconductors: *gaas* : *mn*, *gap* : *mn*. *Journal of Magnetism and Magnetic Materials*, 258:237–240, 2003.

Y. Iye, A. Oiwa, A. Endo, S. Katsumoto, F. Matsukura, A. Shen, H. Ohno, and H. Munekata. Metal-insulator transition and magnetotransport in $iii - v$ compound diluted magnetic semiconductors. *Materials Science and Engineering B*, 63:88–95, 1999.

Yu.A. Izyumov. The hubbard model in the regime of strong electronic correlation. *Physics-Uspekhi*, 38:385–410, 1995.

Yu.A. Izyumov. The $t - j$ model for strongly correlated electrons and high-t_c superconductors. *Physics-Uspekhi*, 40:445–477, 1997.

R.J. Jelitto. The density of states of some simple excitations in solids. *J. Phys. Chem. Solids*, 30:609–626, 1969.

R.C. Jones. Impurity spin wave modes in a simple cubic heisenberg ferromagnet. *J. Phys. C*, 4:2903–2918, 1971.

T. Jungwirth, Jairo Sinova, J. Masek, J. Kucera, and A.H. MacDonald. Theory of ferromagnetic $(iii, mn)v$ semiconductors. *Rev. Mod. Phys.*, 78:809–865, 2006.

T. Kasuya. A theory of metallic ferro- and antiferromagnetism on zener's model. *Prog. Theor. Phys.*, 16:45–51, 1956.

M.P. Kennet, M. Berciu, and R.N. Bhatt. Monte carlo simulations of an impurity-band model for $iii - v$ diluted magnetic semiconductors. *Phys. Rev. B*, 66:045207/1–16, 2002a.

M.P. Kennet, M. Berciu, and R.N. Bhatt. Two-component approach for thermodynamic properties in diluted magnetic semiconductors. *Phys. Rev. B*, 65:115308/1–11, 2002b.

J. Kienert and W. Nolting. Curie temperature of kondo lattice films with finite itinerant charge carrier density. *Phys. Rev. B*, 75:094401/1–9, 2007.

K.A. Kikoin and V.N. Fleurov. *Transition Metal Impurities in Semiconductors*. World Scientific Publishing, Singapore, 1994.

J. Kondo. Resistance minimum in dilute magnetic alloys. *Prog. Theor. Phys.*, 32:37–43, 1964.

H.A. Kramers. Classical idea of electron spin. *Phys. Rev.*, 1:191–195, 1934.

M.A. Krivoglaz and A.A. Smirnov. *The theory of Order-Disorder in Alloys*. American Elservier, New York, 1964.

J. Kudrnovsky, I. Turek, V. Drchal, F. Maca, P. Weinberger, and P. Bruno. Exchange interaction in $ii - vi$ and group-iv diluted magnetic semiconductors. *Phys. Rev. B*, 69:115208/1–11, 2004.

D.A. Lavis and G.M. Bell. *Statistical Mechanics of Lattice Systems vol. II*. Springer, Berlin, 1999. ISBN 3-540-64436-9.

N. Lebedeva and P. Kuivalainen. Shift in the absorption edge due to exchange interaction in ferromagnetic semiconductors. *J. Phys.: Condens. Matter*, 14: 4491–4501, 2002.

L. Ley, M. Taniguchi, J. Ghijsen, and R. L. Johnson. Manganese-derived partial density of states in $cd_{1-x}mn_xte$. *Phys. Rev. B*, 35:2839–2843, 1987.

A.I. Liechtenstein, M.I. Katsnelson, V.P. Antropov, and V.A. Gubanov. Local spin density functional approach to the theory of exchange interactions in ferromagnetic metals and alloys. *J. Magn. Magn. Mater.*, 67:65–74, 1987.

G.V. Loseva, S.G. Ovchinnikov, and G.A. Petrakovskii. *Metal insulator transition in sulphides of* 3*d-metals*. Nauka, Novosybirsk, 1983. in Russian.

T. Matsubara and F. Yonezawa. Note on electronic state of random lattice ii. *Prog. Theor. Phys.*, 35:357–379, 1966.

D.C. Mattis. *The theory of magnetism*. Harper and Row, New York, 1965.

D. Meyer, C. Santos, and W. Nolting. Quantum effects in he qusiparticle structure of the ferromagnetic kondo lattice model. *J.Phys.:Cond.Mat.*, 13: 2531–2548, 2001.

T. Mizokawa and A. Fujimory. $p-d$ exchange interaction for $3d$ transition-metal impurities in $ii-vi$ semiconductors. *Phys. Rev. B*, 56:6669–6672, 1997.

T. Moriya. *Spin Fluctuations in itinerant electron magnetism*. Springer, Berlin, 1985. ISBN 3-540-15422-1.

Yukitoshi Motome and Nobuo Furukawa. Disorder effect on spin excitation in double-exchange systems. *Phys. Rev. B*, 71:014446/1–17, 2005.

W. Müller and W. Nolting. Temperature-dependent quasiparticle band structure of the ferromagnetic semiconductor *eus*. *Phys. Rev. B*, 66:085205/1–9, 2002.

J.A. Mydosh. *Spin glasses: an experimental introduction*. Taylor & Francis, 1993. ISBN 0-7484-0038-9.

E.L. Nagaev. *Physics of magnetic semiconducting*. Nauka, Moscow, 1979. in Russian.

W. Nolting. *Grundkurs Theoretische Physik, band* 7 *Viel-Teilchen-Theorie*. Springer, Berlin, 2005. ISBN 3-540-24117-5.

W. Nolting. Theory of ferromagnetic semiconductors. *Phys. Stat. Sol. B*, 96: 11–54, 1979.

W. Nolting and M. Matlak. Complete analytical solution for the zero bandwidth $s-f$ model. *Phys. Stat. Sol. B*, 123:155–168, 1984.

W. Nolting and A.M. Oles. Effect of finite band filling on the excitation spectrum of the $s-f$ model (magnetic semiconductors). *J. Phys. C*, 13: 823–836, 1980.

W. Nolting, W. Borgiel, and G. Borstel. Coulomb correlation effects in the quasiparticle band structure of ferromagnetic rare-earth insulators. *Phys. Rev. B*, 37:7663–7672, 1988.

W. Nolting, S. Mathi Jaya, and S. Rex. Magnetic polaron in ferro- and antiferromagnetic semiconductors. *Phys. Rev. B*, 54:14455–14466, 1996a.

W. Nolting, S. Rex, and Jaya S. Mathi. Magnetism and electronic structure of local moment ferromagnet. *J. Phys. C*, 9:1301–1330, 1996b.

W. Nolting, G. Reddy, A. Ramakanth, and D. Meyer. Low-density approach to the kondo-lattice model. *Phys. Rev. B*, 64:155109/1–10, 2001.

W. Nolting, G.G. Reddy, A. Ramakanth, D. Meyer, and J. Kienert. Self-energy approach to the correlated kondo lattice model. *Phys. Rev. B*, 67: 024426/1–8, 2003.

W. Nolting, T. Hickel, A. Ramakanth, G.G. Reddy, and M. Lipowczan. Carrier-induced ferromagnetism in concentrated and diluted local-moment systems. *Phys. Rev. B*, 70:075207/1–8, 2004.

H. Ohno. Properties of ferromagnetic $iii - v$ semiconductors. *Journal of Magnetism and Magnetic Materials*, 200:110–129, 1999.

H. Ohno, F. Matsukura, and Y. Ohno. Semiconductor spin electronics. *JSAP International*, 5:4–13, 2002.

E.M. Omelanovskii and V.I. Fistul. *Defect of transition metal ions in semiconductors*. Metalurgija, Moscow, 1983. in Russian.

R.G. Parr and W. Yang. *Density-Functional Theory of Atoms and Molecules*. Oxford University Press, 989.

Clas Persson and Alex Zunger. $s - d$ coupling in zinc-blend semiconductors. *Phys. Rev. B*, 68:073205/1–4, 2003.

S.J. Potashnik, K.C. Ku, R. Mahendiran, S.H. Chun, R.F. Wang, N. Samarth, and P. Schiffer. Saturated ferromagnetism and magnetization deficit in optimally annealed *gamnas* epilayers. *Phys. Rev. B*, 66:012408/1–4, 2002.

D.J. Priour and S. Sarma. Phase diagram of the disordered rkky model in diluted magnetic semiconductors. *Phys. Rev. Lett.*, 97:127201–127205, 2006.

S. Rex, V. Eyert, and W. Nolting. Temperature-dependent quasiparticle band-structure of ferromagnetic gadolinium. *J. Mag. Mag. Mat.*, 192:529–542, 1999.

M.A. Ruderman and C.Kittel. Indirect exchange coupling of nuclear magnetic moments by conduction electrons. *Phys. Rev.*, 96:99–102, 1954.

L.M. Sandratskii and P. Bruno. Electronic structure, exchange interaction and curie temperature in diluted $iii - v$ magnetic semiconductors: $(gacr)as$, $(gamn)as$, $(gafe)as$. *Phys. Rev. B*, 67:214402/1–11, 2003.

C. Santos and W. Nolting. Erratum: Ferromagnetism in the kondo-latice model. *Phys. Rev. B*, 66:019901(E), 2002a.

C. Santos and W. Nolting. Ferromagnetism in the kondo-lattice model. *Phys. Rev. B*, 65:144419/1–11, 2002b.

B. Sanyal, L. Bergqvist, and O. Eriksson. Ferromagnetic materials in the zinc-blende structure. *Phys. Rev. B*, 68:54417/1–7, 2003.

R. Schiller. *Correlation effects and temperature dependencies in thin ferromagnetic films - magnetism and electronic structure.* PhD thesis, Humboldt Universität zu Berlin, Germany, 2000. http://edoc.hu-berlin.de/dissertationen/schiller-roland-2000-11-01/PDF/Schiller.pdf.

A. Singh, S.K. Das, A. Sharma, and W. Nolting. Spin dynamics in the diluted ferromagnetic kondo lattice model. *J.Phys.:Cond.Mat.*, 19:236213/1–16, 2007.

Avinash Singh, Animesh Datta, K. Das Subrat, and Vijay A. Singh. Ferromagnetism in a dilute magnetic semiconductor: Generalized rkky interaction and spin-wave excitations. *Phys. Rev. B*, 68:235208/1–9, 2003.

E.J. Singley, R. Kawakami, D.D. Awscholom, and D. N. Basov. Infrared probe of itinerant ferromagnetism in *gamnas*. *Phys. Rev. Lett.*, 29:097203/1–4, 2002.

J.C. Slater. Atomic shielding constants. *Phys. Rev.*, 36:57–64, 1930.

S.Schwieger and W.Nolting. Long-range superexchange: An exchange interaction through empty bands. *Phys. Rev. B*, 65:205210/1–5, 2002.

K. Das Subrat and Avinash Singh. Enhancement of spin stiffness with dilution in a ferromagnetic kondo lattice model. *cond-mat*, 0506523, 2005.

Shih-Jye Sun and Hsiu-Hau Lin. Deluted magnetic semiconductor at finite temperatures. *Phys. Rev. Lett.*, cond-mat:0303328, 2003.

M. Takahashi and K. Kubo. Coherent-potential approach o magnetic and chemical disorder in diluted magnetic semiconductors. *Phys. Rev. B*, 60: 15858–15864, 1999.

M. Takahashi and K. Kubo. Mechanism of carrier-induced ferromagnetism in magnetic semiconductors. *Phys. Rev. B*, 66:153202/1–4, 2002.

M. Takahashi and K. Mitsui. Single-site approximation for $s - f$ model in ferromagnetic semiconductors. *Phys. Rev. B*, 54:11298–11304, 1996.

Masao Takahashi. Optical band edge of diluted magnetic semiconductors. *Phys. Rev. B*, 70:035207/1–16, 2004.

G. Tang and W. Nolting. Carrier-induced ferromagnetism in diluted local-moment systems. *Phys. Rev. B*, 75:024426/1–11, 2007.

A. Theumann and R.A. Tahir-Kheli. Excitations in randomly diluted ferromagnets. *Phys. Rev. B*, 12:1796–1818, 1975.

G.E. Uhlenbeck. Successive approximation methods in classical statistical mechanics. *Physica*, 26 (Suppl.1):S17–S29, 1967.

G.E. Uhlenbeck and G.W. Ford. *Studies in Statistical Mechanics*. Am. Math. Soc., Providence, 1962.

S. Vonsovskii. Electron theory of transition metals. *Zh. Eksperim. i Teor. Fiz. (Soviet Phys. JETP)*, 16:981, 1946.

T. Wojtowicz, G. Cywinski, W.L. Lim, X. Liu, M. Dobrowolska, J. K. Furdyna, K. M. Yu, W. Walukiewicz, G.B. Kim, M. Cheon, X. Chen, S.M. Wang, and H. Luo. *inmnsb* - a new narrow gap ferromagnetic semiconductor. *Appl. Phys. Lett.*, 82:4310–4312, 2003.

Min-Fong Yang, Shih-Jye Sun, and Ming-Che Chang. Comment on theory of diluted magnetic semiconductor ferromagnetism. *Phys. Rev. Lett.*, 86:5636, 2001.

K. Yosida. Magnetic properties of $cu - mn$ alloys. *Phys. Rev.*, 106:893–898, 1957.

I.R. Yukhnovskii. *Phase Transitions of the Second Order. Collective Variables Method*. World Scientific, Singapore, 1987.

I.R. Yukhnovskii and Z.A. Gurskii. *Quantum-statistical Theory of Disordered Systems*. Naukova Dumka, Kiev, 1991. in Russian.

C. Zener. Interaction between the s-shells in the transition metalss. ii. ferromagnetic compounds of manganese with perovskite structure. *Phys. Rev.*, 82:403–405, 1951.

C. Zhou, M.P. Kennett, X. Wan, M. Berciu, and R.N. Bhatt. Exchange anisotropy, disorder, and frustration in diluted, predominantly ferromagnetic, heisenberg spin systems. *Phys. Rev. B*, 69:144419/1–9, 2004.

J.M. Ziman. *Models of disorder: The theoretical physics of homogeneously disordered systems*. Cambridge University Press, Cambridge, 1979.

D.N. Zubarev. Double-time green functions in statistical physics. *Soviet Phys. Usp.*, 71:71–80, 1960.

Abbildungsverzeichnis

2.1. There is a schematic presentation of the crystal lattice Heisenberg model. A circle in the lattice node shows an atom. An arrow on an atom means the magnetic moment. There are magnetic interaction between any two magnetic atoms. On the figure the interaction between nearest-neighbor, next-nearest-neighbor, ... atoms are shown by red, green, ... colors. 9

2.2. There is a schematic presentation of the disorder crystal lattice Heisenberg model. A circle in the lattice node is shown an atom. An arrow on an atom is shown the magnetic moment. There are magnetic interaction between any two magnetic atoms. On the figure the interaction between nearest-neighbor, next-nearest-neighbor, ... atoms are shown by red, green, ... colors. 13

2.3. The magnetic density of states (DOS) in a simple cubic lattice for the Heisenberg model (Eq. 2.11) for a case only short range interaction $J_1 = 0.001eV$ at $T = 0$, $S = 1/2$. 17

2.4. The dependence of magnetization on temperature for the Heisenberg model that was obtained from the DOS presented on the Fig. 2.3. 18

2.5. Quasiparticle magnon DOS at fixed model parameters $S = 1/2$, $T = 0$ for different values of the concentrations of magnetic atoms x, and additional assumption about magnetic interaction in the crystal lattice $J_1 = 1meV; J_2 = 0.01meV; J_3 = 0.001meV$. 18

2.6. Quasiparticle magnon DOS at fixed model parameters $S = 1/2$, $T = 0$ for different values of the concentrations of magnetic atoms x, and additional assumption about magnetic interaction in the crystal lattice $J_1 = 1meV; J_2 = 0.5meV; J_3 = 0.1meV$. . . 19

2.7. The dependence of magnetization on temperature for the disordered HM that was obtained from the DOS presented on the Fig. 2.6 20

3.1. There is a schematic presentation of the the disordered Kondo-lattice model. 25

3.2. Density of electron states for the disordered KLM at $x = 0.95$, $U = \infty$, $n = 0.06$, $S = 5/2$, $J = 0.4$ for ferromagnetic $\langle S^z \rangle = S$ and paramagnetic $\langle S^z \rangle = 0$ cases 27

3.3. Density of electron states for the disordered KLM at $x = 0.1$, $U = \infty$, $n = 0.06$, $S = 5/2$, $J = 0.4$ for ferromagnetic $\langle S^z \rangle = S$ and paramagnetic $\langle S^z \rangle = 0$ cases 27

3.4. Dependence of the total band occupation $n_\uparrow + n_\downarrow$ on the position of the Fermi edge at $T = 0$, $S = 5/2$, $J = 0.6$, $W = 0.9$ for a different value of concentration of the magnetic atoms. 28

3.5. Dependence of the electron polarization on the position of the Fermi edge at $T = 0$, $S = 5/2$, $J = 0.6$, $W = 0.9$ for a different value of concentration of the magnetic atoms. 29

3.6. Density of electron states for the disordered KLM at $x = 0.9$, $S = 5/2$, $J = 0.4$ for ferromagnetic $\langle S^z \rangle = S$ and paramagnetic $\langle S^z \rangle = 0$ cases 30

3.7. Density of electron states for the disordered KLM at $x = 0.1$, $S = 5/2$, $J = 0.4$ for ferromagnetic $\langle S^z \rangle = S$ and paramagnetic $\langle S^z \rangle = 0$ cases. 31

3.8. Schematic picture of the lattice and the electron processes. . . . 33

3.9. Density of electron states in the cluster approximation for the disordered KLM at $S = 1/2$, $J = 1$, $W = 0.5$ for ferromagnetic $\langle S^z \rangle = S$ case at the different crystal field parameters 39

3.10. Density of electron states in the cluster approximation for the disordered KLM at $S = 1/2$, $J = 1$, $W = 0.5$ for ferromagnetic $\langle S^z \rangle = S$ case at the different crystal field parameters 40

3.11. Density of electron states in the cluster approximation for the disordered KLM at $S = 1/2$, $J = 1$, $W = 0.5$ for ferromagnetic $\langle S^z \rangle = S$ case at the different crystal field parameters 40

4.1. Flowchart exhibiting the self consistent determination of the magnetization $\langle S^z \rangle$. The terminologies are as explained in the text. 46

4.2. Dependence of the MRKKY interaction (Eq. 3.10) on the distance R between magnetic atoms in a simple cubic lattice ($R = 1$ is a first shell(nearest-neighbors atoms),$R = \sqrt{2}$ is a second shell(next nearest-neighbors atoms) and so on) at fixed parameters $W = 0.9, S = 5/2, x = 0.1, T = 0, \langle S^z \rangle = S$ of the model for three different coupling $J = 0.2, J = 0.4, J = 0.9$ and three different values of a small electron concentration $n/x = 1, n/x = 0.6, n/x = 0.2$. In the inset is the electron DOS for the same parameters. The Fermi edge is indicated for the band occupation $n/x = 0.6$. 47

4.3. Dependence of the conventional RKKY interaction (Eq. 3.10) and MRKKY on the distance R between magnetic atoms in a simple cubic lattice ($R = 1$ is a first shell(nearest-neighbors atoms),$R = \sqrt{2}$ is a second shell(next nearest-neighbors atoms) and so on) at fixed parameters $W = 0.5, S = 5/2, x = 1, T = 0, \langle S^z \rangle = S, J = 0.0001$ of the model for three different values of a small electron concentration $n = 0.02, n = 0.06, n = 0.1$. The terminologies are as explained in the text. 48

4.4. Quasiparticle electron(left column) and magnon (right column) density of states(DOS) at fixed model parameters $W = 0.5, S = 5/2, x = 0.1, n/x = 0.6$ for three different couplings and for different values of the crystal field parameters. The inset shows dependence of the MRKKY interaction on the distance R between magnetic atoms in simple cubic lattice($R = 1$ is a first shell, $R = t\sqrt{2}$ is a second shell, and $R = \sqrt{3}$ is a third shell). . 50

4.5. Dependence of the nearest-neighbor effective exchange integral J_1, the next-nearest-neighboring one J_2 and J_3 on the exchange coupling J at $W = 0.5, n = 0.06, T = 0$, for different values of concentration x and two value of $S = 1/2, S = 5/2$ which were calculated by using of the zero-bandwith limit (the atomic limit) of the correlated KLM. 52

4.6. Dependence of the nearest-neighbor effective exchange integral J_1 on the exchange coupling J at $W = 0.5, n = 0.06, S = 5/2, T = 0$, for different values of concentration x using two method of calculation for the electron spectrum of the disorder KLM. In the labels we use AL and ISA which mean that the results were calculated by used the zero-bandwidth atomic analogy limit and the Interpolating self-energy approach, respectively. 53

4.7. Dependence of the nearest-neighbor effective exchange integral J_1 on the exchange coupling J at $W = 0.9, S = 5/2, T = 0$, for different values of concentration x and different values of a band occupation $n = 0.02, n = 0.06, n = 0.1$. 54

4.8. Dependence of the nearest-neighbor effective exchange integral J_1 and the next-nearest-neighboring one J_2 on the exchange coupling J at $W = 0.9eV, S = 5/2, T = 0$ for different values of moment-concentration x without crystal field effects. 54

4.9. Electron DOS calculated with $W = 0.5, J = 1.2, S = 1/2, n = 0.6, T = 0$ for different values of the concentration x. 55

4.10. Magnon DOS calculated self-consistently by use of the VCA with the same parameters as those in Fig. 4.9 for different values of the concentration x. 56

4.11. Magnon DOS calculated self-consistently by use of the Low Quadratic Approximation with the same parameters as those in Fig. 4.9 for different values of the concentration x. 56

4.12. Self-consistent calculation of the dependence of the magnetization $\langle S^z \rangle$ on temperature by use of the VCA approximation with the same parameters as those in Fig. 4.9 for different values of the concentration x. 57

4.13. Self-consistent calculation of the dependence of the magnetization $\langle S^z \rangle$ on temperature by use of the Low Quadratic Approximation with the same parameters as those in Fig. 4.12 for different values of the concentration x. 57

4.14. Dependence of the nearest-neighbor effective exchange integral J_1 on the temperature T with the same parameters as those in Fig. 4.10 for different values of the concentration x. 58
4.15. Self-consistent calculation of the dependence of the magnetization $\langle S^z \rangle$ on temperature by use of the Low Quadratic Approximation with the same parameters as those in Fig. 4.12 for the concentration $x = 0.1$. 59
4.16. Dependence of the Curie temperature T_c on the exchange coupling J at $W = 0.5eV, S = 5/2, x = 0.1$ and tree different value of a small electron concentration $n/x = 0.1, n/x = 0.6, n/x = 1$ without crystal field parameters influence. 60
4.17. Dependence of the Curie temperature T_c on the exchange coupling J at $W = 0.5eV, n = 0.06, x = 0.1, S = 5/2$ for the case of finite crystal field parameters. 60
4.18. Self-consistent calculation of the dependence of the magnetization $\langle S^z \rangle$ on temperature by use of the VCA approximation with the same parameters as those in Fig. 4.17 for different values of the concentration x. 61

A.1. Dependence of the imagery part of the $C_i(E)$ function (Eq. 3.10) on the energy E in a simple cubic lattice for several shells. In the inset is the shell structure of the given cluster. 67

B.1. Binary diagrams on the square lattice and their topological equivalent ones. 74
B.2. a) Irreducible diagram, b) Non-irreducible diagram. 75

Tabellenverzeichnis

A.1. Several topological parameters for a simple cubic lattice 69

Selbständigkeitserklärung

Hiermit erkläre ich, die vorliegende Arbeit selbstständig ohne unerlaubte Hilfe verfasst und nur die angegebene Literatur und die angegebenen Hilfsmittel verwendet zu haben.

Kyiv, den 5 März 2009 Vadym Bryksa